

Wolfgang Eckstein

## **Sputtered Energy Coefficient and Sputtering Yield**

**IPP 17/29**  
**Dezember, 2011**

# Sputtered Energy Coefficient and Sputtering Yield

W.Eckstein

Max-Planck-Institut für Plasmaphysik  
Boltzmannstr.2, D-85748 Garching  
[wolfgang.eckstein@ipp.mpg.de](mailto:wolfgang.eckstein@ipp.mpg.de)

December 6, 2011

## 1 Abstract

This report gives an overview of available calculated sputtered energy coefficients of energetic ions bombarding elemental targets. The energy and angular dependences of the sputtered energy coefficient are fitted by simple formulae for a large number of elemental targets and light (hydrogen and helium) and heavy (mainly noble gases and selfbombardment) bombarding atoms. The incident energies cover a range from 10 to  $10^5$  eV, in some cases up to MeV energies.

## 2 Introduction

In recent years surveys on sputtering [1], reflection [2], and mean penetration depths [3] have been published, comparing experimental and calculated data as well as fitting available calculated values. Based on the same calculations this report provides values fits for the energy and angular dependence of the sputtered energy coefficient and the sputtering yield of energetic ions bombarding solids.

Bombarding a solid (or liquid) with energetic ions (or neutrals) leads to backscattering, sputtering and implantation. Besides the sputtering yield,  $Y$  (number of sputtered atoms normalized to the number of incident ions), the sputtered energy coefficient,  $Y_E$  (energy of the sputtered atoms normalized to the energy of the incident ions) characterizes the energy of the sputtered atoms. The ratio  $(Y_E/Y)E_0$  delivers the mean energy of the sputtered atoms, where  $E_0$  is the energy of the incident ion.

In [1] the sputtering yield has been discussed in great detail, whereas the sputtered energy coefficient (sometimes called sputtering efficiency) was not considered thoroughly because of the lack of experimental data.

## 3 Calculational Methods

The calculated results reported in this review are determined with a Monte Carlo program based on the binary collision model [4]. The programs used are TRIM.SP [4, 5] and the newest versions of SDTrimSP [6, 7]. The most important input for the program is the interaction potential. In the programs mentioned, mostly the WHB (KrC) potential [8] is applied; but other potentials such as the ZBL [9] and Moliere [10] potentials are also used sometimes. All these potentials are purely repulsive and only dependent on the interatomic distance. For Si a special potential with an attractive part has been used in a few cases [11]. Another important input is the electronic (inelastic) energy loss. Here, an equipartition of the local Oen-Robinson model [12] and the nonlocal velocity proportional loss [13, 14] is applied at low energies (1 eV to 20 keV) for hydrogen and helium, and for heavy ions in the whole energy range (1 to  $10^6$  eV) investigated. At high energies the formulae of Ziegler [15] for helium, and the formulae of Andersen and Ziegler [16] for hydrogen are used. Other input parameters for the calculations [4] are the surface binding energy of target atoms,  $E_{sb}$ , which is only important in reflection for selfbombardment, the binding energy of projectiles,  $E_{sp}$ , to the target surface (about 1 eV), which is only of importance for hydrogen and nitrogen (for most elements but not for Cu, Ag, Au), and finally a cutoff energy of projectiles of 0.5 eV. For other calculational approaches see [4].

Sputtered energy coefficient values calculated with TRIM, TRIM.SP and SDTrimSP are documented in [17, 18, 19], which implies that all calculated values are only valid for zero fluence (static case) or in other words, the influence of implanted species are not taken into account. The absolute error depends

on the applied interaction potential and on the inelastic energy loss model; it should be smaller than a factor of two, in most cases better than 30%. The statistical error is usually better than a few percent, in many cases better than 1%. References [17, 18, 19] contain all the calculated values used for the fits. These references provide also more but not enough calculated values for special cases to make a good fit; these values do not appear in this report.

The implantation of bombarding species in the target and the resulting change of the target composition with fluence can be treated by a dynamical program like TRIDYN [4, 20] or in the dynamic mode of SDTrimSP [6, 7].

## 4 Fitting

The fit formulae used here are similar to those applied in [6] (the corrected error which appeared in [1] can be found in [19]).

$$Y_E(E_0) = q s_n^{Krc}(\varepsilon_L) \frac{\left(\frac{E_0}{E_{th}} - 1\right)^\mu}{\lambda + \left(\frac{E_0}{E_{th}} - 1\right)^\mu} \quad \text{with} \quad (1)$$

$$s_n^{Krc}(\varepsilon_L) = \left( \frac{0.5 \ln(1 + 1.2288\varepsilon_L)}{(w(\varepsilon_L))^\nu} \right)^n \quad (2)$$

The value  $n$  is 2 for the light ions (hydrogen and helium) and 1 for heavy ions (nitrogen, oxygen, noble gases and selfbombardment).

$$w(\varepsilon_L) = \varepsilon_L + 0.1728\sqrt{\varepsilon_L} + 0.008\varepsilon_L^{0.1504} \quad (3)$$

$$\varepsilon_L = E_0 \frac{M_2}{M_1 + M_2} \frac{a_L}{Z_1 Z_2 e^2} = E_0 / \varepsilon \quad (4)$$

The fitting is performed in the energy range from 1 to 20 keV for light ions, and from 10 to 200 keV for heavy ions in most cases, but the same formula also applies to higher energies up to a few MeV as shown for a few cases of several ions on Si, Ti, Cu, Ag, Au. The fitting parameters  $\lambda, q, \mu, E_{th}, \nu$  are provided in tables 1 to 9. It should be mentioned, that the fitting parameters are only valid in the energy range given in the plots.

For the angular dependence of the sputtered energy coefficient the same fit formula as for the sputtering yield is used ([1, 21]):

$$\frac{Y(E_0, \theta_0)}{Y(E_0, 0)} = \left\{ \cos \left[ \left( \frac{\theta_0}{\theta_0^*} \frac{\pi}{2} \right)^c \right] \right\}^{-f} \exp \left\{ b \left( 1 - 1 / \cos \left[ \left( \frac{\theta_0}{\theta_0^*} \frac{\pi}{2} \right)^c \right] \right) \right\} \quad (5)$$

$$\theta_0^* = \pi - \arccos \sqrt{\frac{1}{1 + E_0/E_{sp}}} \geq \frac{\pi}{2} \quad (6)$$

$\theta_0^*$  takes care of the effect, that an angle of incidence of  $90^\circ$  cannot be reached, if the projectile experience a binding energy  $E_{sp}$  (to simulate a chemical binding).  $E_{sp} = E_{sb}$  for selfbombardment with  $E_{sb}$  being the surface binding energy (heat of sublimation),  $E_{sp} = 1$  eV is assumed for hydrogen isotopes and nitrogen,  $E_{sp} = 0$  for nobel gases. This projectile binding effect is only important at low energies and especially for selfbombardment. If  $E_{sp} = 0$ ,  $\theta_0^*$  becomes  $\pi/2$  and formula (5) is close to the Yamamura formula [22] besides the parameter  $c$ . If  $E_{sp} > 0$  the projectile experiences an acceleration and a refraction (decrease of the angle of incidence). The angle  $\theta_{0m}$ , at which the angular dependence reaches its maximum, is determined by

$$\theta_{0m} = \frac{2}{\pi} \theta_0^* (\arccos(b/f))^{1/c} \quad (7)$$

The values of the parameters  $f, c, b$  obtained by fitting the calculated values of the sputtered energy coefficient with Bayesian statistics are provided in tables 10 to 24 together with values of  $Y_E(E_0, \alpha), E_{sp}, \theta_0^*, \theta_{0m}$ , where  $\alpha$  is the angle of incidence (counted from the surface normal in degree).

## 5 Energy Dependence of the Sputtered Energy Coefficient

Generally, for each elemental target and several incident ions a plot is provided. The fits using formula (1) describe the energy dependence quite well. The reason for the different fits ( $n$ ) for light and heavy ions is the stronger decrease of  $Y_E$  for light ions at higher energies in the energy range investigated. The threshold energy determined by the fits agree well with those given in [1], often better than 1 eV, but in some cases the discrepancy is a few eV.

There are no experimental data for  $Y_E$  available to compare with calculated values.

The energy dependence of the sputtered energy coefficient shows a maximum at lower a lower energy than the corresponding sputtering yield.

The fits are shown in figures 1 to 9. The fitting parameters of formula (1) are provided in tables 1 to 9. It should be mentioned that the scales in the figures are not always the same, and that the fits are only valid in the energy range indicated in the figures.

The relative sputtered energy coefficient,  $Y_E/Y$ , shows in the case for Ag, approximately, a decreasing power dependence versus the energy of the incident ions, whereas the mean energy of the sputtered atoms,  $(Y_E/Y)E_0$ , exhibits an increasing power dependence, neglecting the threshold region, see Fig.10.

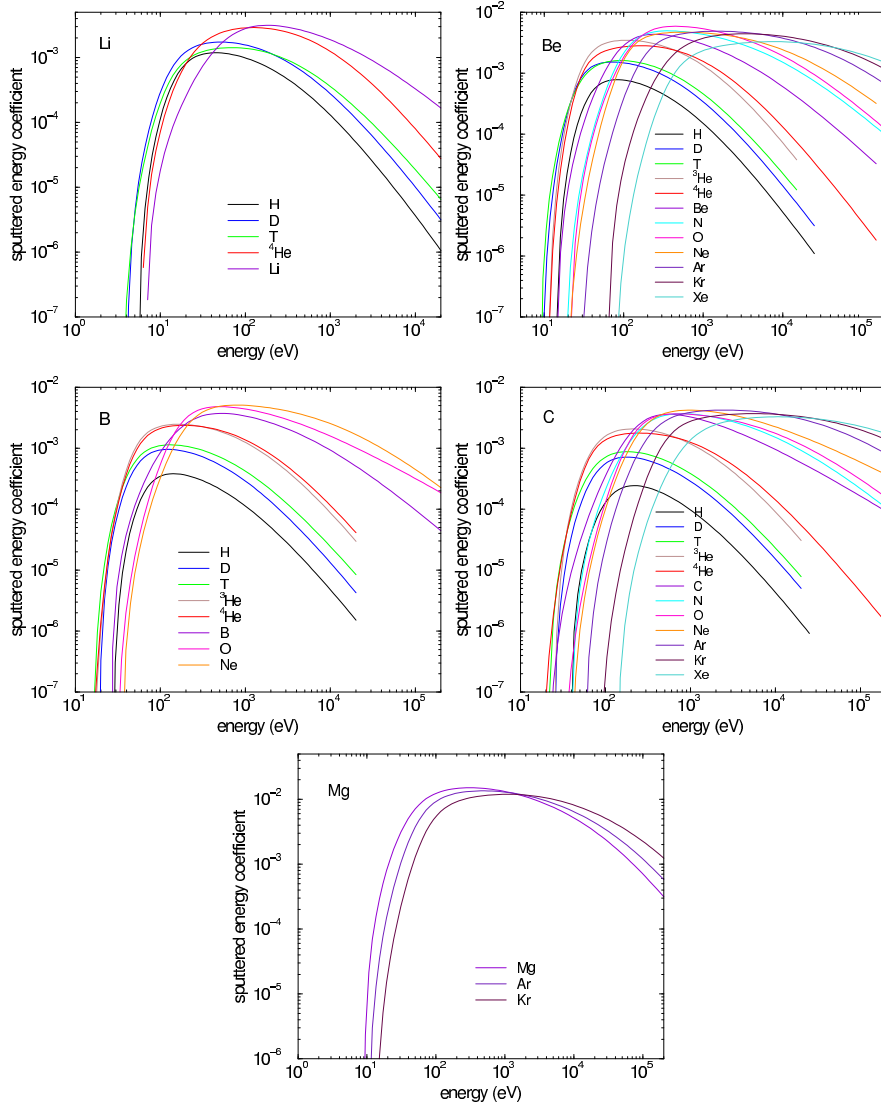


Figure 1: Sputtered energy coefficient versus the incident energy for several ion species bombarding Li, Be, B, C, Mg. Lines are fits to calculated values (parameters see table 1).

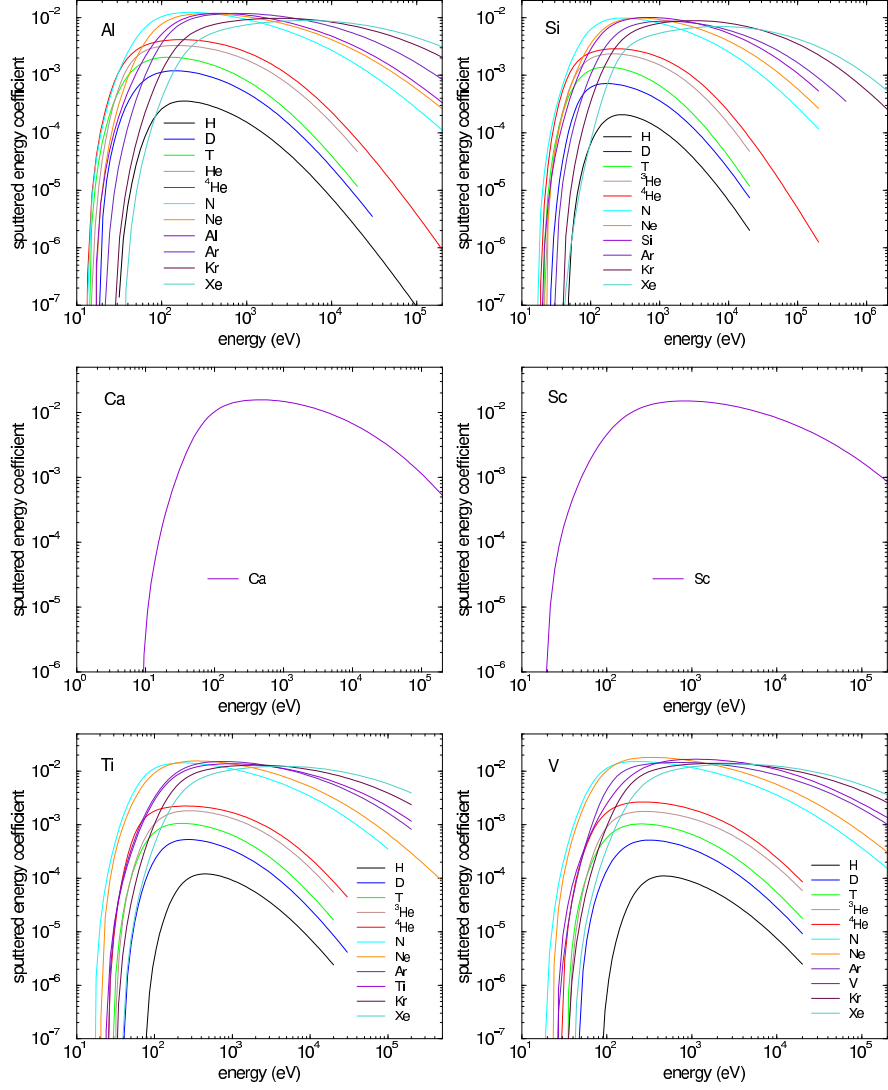


Figure 2: Sputtered energy coefficient versus the incident energy for several ion species bombarding Al, Si, Ca, Sc, Ti, V. Lines are fits to calculated values (parameters see table 2).

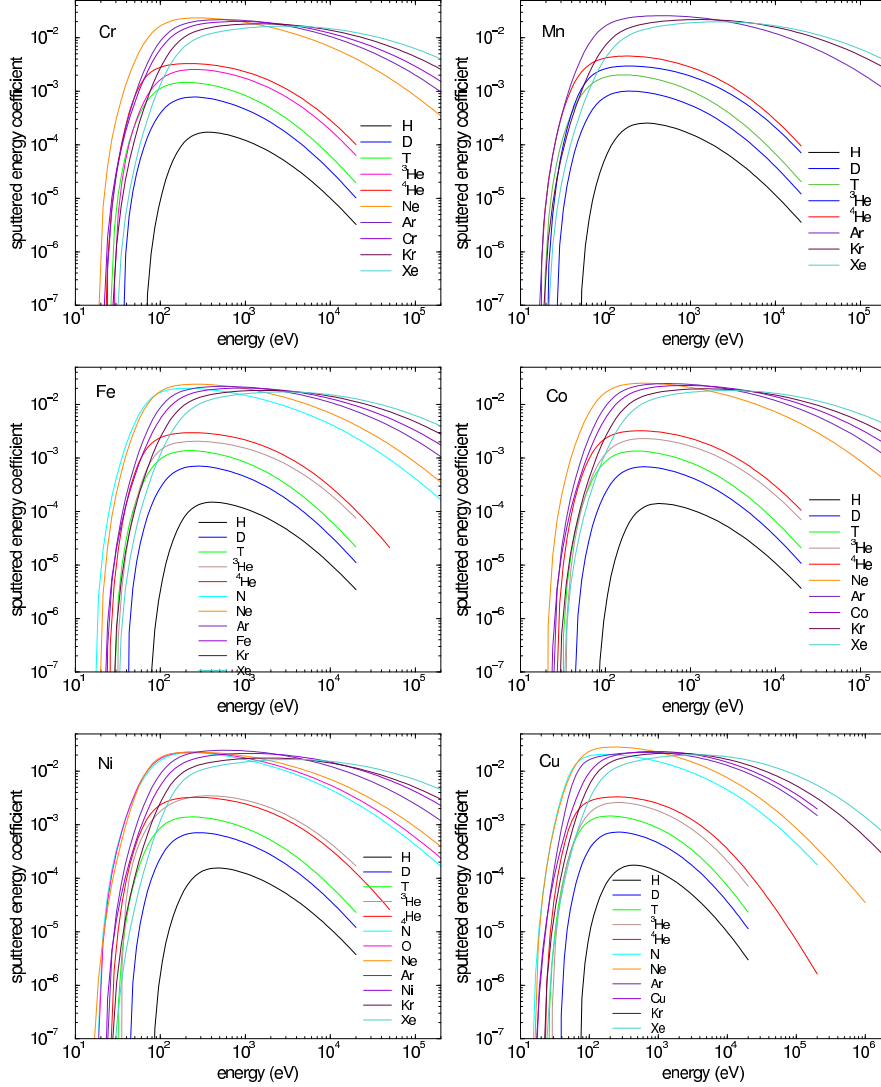


Figure 3: Sputtered energy coefficient versus the incident energy for several ion species bombarding Cr, Mn, Fe, Co, Ni, Cu. Lines are fits to calculated values (parameters see tables 3 and 4).

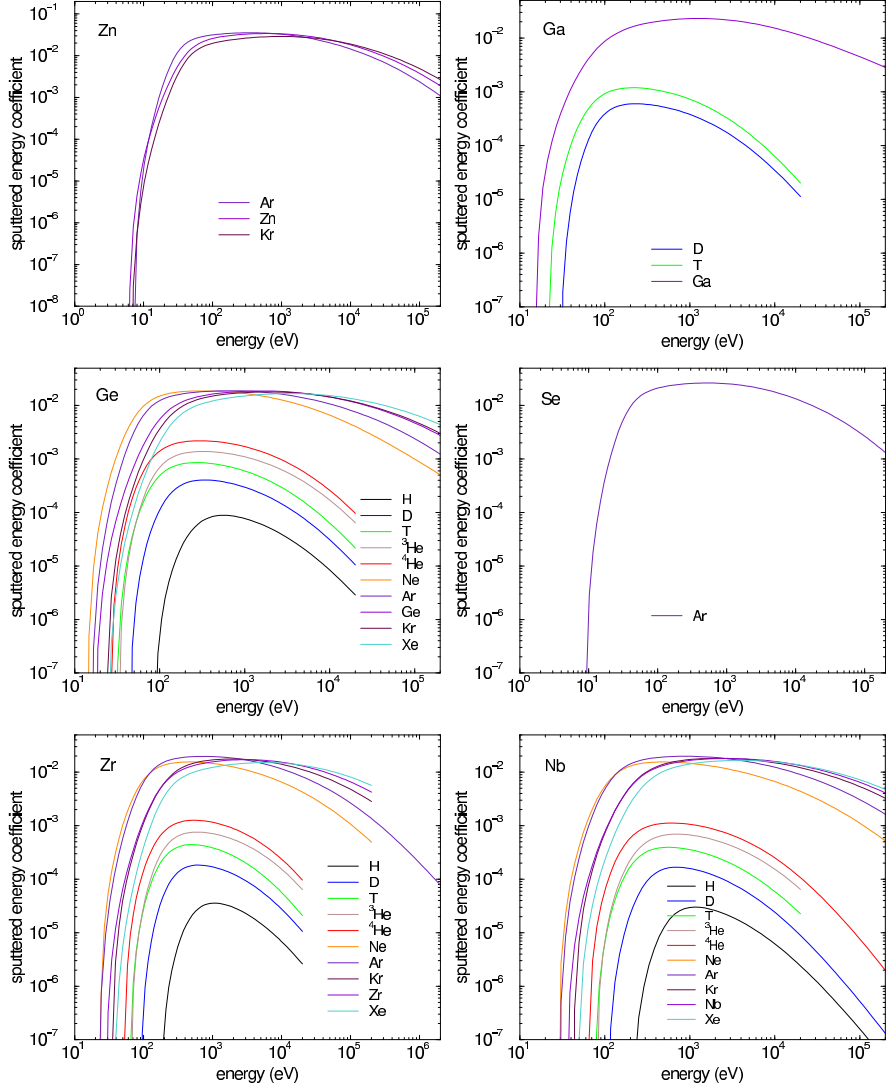


Figure 4: Sputtered energy coefficient versus the incident energy for several ion species bombarding Zn, Ga, Ge, Se, Zr, Nb. Lines are fits to calculated values (parameters see tables 4 and 5).

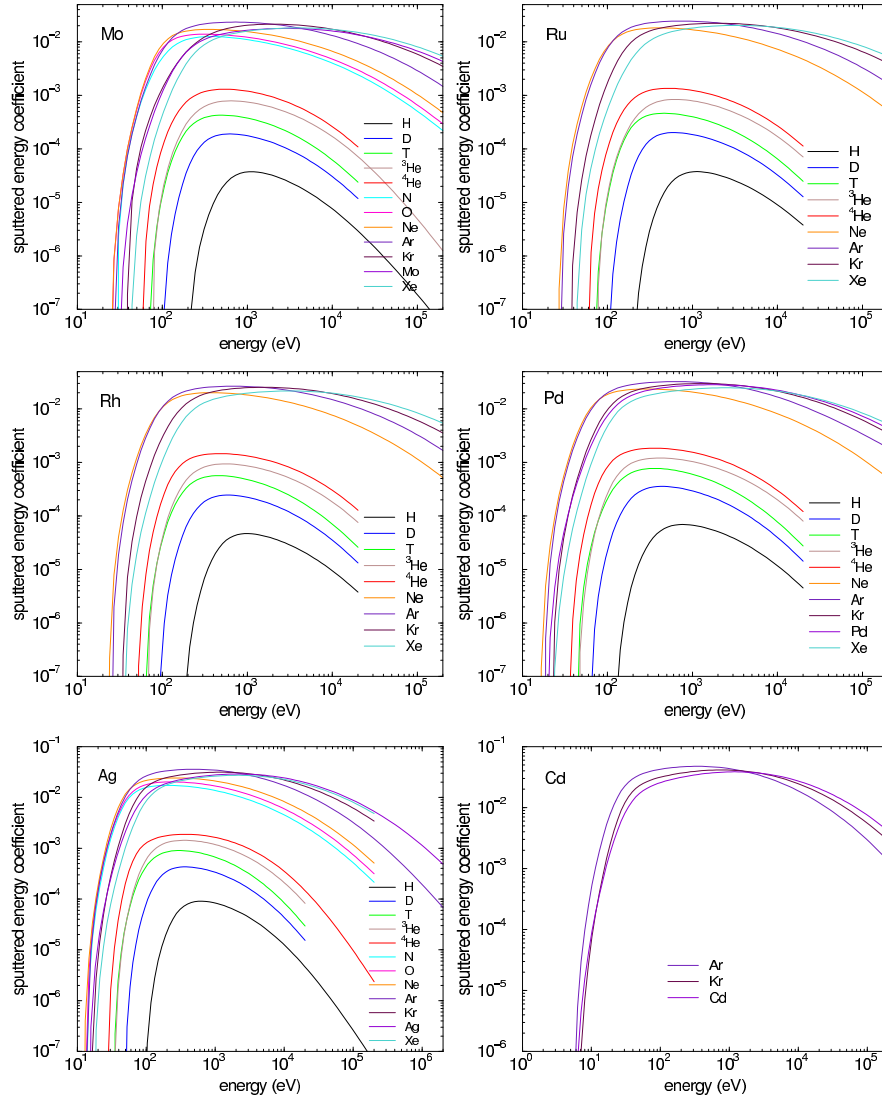


Figure 5: Sputtered energy coefficient versus the incident energy for several ion species bombarding Mo, Ru, Rh, Pd, Ag, Cd. Lines are fits to calculated values (parameters see tables 5 and 6).

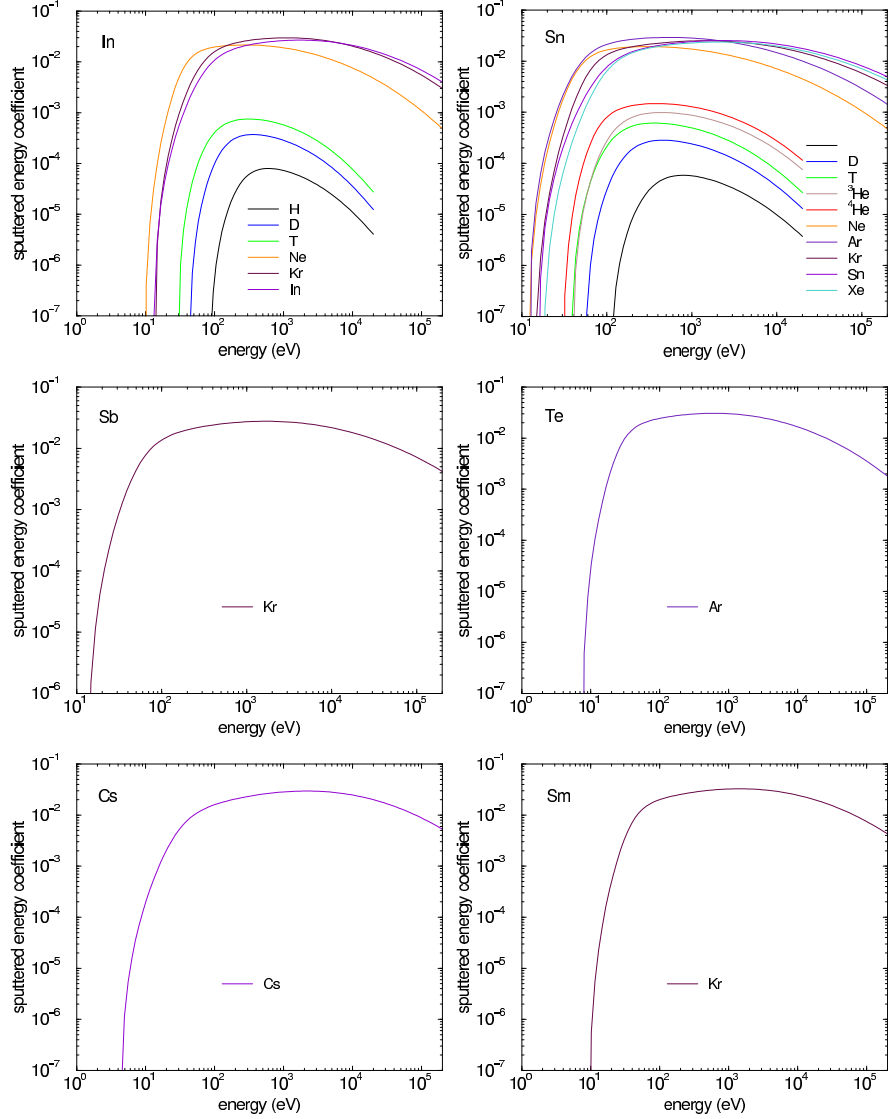


Figure 6: Sputtered energy coefficient versus the incident energy for several ion species bombarding In, Sn, Sb, Te, Cs, Sm. Lines are fits to calculated values (parameters see tables 6 and 7).

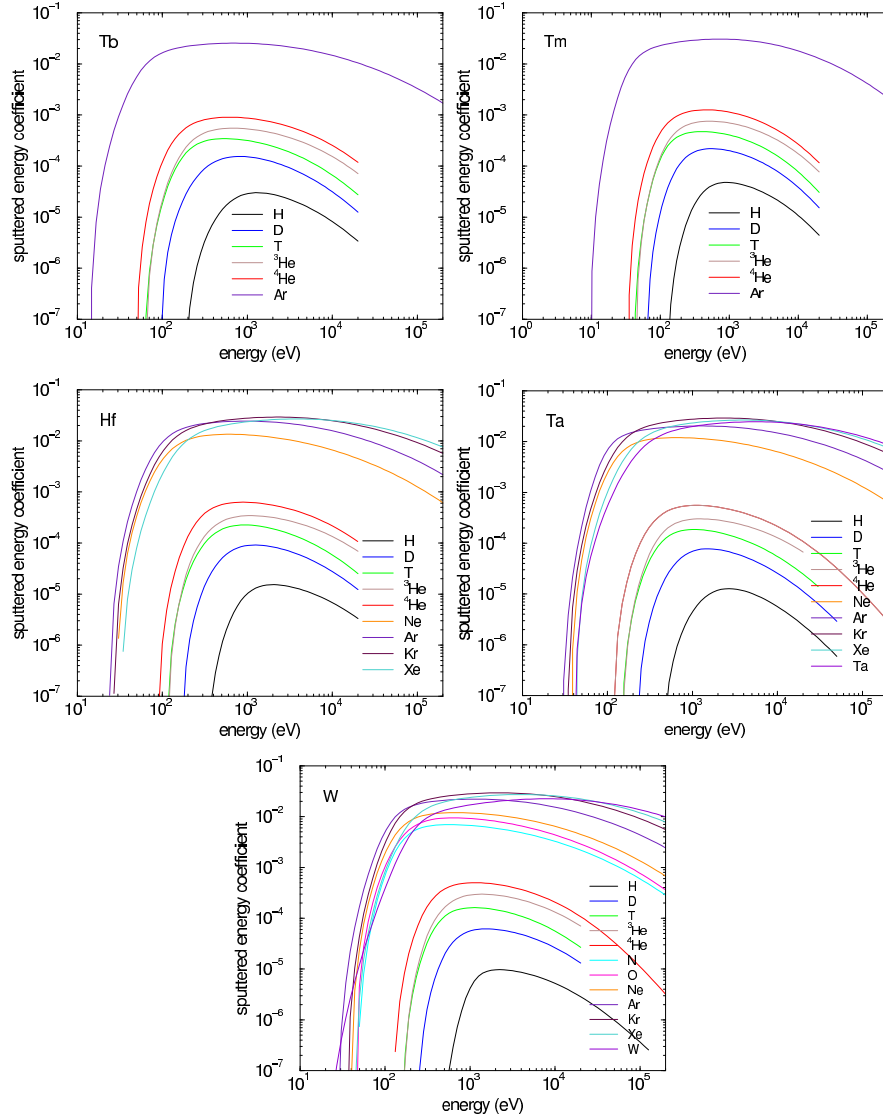


Figure 7: Sputtered energy coefficient versus the incident energy for several ion species bombarding Tb, Tm, Hf, Ta, W. Lines are fits to calculated values (parameters see tables 7 and 8).

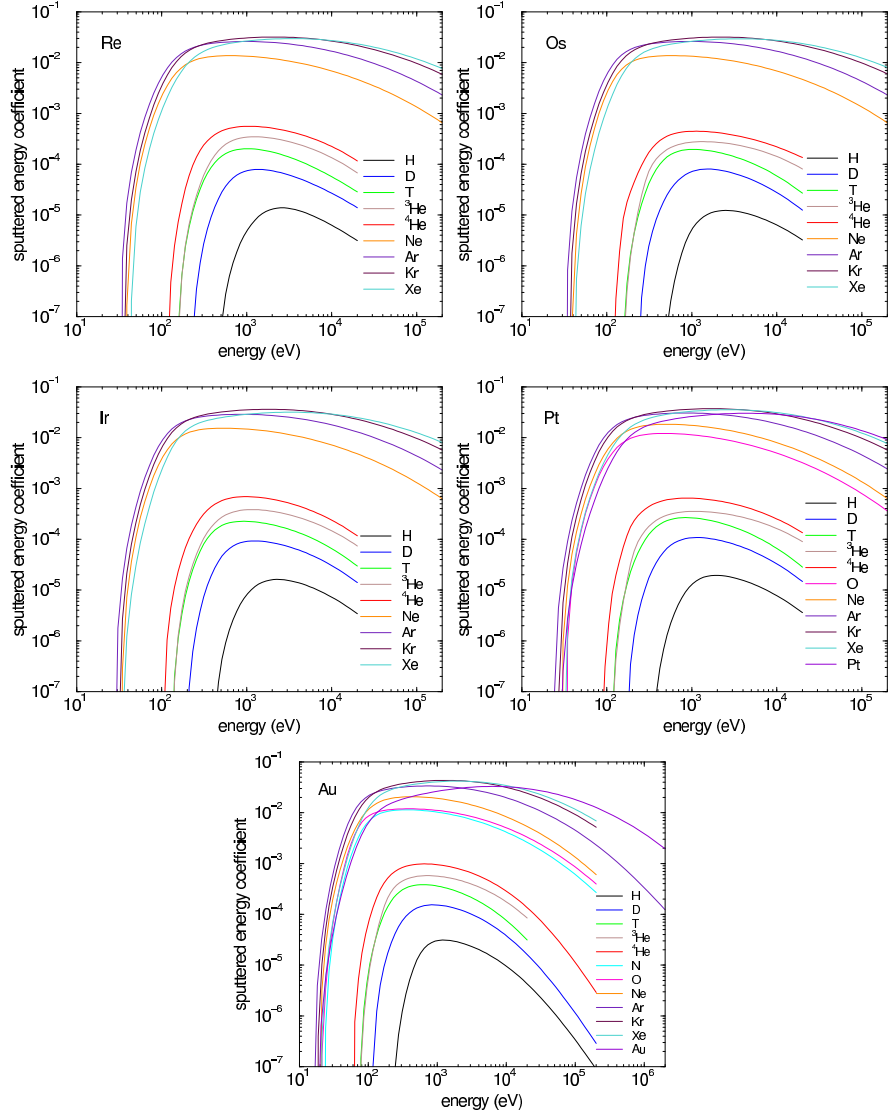


Figure 8: Sputtered energy coefficient versus the incident energy for several ion species bombarding Re, Os, Ir, Pt, Au. Lines are fits to calculated values (parameters see tables 8 and 9).

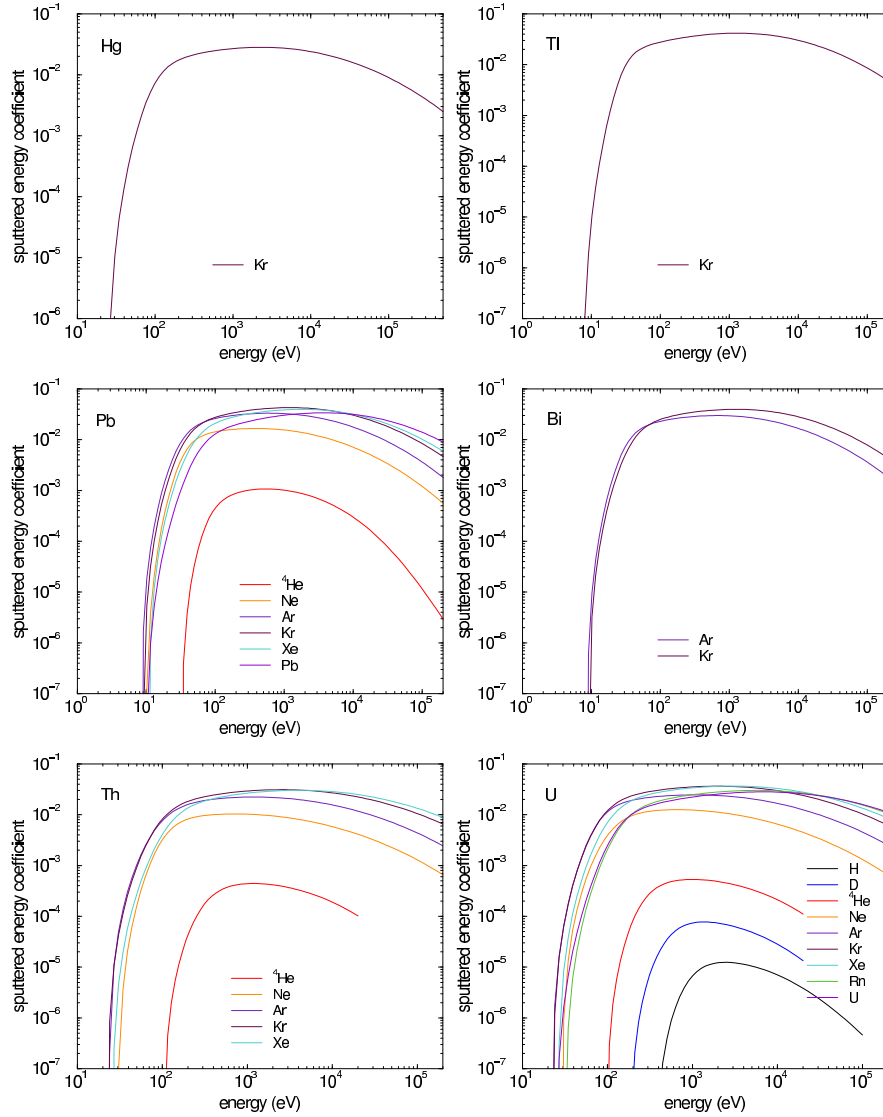


Figure 9: Sputtered energy coefficient versus the incident energy for several ion species bombarding Hg, Tl, Pb, Bi, Th, U. Lines are fits to calculated values (parameters see table 9).

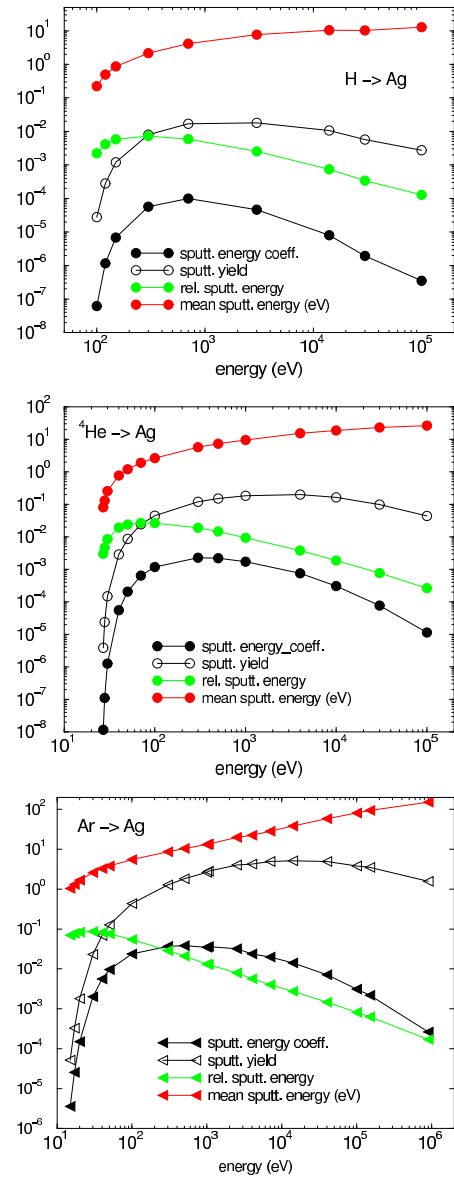


Figure 10: Sputtered energy coefficient, sputtering yield, relative sputtered energy coefficient, mean energy of sputtered atoms versus the incident energy for  $H$ ,  ${}^4He$ ,  $Ar$  bombarding  $Ag$ . Lines are drawn to guide the eye.

## 6 Angular Dependence of the sputtered energy coefficient

Similarly as in the energy dependence, the angular dependence of the sputtered energy coefficients is provided for each ion-target combination. Formula (2) can well describe the angular dependence. In addition to the plots of  $Y_E$  the corresponding plots of  $Y$  are provided, because only a few special where experimental data were available are shown in [1].

The use of different interaction potentials in the calculations leads to different values of the sputtered energy coefficient; these differences are usually smaller than a factor of two, for the mostly used potentials (WHB [8] and ZBL [9] these differences are in most cases smaller than 20%.

There is a tendency, that the maximum of the angular distribution of  $Y_E$  is a few degrees at larger angles than  $Y$ .

The fits of the angular dependence are shown in figures 11 to 43. Fitting parameters for  $Y_E(E_0, \alpha)$  are provided in tables 10 to 24. There are also parameters given for the sputterung yield,  $Y(E_0, \alpha)$ , of some combinations in table 25 not covered in [1]. For a few cases, there exist no data of  $Y_E$  but for  $Y$ .

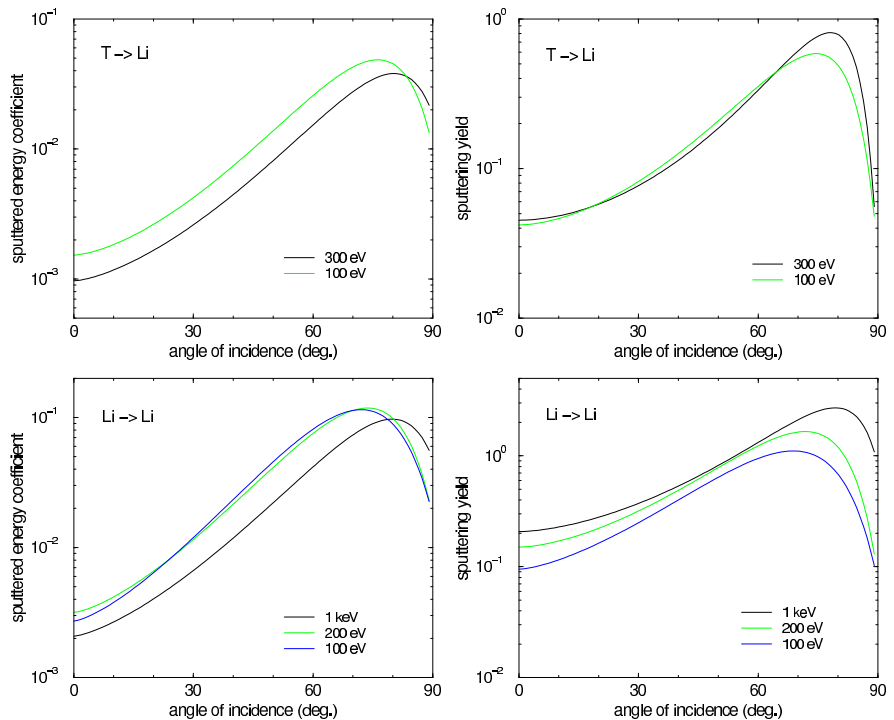


Figure 11: Sputtered energy coefficient and sputtering yield versus the angle of incidence for the bombardment of Li with T and Li at different incident energies. Lines are fits to calculated values (parameters see table 10 and [1]).

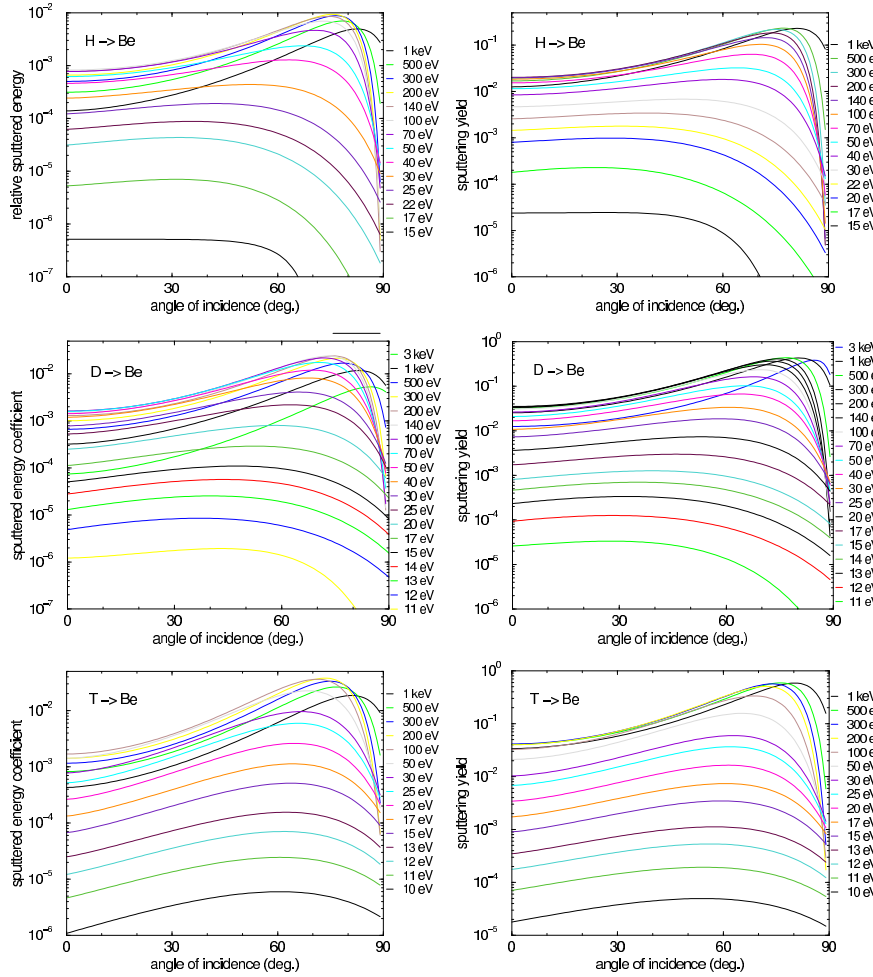


Figure 12: Sputtered energy coefficient and sputtering yield versus the angle of incidence for the bombardment of Be with H, D, and T at different incident energies. Lines are fits to calculated values (parameters see table 10 and [1]).

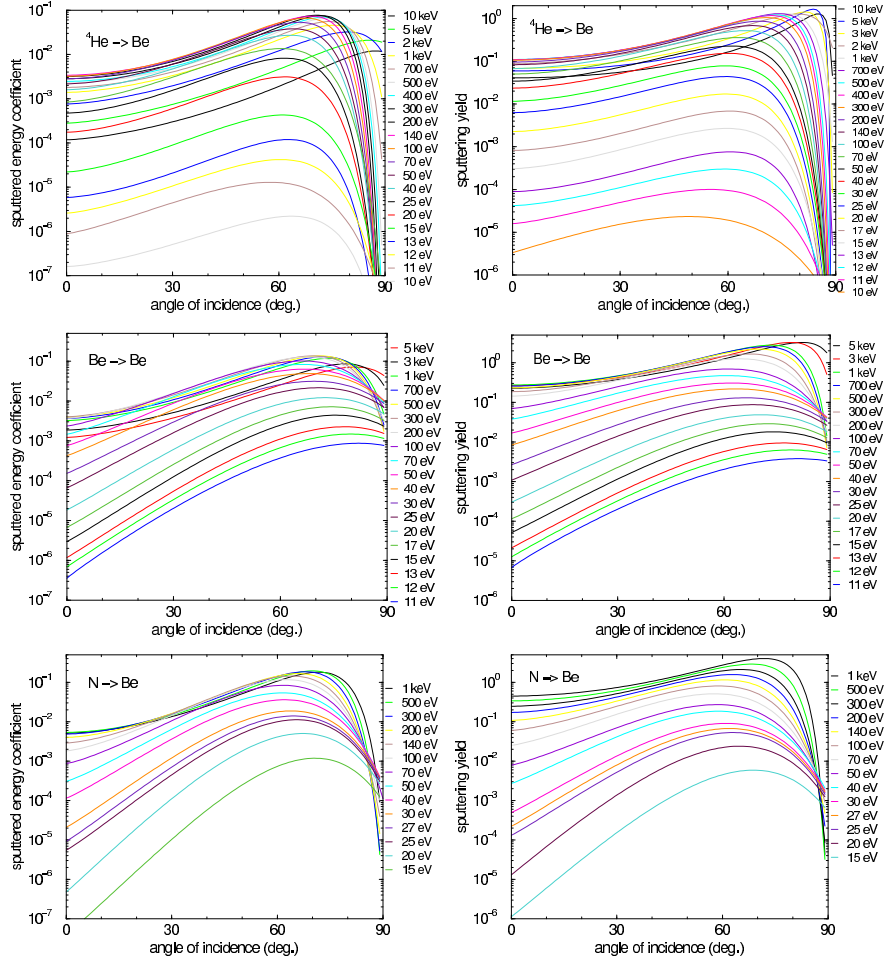


Figure 13: Sputtered energy coefficient and sputtering yield versus the angle of incidence for the bombardment of Be with  ${}^4\text{He}$ , Be, and N at different incident energies. Lines are fits to calculated values (parameters see tables 11, 12 and [1]).

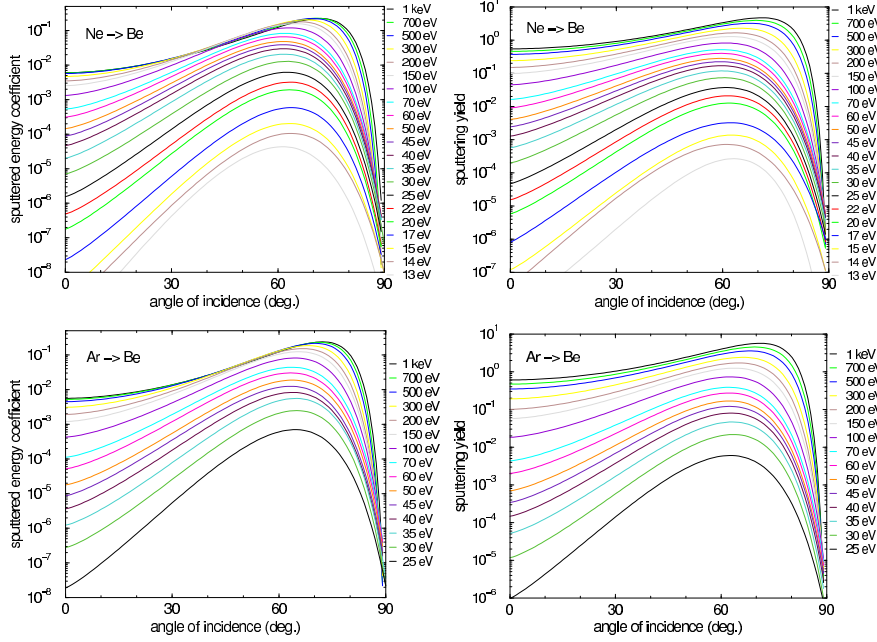


Figure 14: Sputtered energy coefficient and sputtering yield versus the angle of incidence for the bombardment of Be with Ne and Ar at different incident energies. Lines are fits to calculated values (parameters see table 12 and [1]).

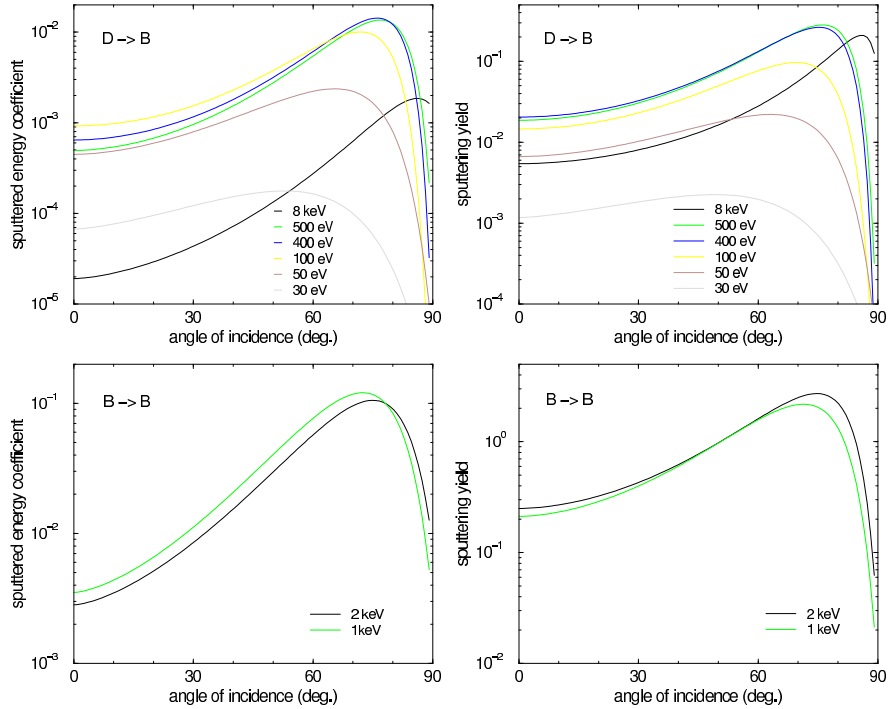


Figure 15: Sputtered energy coefficient and sputtering yield versus the angle of incidence for the bombardment of B with D and B at different incident energies. Lines are fits to calculated values (parameters see table 13 and [1]).

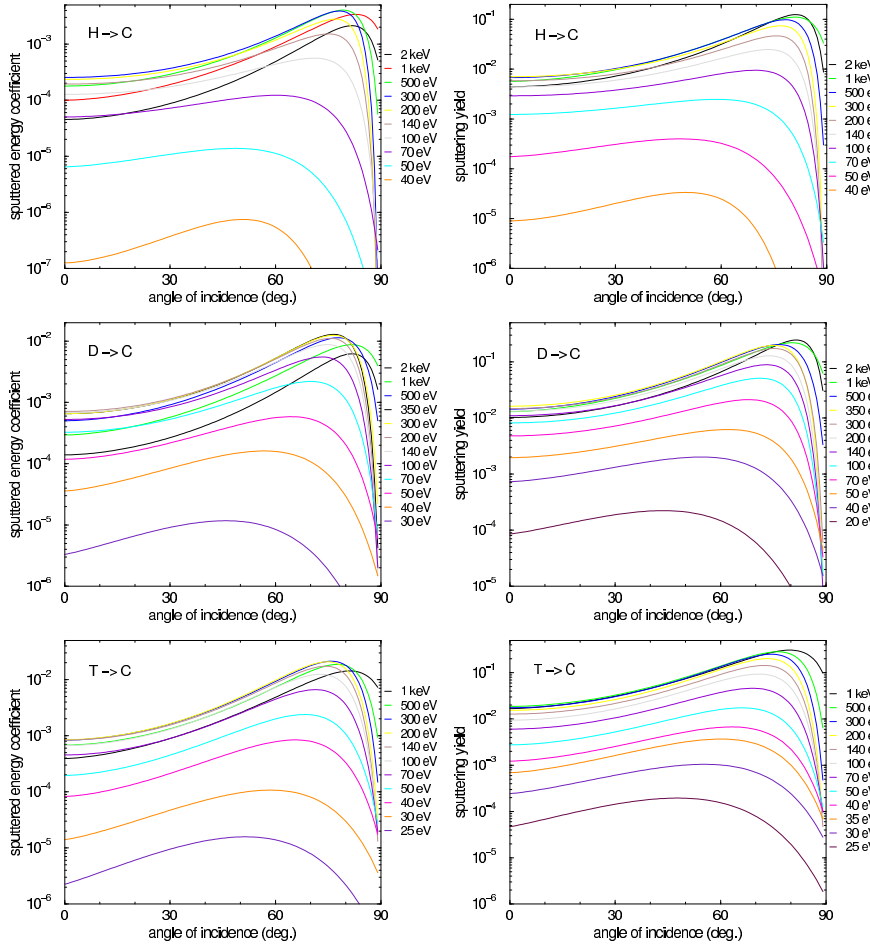


Figure 16: Sputtered energy coefficient and sputtering yield versus the angle of incidence for the bombardment of C with H, D, T at different incident energies. Lines are fits to calculated values (parameters see table 13 and [1]).

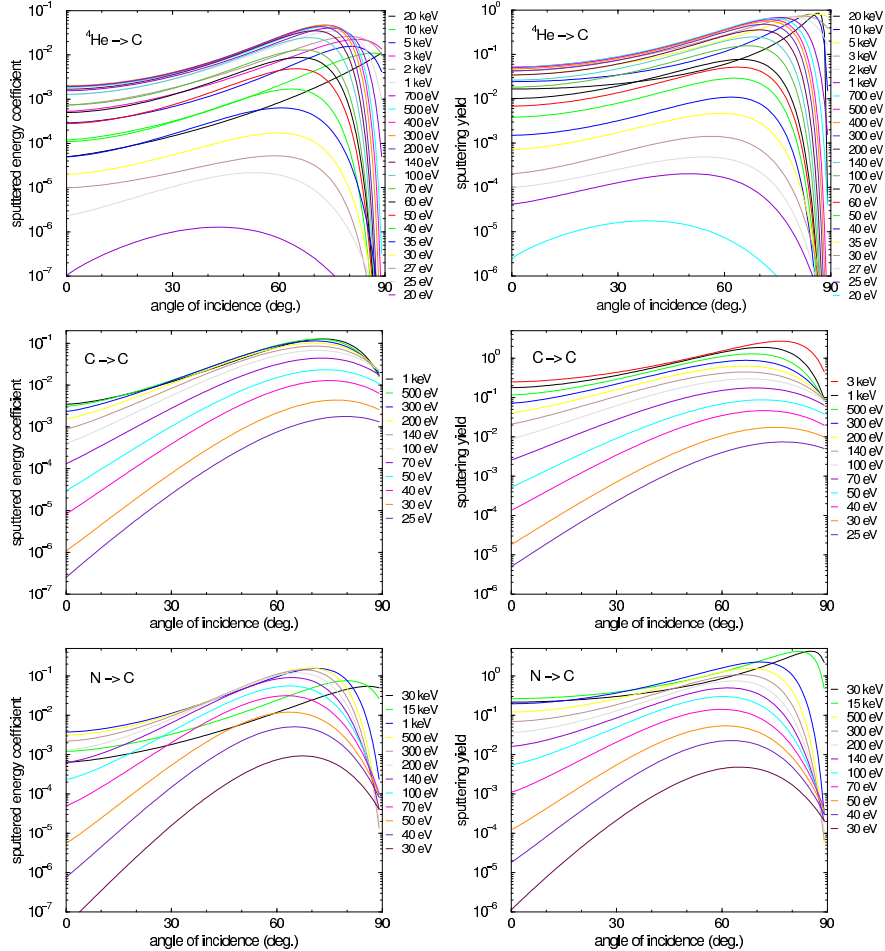


Figure 17: Sputtered energy coefficient and sputtering yield versus the angle of incidence for the bombardment of C with  ${}^4\text{He}$ , C, N at different incident energies. Lines are fits to calculated values (parameters see table 14 and [1]).

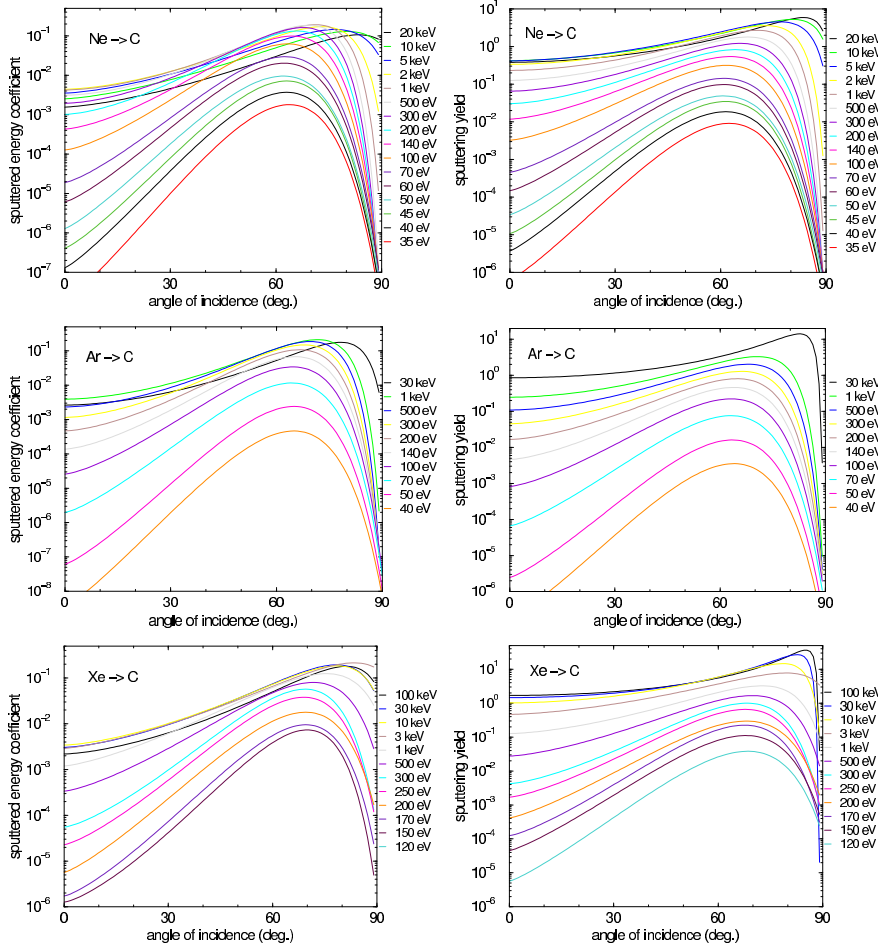


Figure 18: Sputtered energy coefficient and sputtering yield versus the angle of incidence for the bombardment of C with Ne, Ar, Xe at different incident energies. Lines are fits to calculated values (parameters see table 15 and [1]).

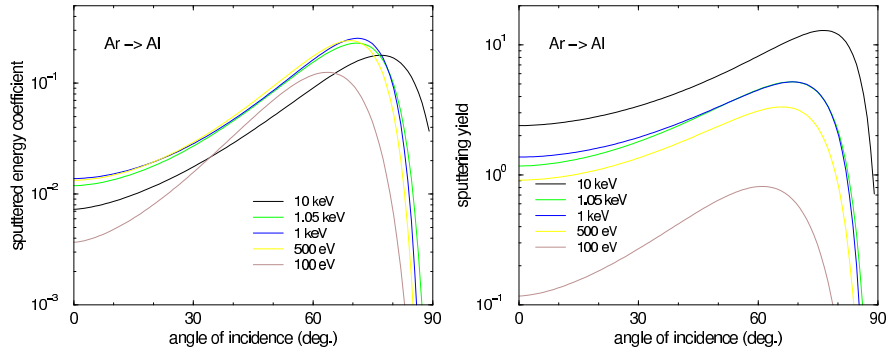


Figure 19: Sputtered energy coefficient and sputtering yield versus the angle of incidence for the bombardment of Al with Ar at different incident energies. Lines are fits to calculated values (parameters see table 15 and [1]).

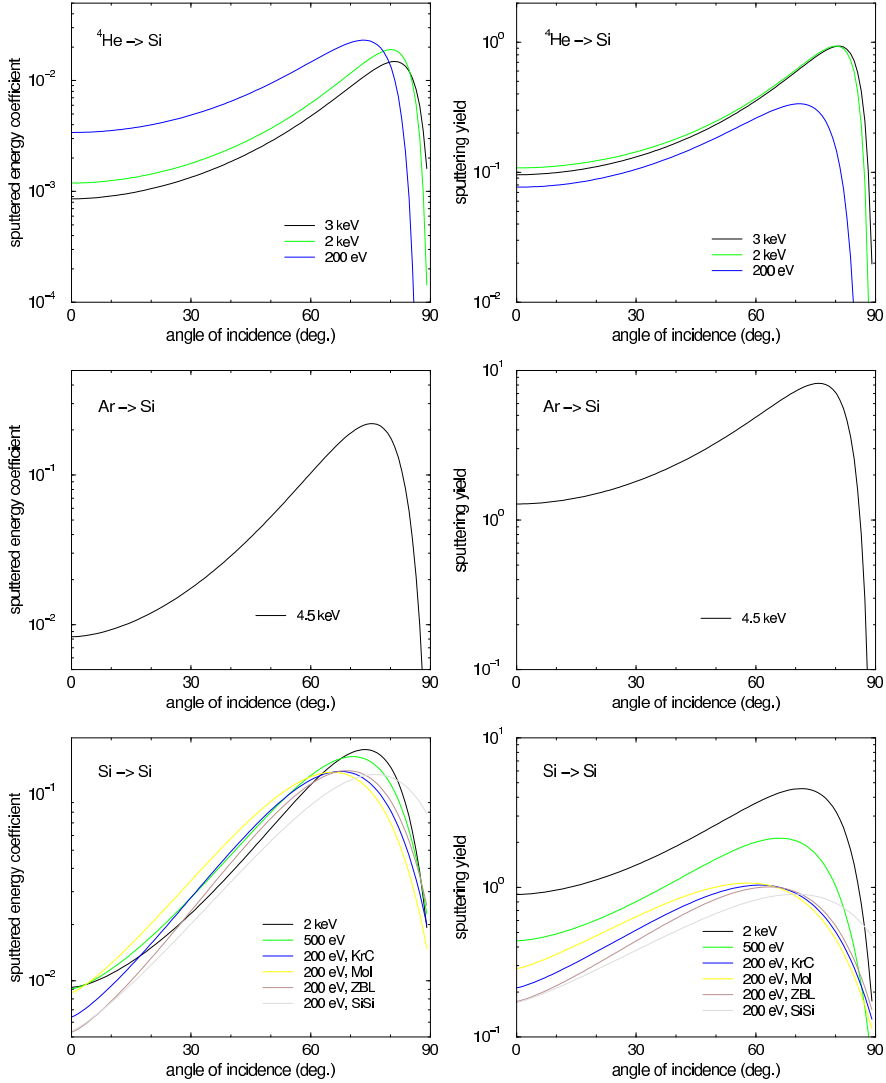


Figure 20: Sputtered energy coefficient and sputtering yield versus the angle of incidence for the bombardment of Si with  ${}^4\text{He}$ , Ar, Si at different incident energies. Lines are fits to calculated values (parameters see tables 15, 16 and [1]).

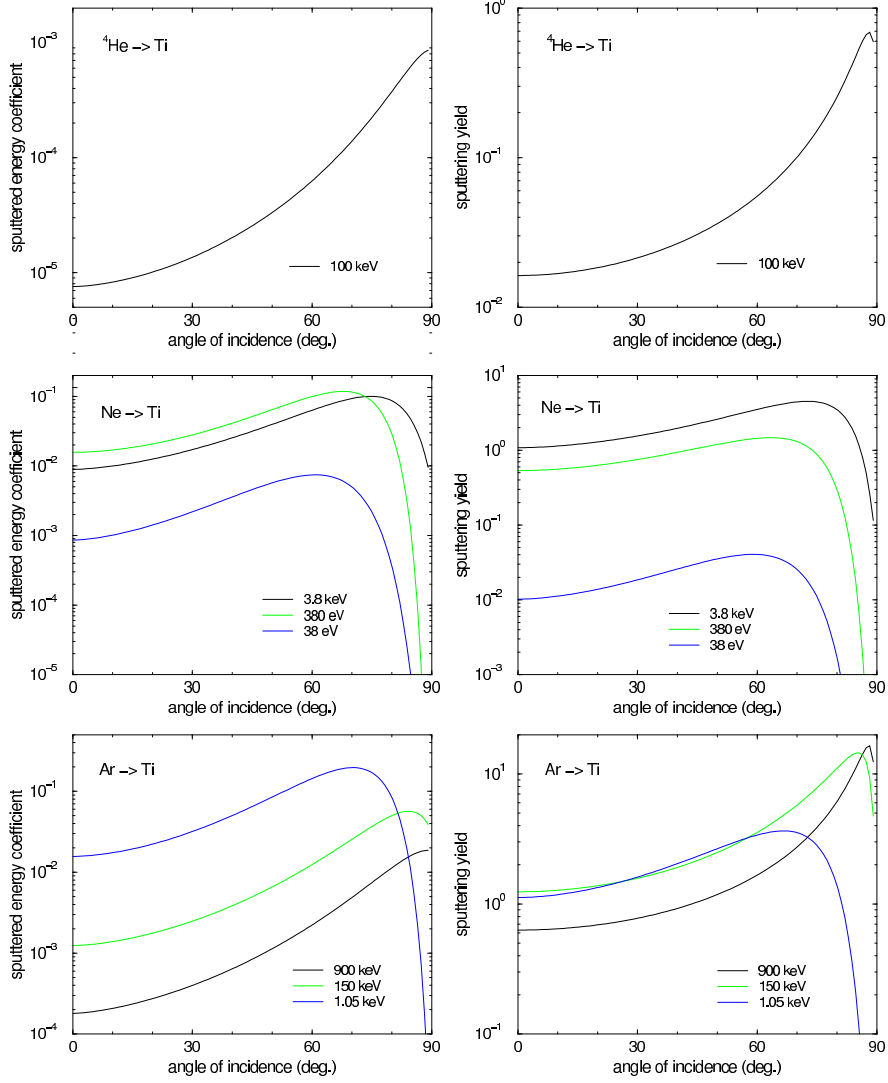


Figure 21: Sputtered energy coefficient and sputtering yield versus the angle of incidence for the bombardment of Ti with  ${}^4\text{He}$ , Ne, Ar at different incident energies. Lines are fits to calculated values (parameters see table 16 and [1]).

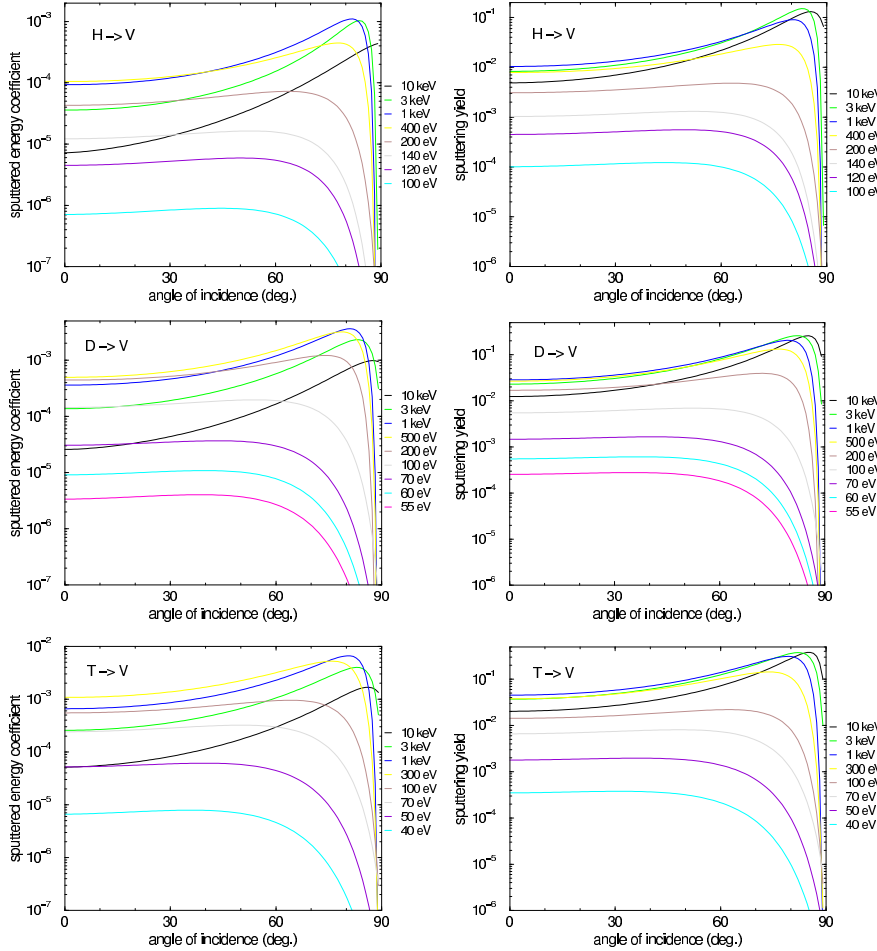


Figure 22: Sputtered energy coefficient and sputtering yield versus the angle of incidence for the bombardment of V with H, D, T at different incident energies. Lines are fits to calculated values (parameters see table 16 and [1]).

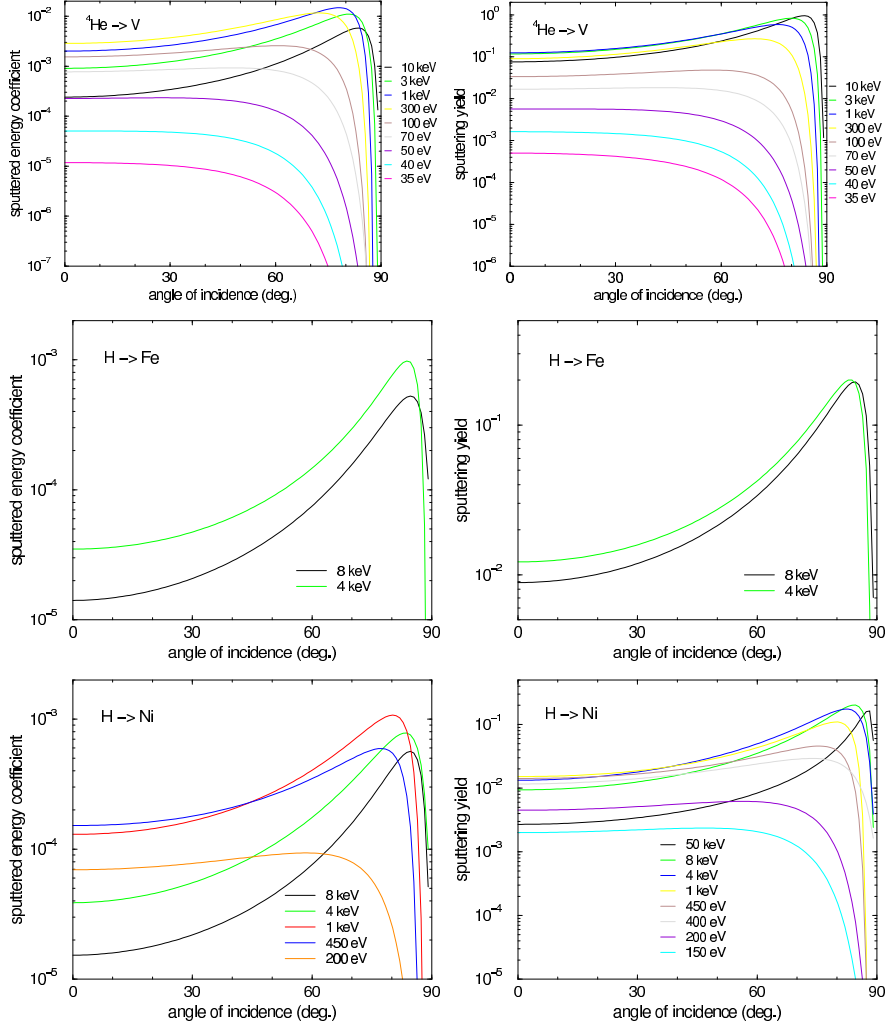


Figure 23: Sputtered energy coefficient and sputtering yield versus the angle of incidence for the bombardment of V with  ${}^4\text{He}$ , and Fe and Ni with H at different incident energies. Lines are fits to calculated values (parameters see tables 16, 17 and [1]).

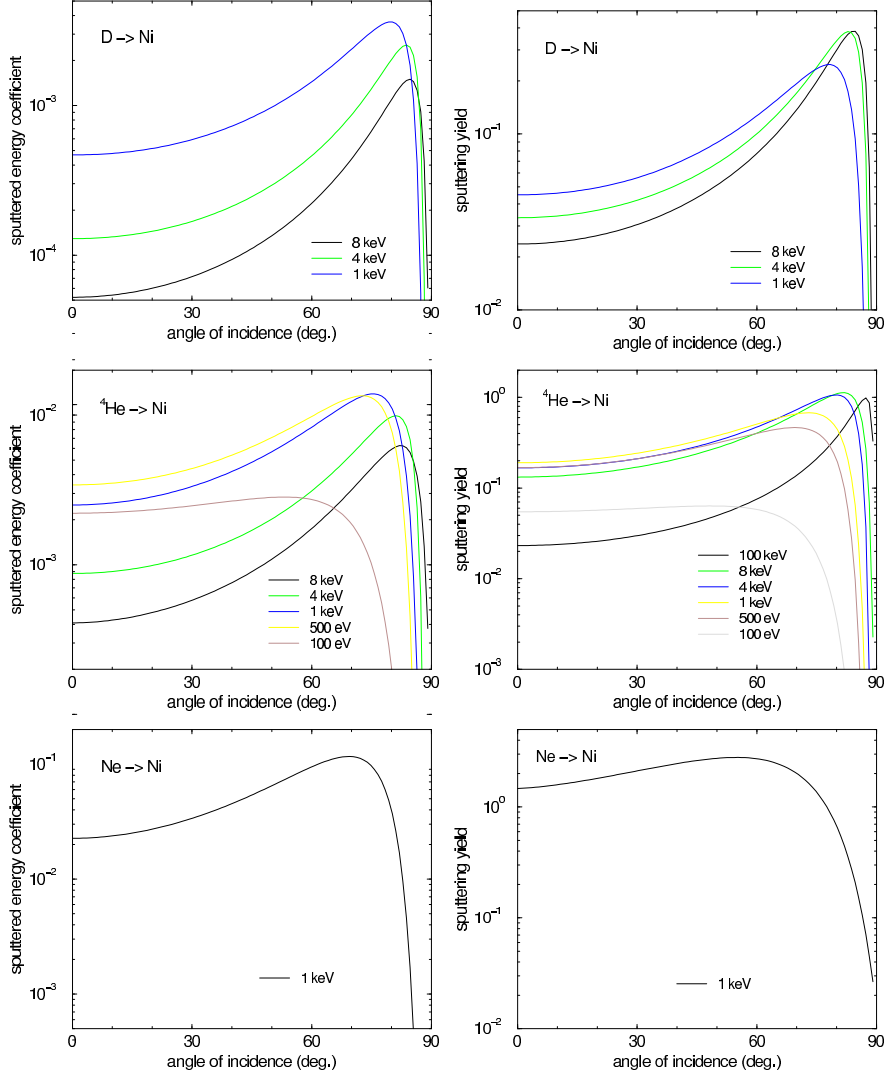


Figure 24: Sputtered energy coefficient and sputtering yield versus the angle of incidence for the bombardment of Ni with D,  $^4\text{He}$ , Ne at different incident energies. Lines are fits to calculated values (parameters see table 17 and [1]).

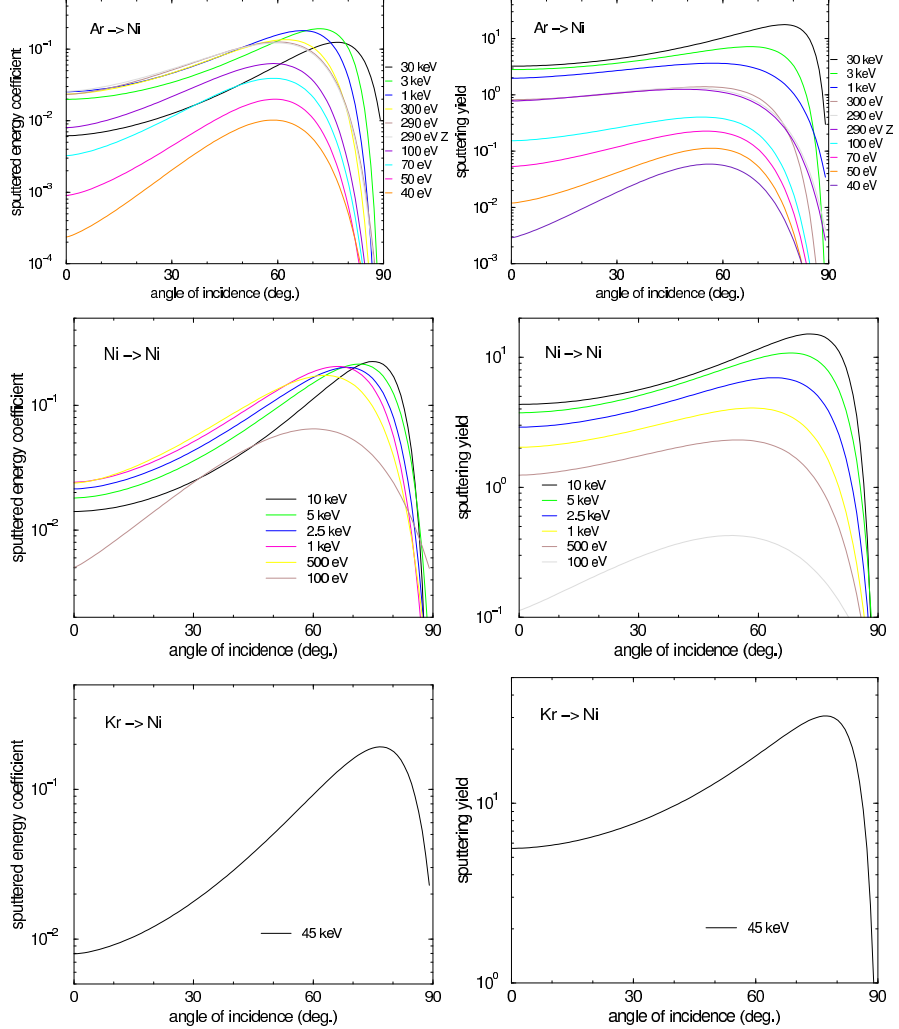


Figure 25: Sputtered energy coefficient and sputtering yield versus the angle of incidence for the bombardment of Ni with Ar, Ni, Kr at different incident energies. Lines are fits to calculated values (parameters see table 17 and [1]).

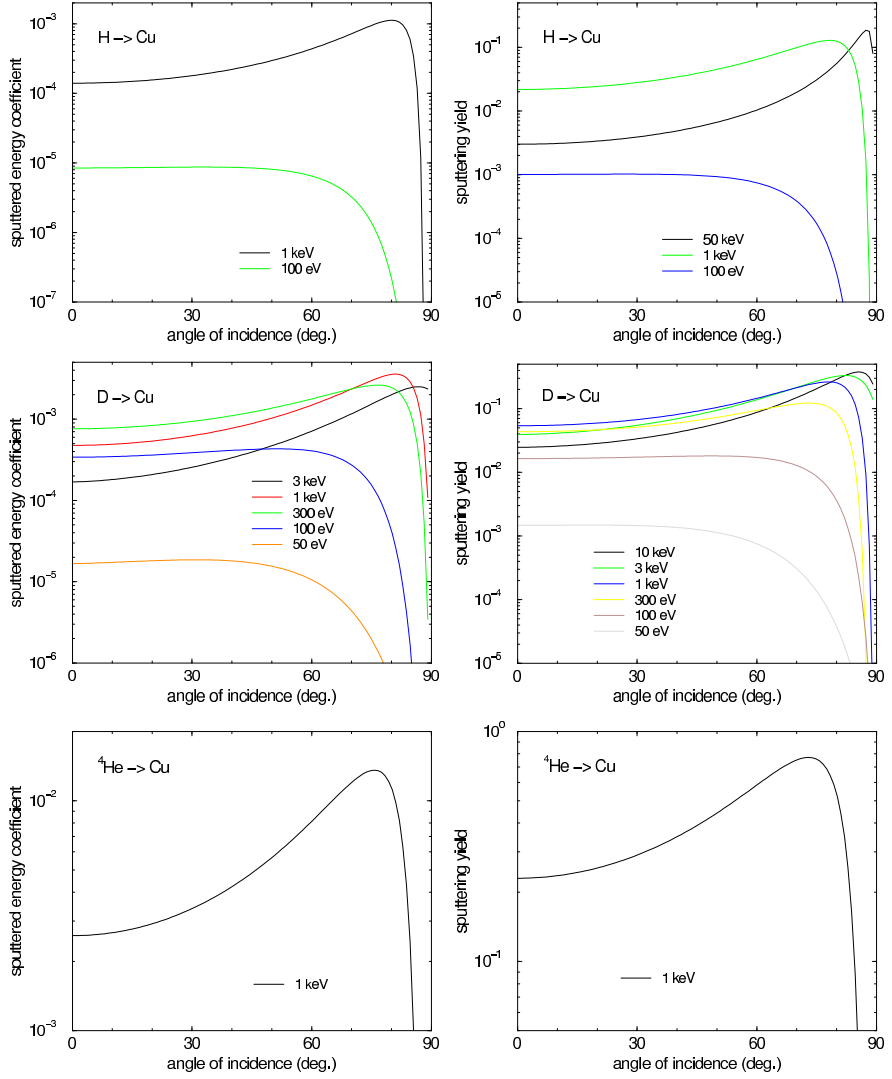


Figure 26: Sputtered energy coefficient and sputtering yield versus the angle of incidence for the bombardment of Cu with H, D,  ${}^4He$  at different incident energies. Lines are fits to calculated values (parameters see table 18 and [1]).

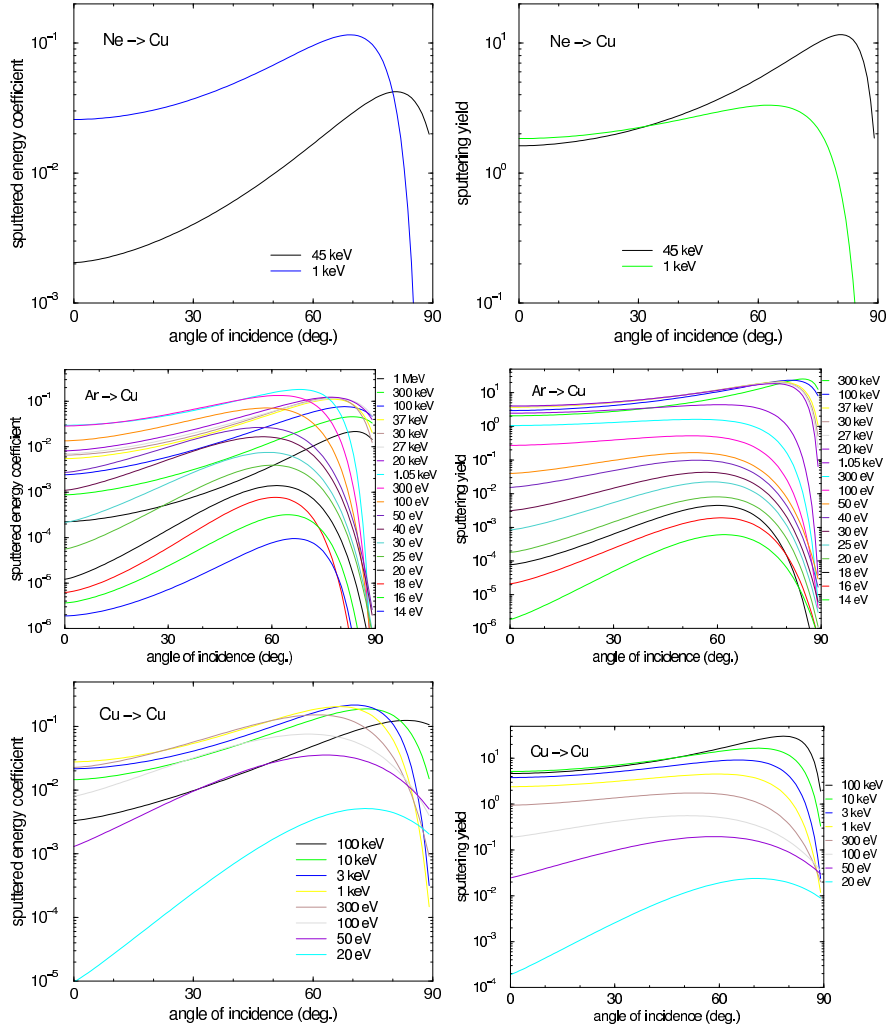


Figure 27: Sputtered energy coefficient and sputtering yield versus the angle of incidence for the bombardment of Cu with Ne, Ar, Cu at different incident energies. Lines are fits to calculated values (parameters see table 18 and [1]).

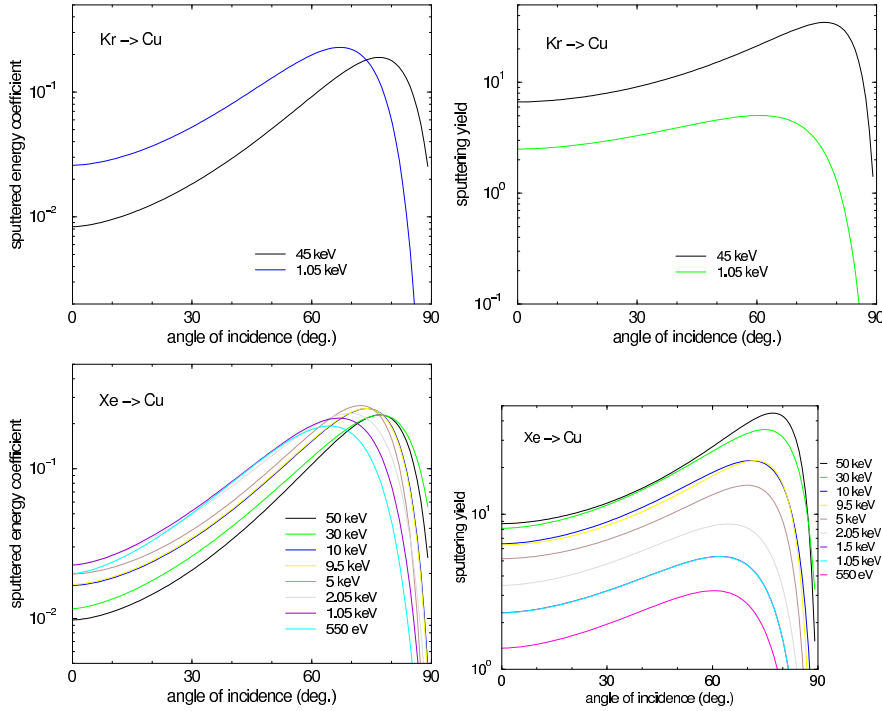


Figure 28: Sputtered energy coefficient and sputtering yield versus the angle of incidence for the bombardment of Cu with Kr, Xe at different incident energies. Lines are fits to calculated values (parameters see table 18 and [1]).

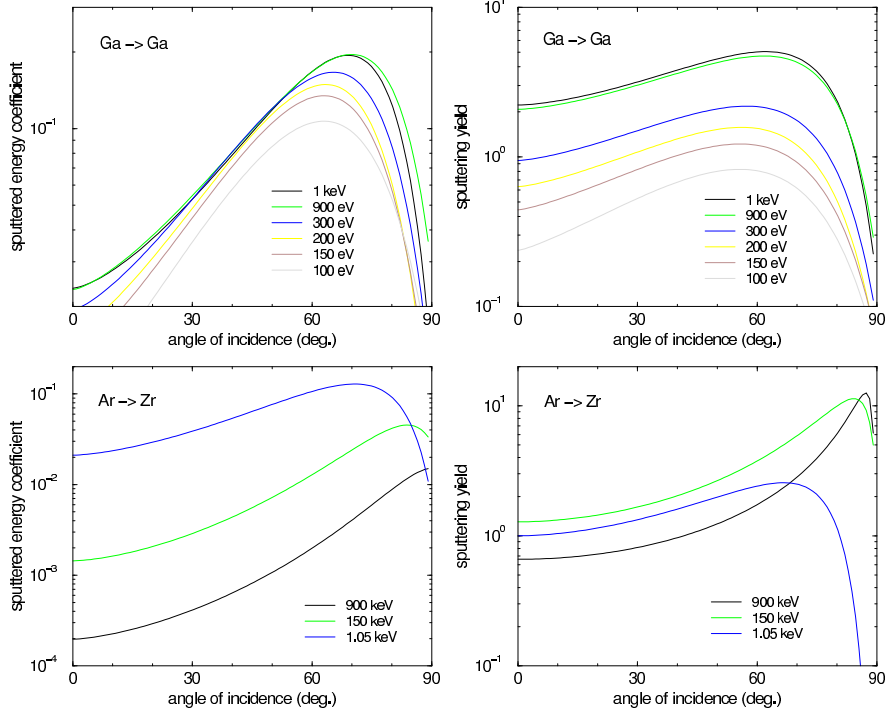


Figure 29: Sputtered energy coefficient and sputtering yield versus the angle of incidence for the bombardment of Ga with Ga, and of Zr with Ar at different incident energies. Lines are fits to calculated values (parameters see table 19 and [1]).

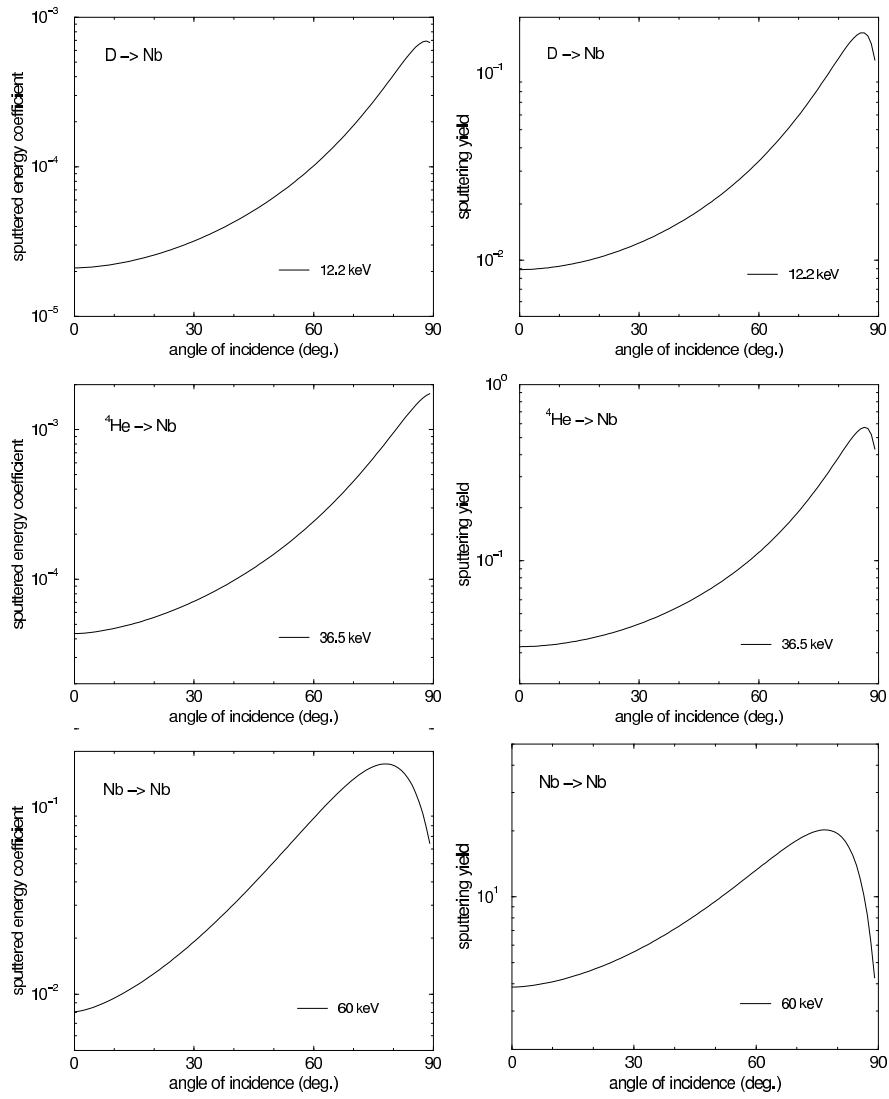


Figure 30: Sputtered energy coefficient and sputtering yield versus the angle of incidence for the bombardment of Nb with D,  ${}^4He$ , Nb at different incident energies. Lines are fits to calculated values (parameters see table 19 and [1]).

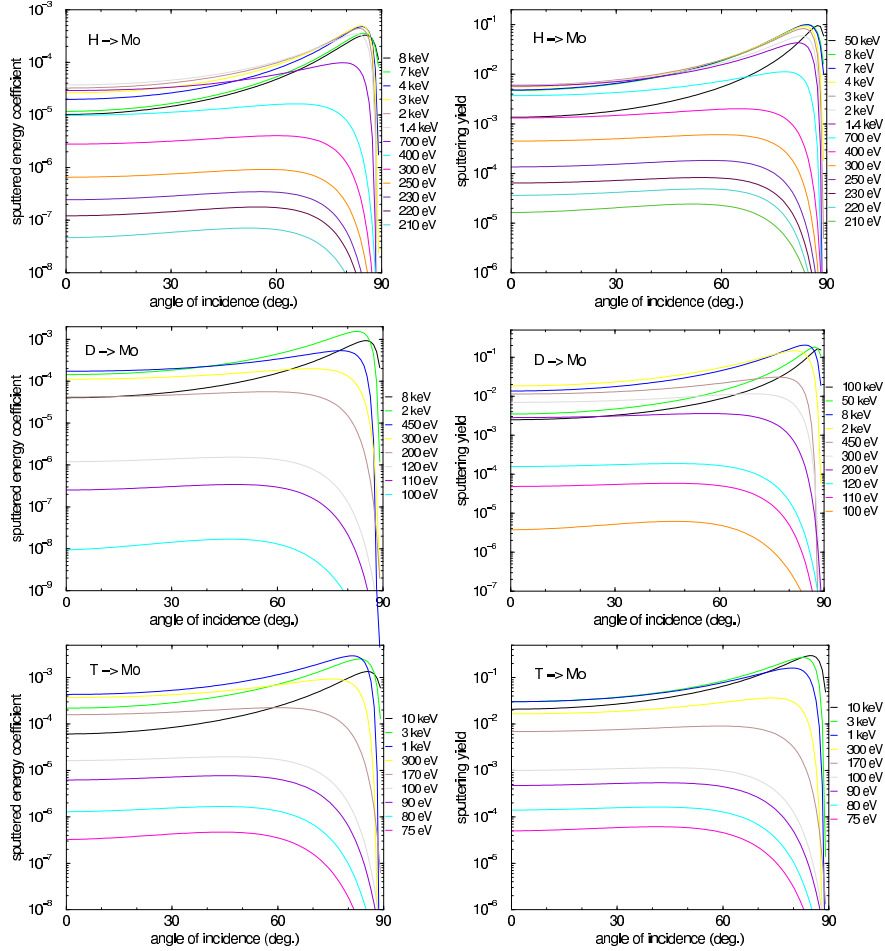


Figure 31: Sputtered energy coefficient and sputtering yield versus the angle of incidence for the bombardment of Mo with H, D, T at different incident energies. Lines are fits to calculated values (parameters see tables 19, 20 and [1]).

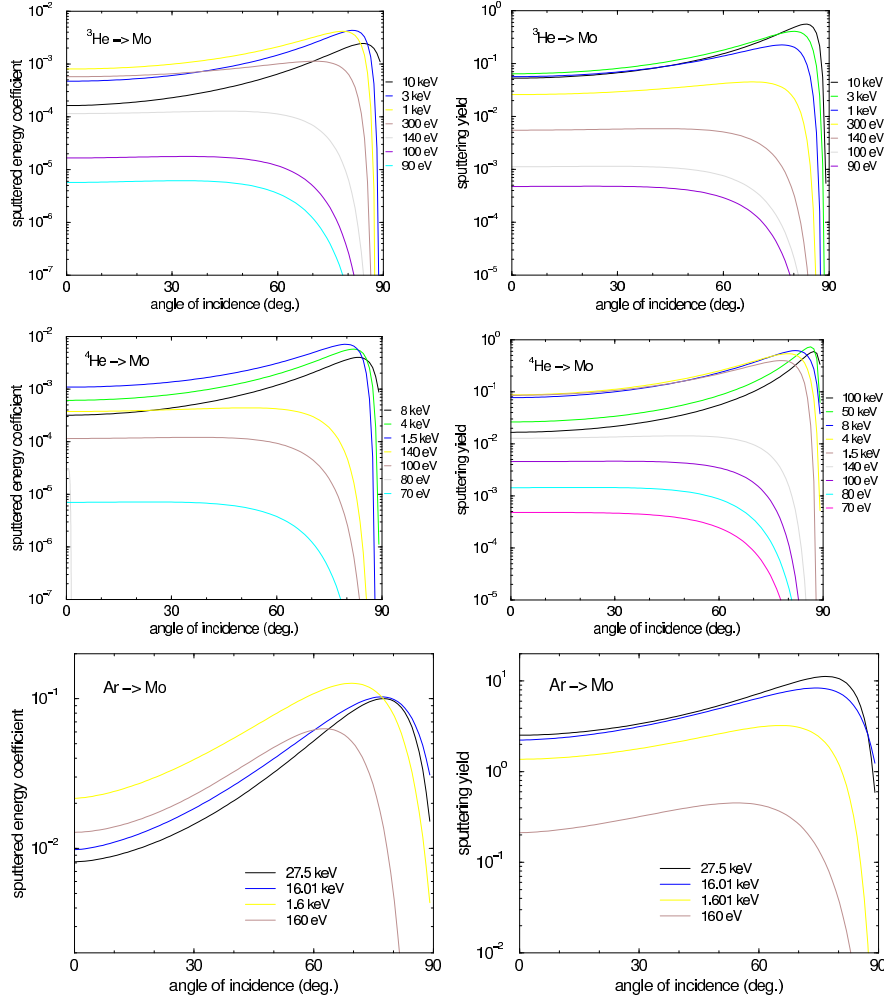


Figure 32: Sputtered energy coefficient and sputtering yield versus the angle of incidence for the bombardment of Mo with  ${}^3\text{He}$ ,  ${}^4\text{He}$ , Ar at different incident energies. Lines are fits to calculated values (parameters see table 20 and [1]).

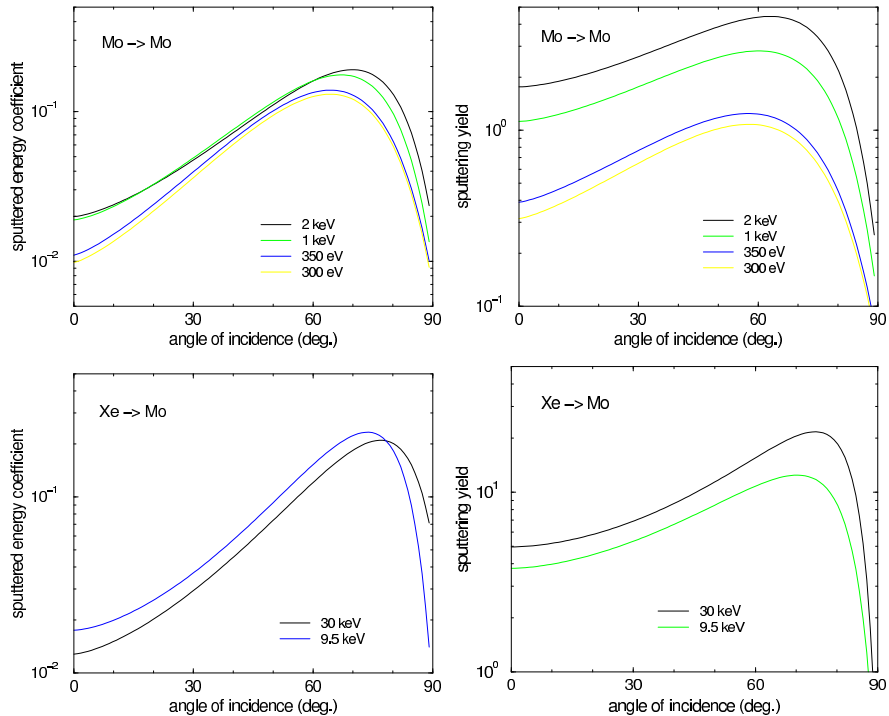


Figure 33: Sputtered energy coefficient and sputtering yield versus the angle of incidence for the bombardment of Mo with Mo, Xe at different incident energies. Lines are fits to calculated values (parameters see table 20 and [1]).

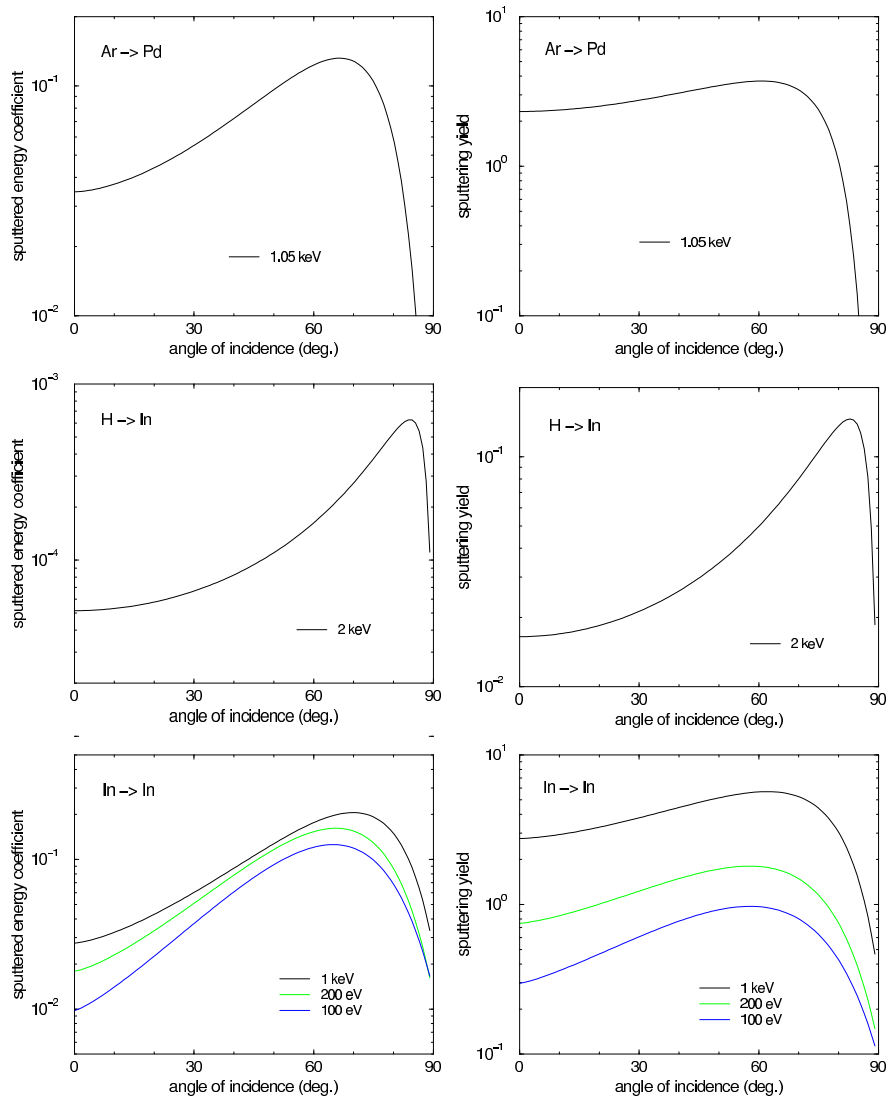


Figure 34: Sputtered energy coefficient and sputtering yield versus the angle of incidence for the bombardment of Pd with Ar, and of In with H and In at different incident energies. Lines are fits to calculated values (parameters see table 21 and [1]).

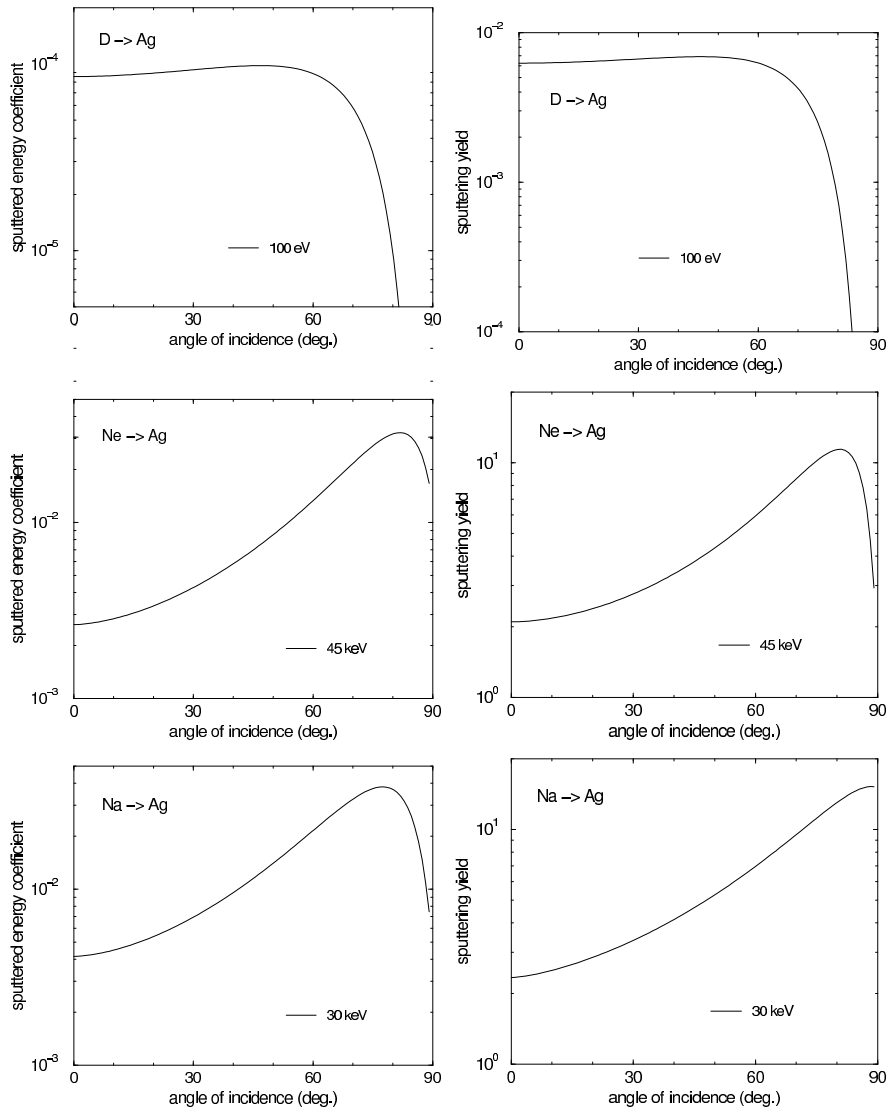


Figure 35: Sputtered energy coefficient and sputtering yield versus the angle of incidence for the bombardment of Ag with D, Ne, Na at different incident energies. Lines are fits to calculated values (parameters see table 21 and [1]).

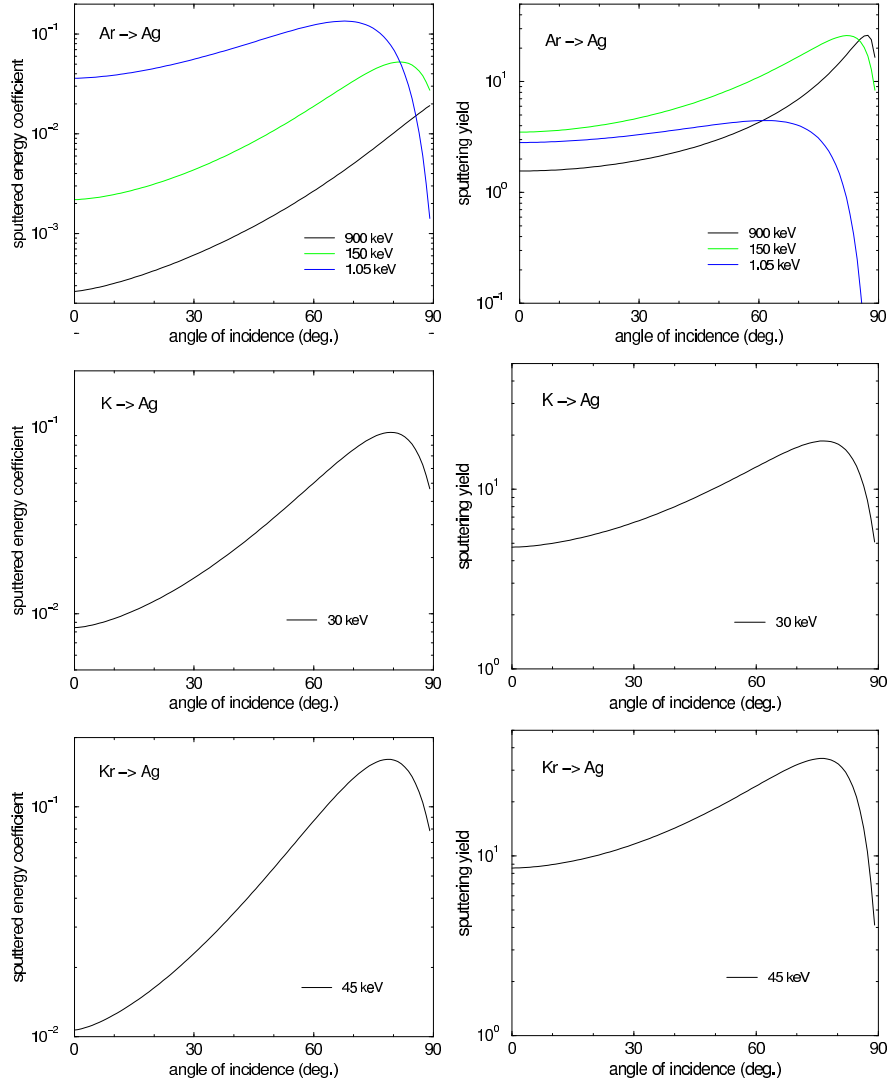


Figure 36: Sputtered energy coefficient and sputtering yield versus the angle of incidence for the bombardment of Ag with Ar, K, Kr at different incident energies. Lines are fits to calculated values (parameters see table 21 and [1]).

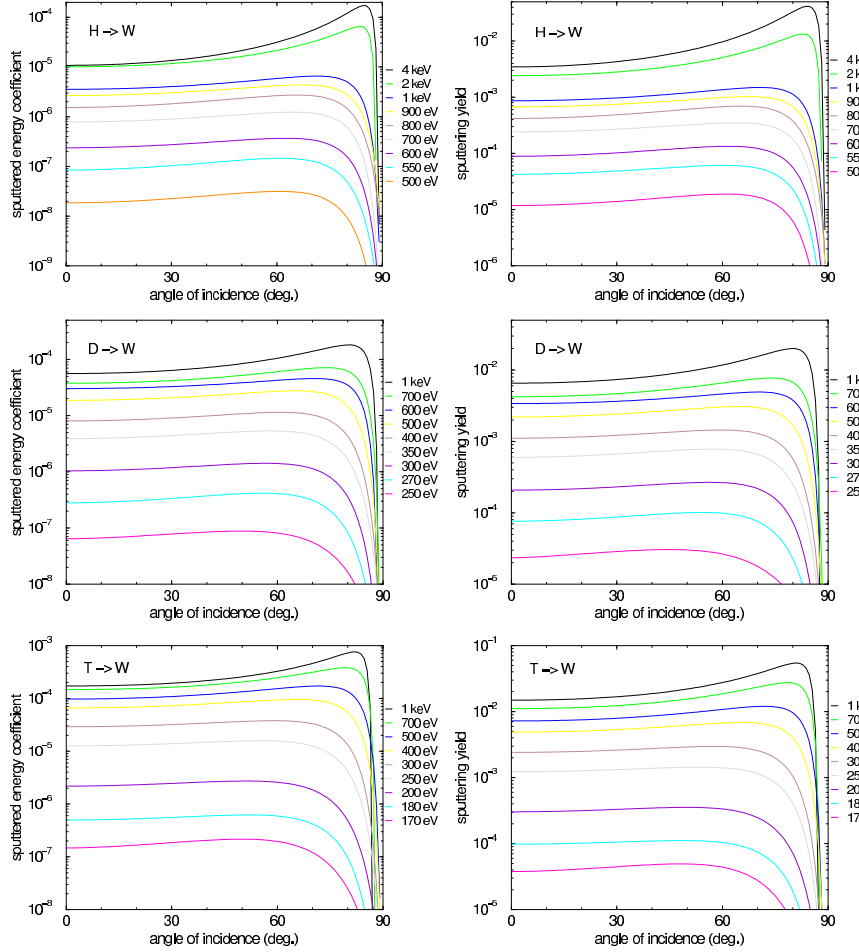


Figure 37: Sputtered energy coefficient and sputtering yield versus the angle of incidence for the bombardment of W with H, D, T at different incident energies. Lines are fits to calculated values (parameters see table 21 and [1]).

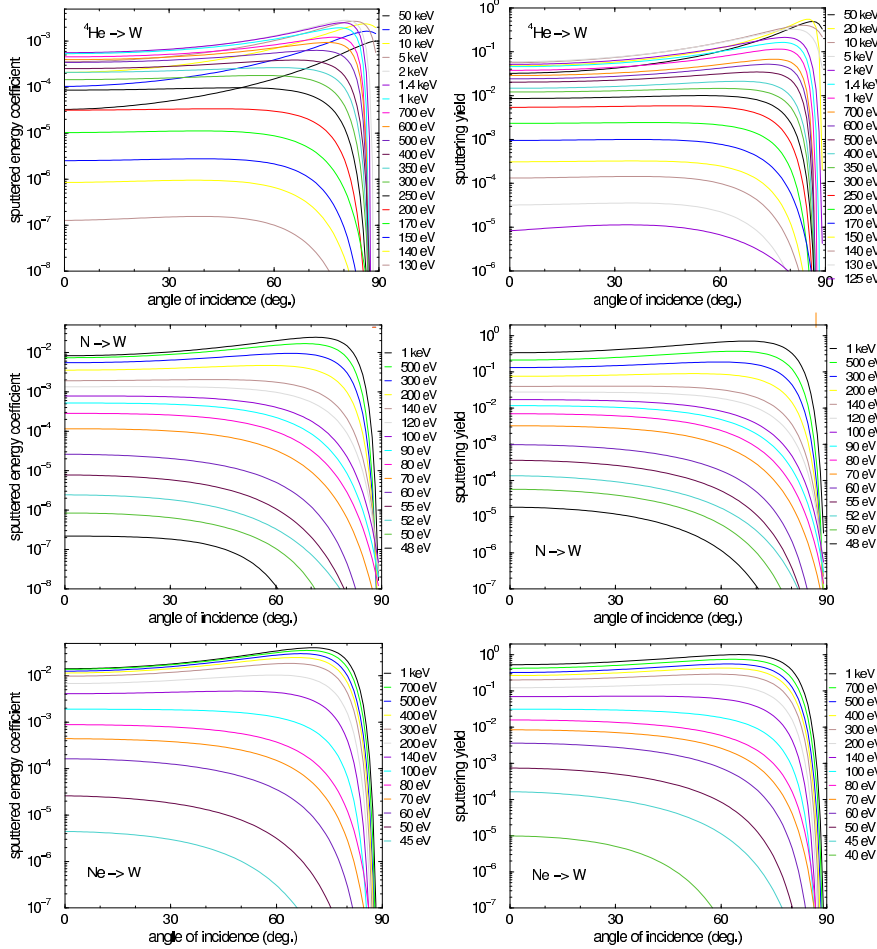


Figure 38: Sputtered energy coefficient and sputtering yield versus the angle of incidence for the bombardment of W with  ${}^4\text{He}$ , N, Ne at different incident energies. Lines are fits to calculated values (parameters see table 22 and [1]).

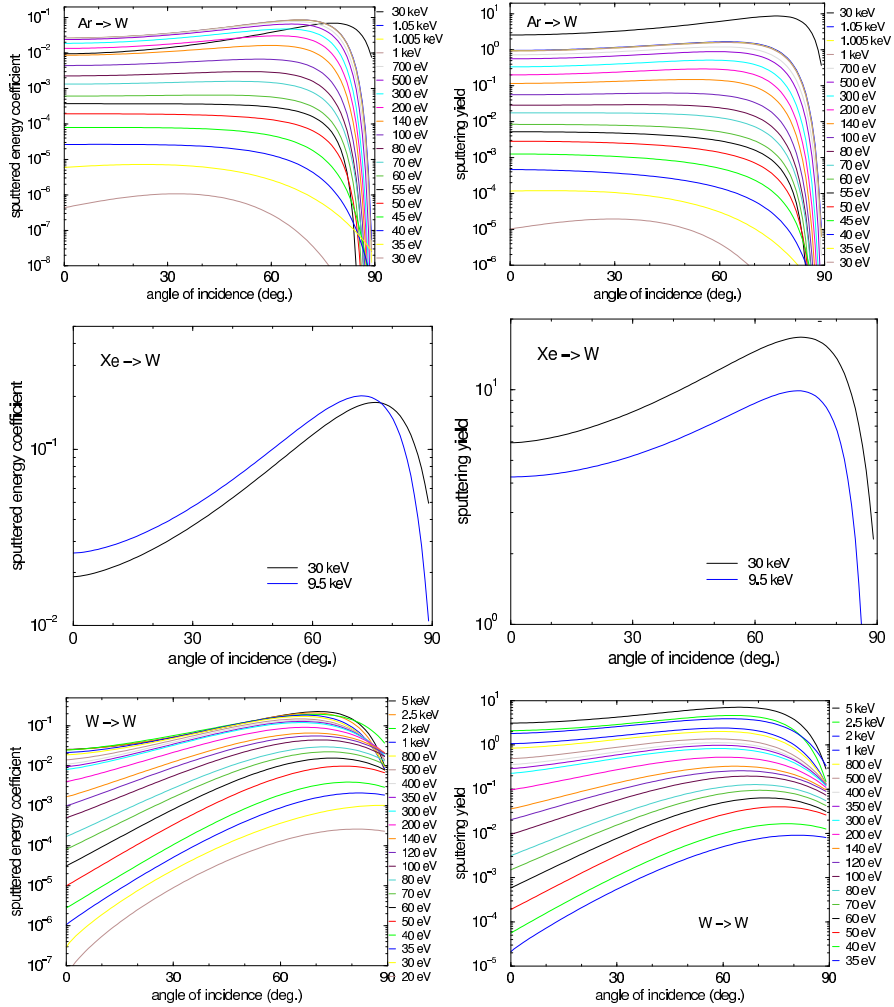


Figure 39: Sputtered energy coefficient and sputtering yield versus the angle of incidence for the bombardment of W with Ar, Xe, W at different incident energies. Lines are fits to calculated values (parameters see table 23 and [1]).

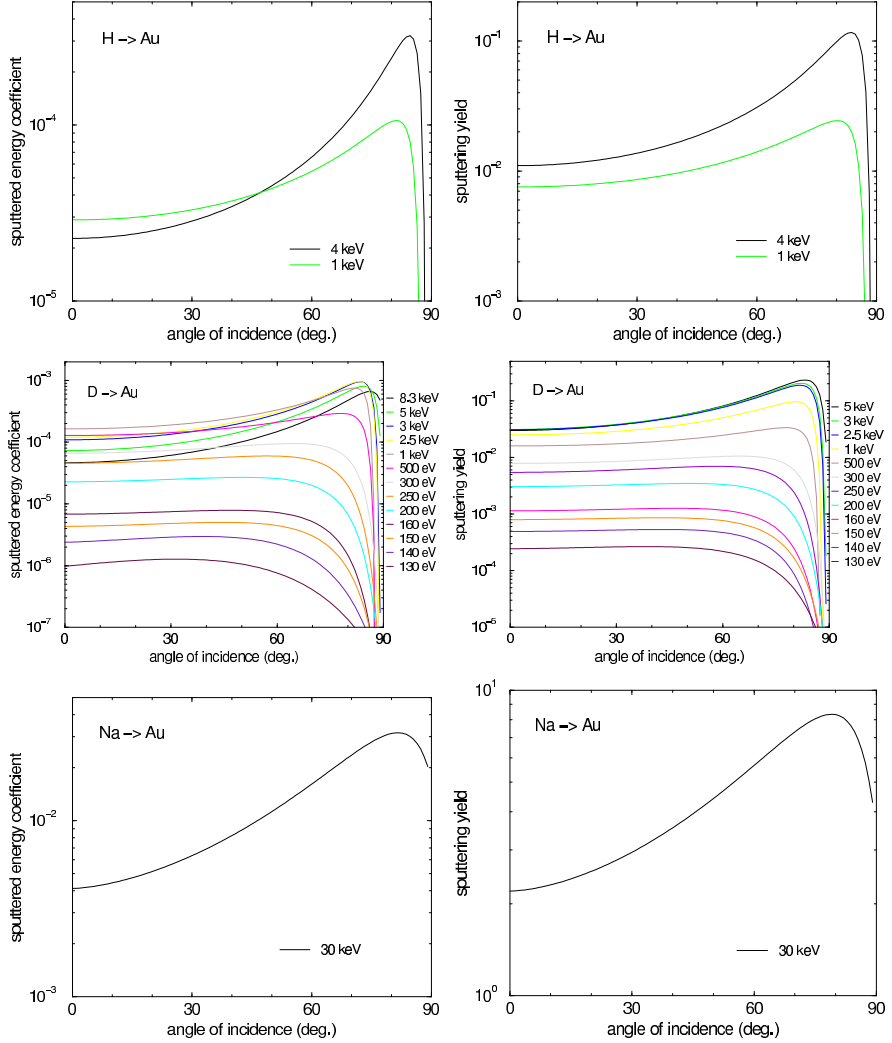


Figure 40: Sputtered energy coefficient and sputtering yield versus the angle of incidence for the bombardment of Au with H, D, Na at different incident energies. Lines are fits to calculated values (parameters see table 24 and [1]).

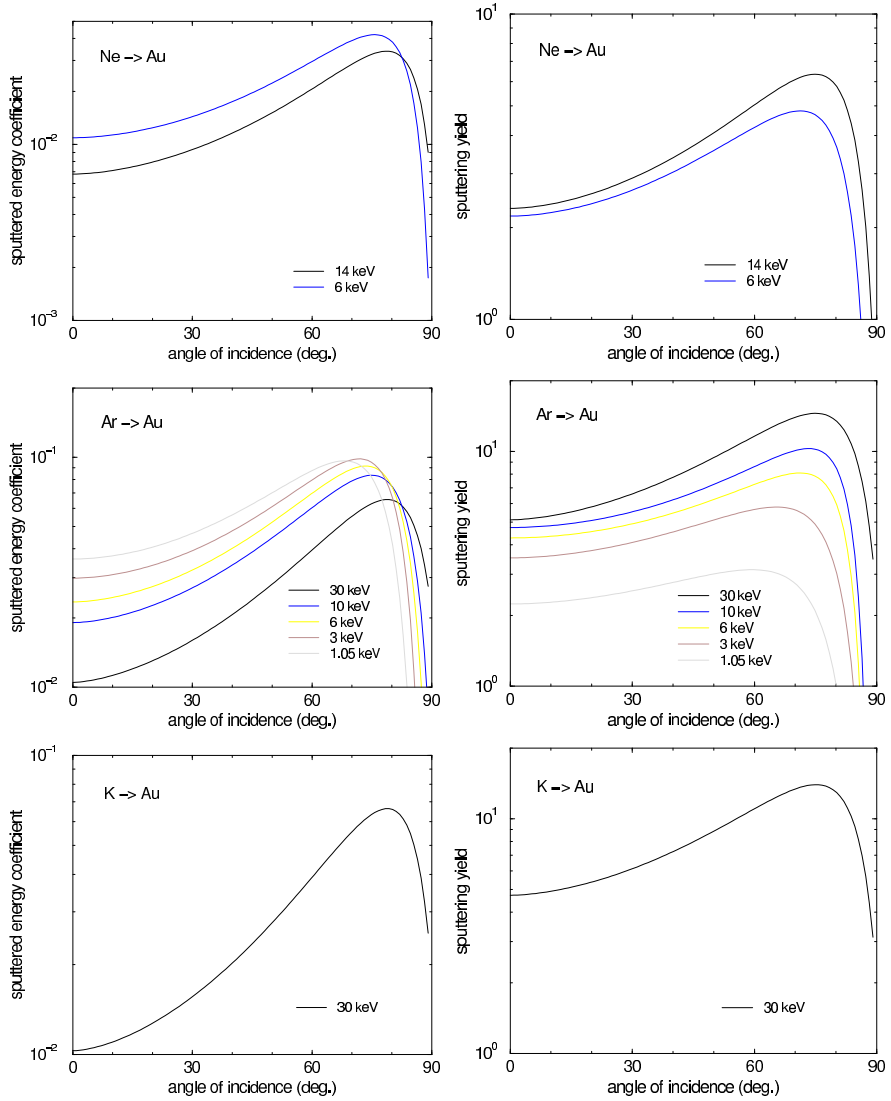


Figure 41: Sputtered energy coefficient and sputtering yield versus the angle of incidence for the bombardment of Au with Ne, Ar, K at different incident energies. Lines are fits to calculated values (parameters see table 24 and [1]).

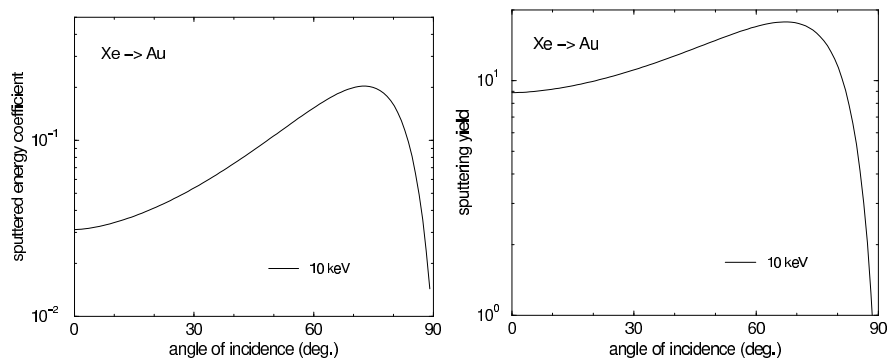


Figure 42: Sputtered energy coefficient and sputtering yield versus the angle of incidence for the bombardment of Au with Xe at different incident energies. Lines are fits to calculated values (parameters see table 24 and [1]).

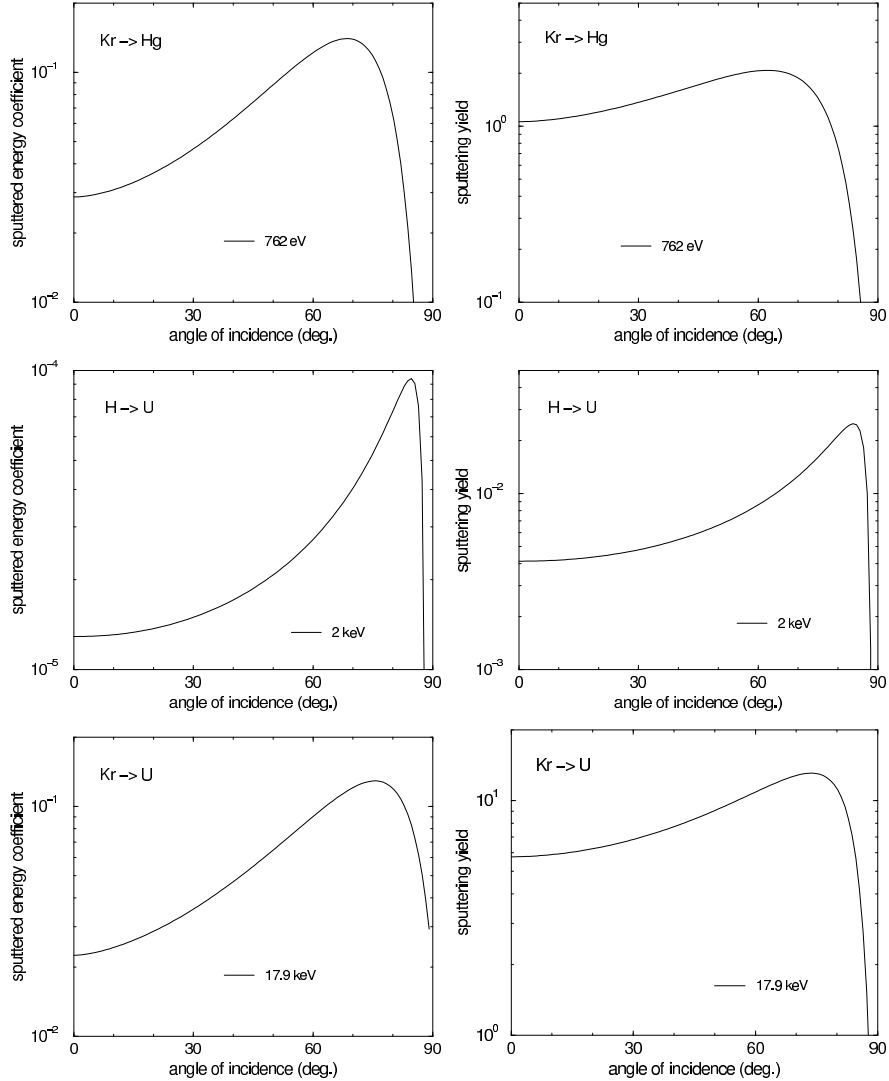


Figure 43: Sputtered energy coefficient and sputtering yield versus the angle of incidence for the bombardment of Hg with Kr and of U with H and Kr at different incident energies. Lines are fits to calculated values (parameters see table 24 and [1]).

## References

- [1] R. Behrisch, W.Eckstein, eds., *Sputtering*, (Springer, Berlin Heidelberg New York 2007)
- [2] W. Eckstein, IPP Report 17/12, Garching (2009)
- [3] W. Eckstein, IPP Report 17/20, Garching (2010)
- [4] W. Eckstein, *Computer Simulation of Ion-Solid Interactions*, Springer Series in Material Science, Vol.10, (Springer, Berlin Heidelberg New York 1991)
- [5] J.P. Biersack, W. Eckstein, Appl. Phys. 34 (1984) 73
- [6] W. Eckstein, R. Dohmen, A. Mutzke, R. Schneider, Report IPP 12/3, Garching 2007
- [7] A. Mutzke, R. Schneider, W. Eckstein, R. Dohmen, Report IPP 12/8, Garching 2011
- [8] W.D.Wilson, L.G.Haggmark, J.P. Biersack, Phys. Rev. B 15 (1977) 2458
- [9] J.F. Ziegler, J.P. Biersack, U. Littmark, The Stopping and Range of Ions in Solids, The Stopping and Range of Ions in Matter, Vol. 1, ed. by J.F. Ziegler (Pergamon, New York 1985)
- [10] G. Molière, Z. Naturf. A2 (1947) 133
- [11] W. Eckstein, S. Hackel, D. Heinemann, B. Fricke, Z. Phys. D 24 (1992) 171
- [12] O.S. Oen, M.T. Robinson, Nucl. Instrum. Meth. 132 (1976) 647
- [13] E. Fermi, E. Teller, Phys. Rev. 72 (1947) 399
- [14] J. Lindhard, M. Scharff, Phys. Rev. 124 (1961) 128
- [15] J.F. Ziegler, In Helium Stopping Powers and Ranges in All Elements, The Stopping and Range of Ions in Matter, Vol. 4, ed. by J.F. Ziegler (Pergamon, New York 1977)
- [16] H.H. Andersen, J.F. Ziegler, In Hydrogen Stopping Powers and Ranges in All Elements, The Stopping and Range of Ions in Matter, Vol. 3, ed. by J.F. Ziegler (Pergamon, New York 1985)
- [17] W. Eckstein, IPP Report 9/117, Garching (1998)
- [18] W. Eckstein, IPP Report 9/132, Garching (2002)
- [19] W. Eckstein, calculated values can be retrieved via ftp:  
<ftp://rzg.mpg.de/ftp/pub/ipp/eckstein/rep05>

- [20] W. Möller, W. Eckstein, J.P. Biersack, Comp. Phys. Commun. 51 (1988) 355
- [21] W. Eckstein, R. Preuss, J. Nucl. Mater. 320 (2003) 209
- [22] Y. Yamamura, Y. Itikawa, N. Itoh, IPPJ-AM-26, Nagoya (1993)

Table 1: Fitting parameters  $\lambda, q, \mu, E_{th}, \nu$ , for the energy dependence of the sputtered energy coefficient,  $Y_E$ , at normal incidence for different ions and targets. The lower limit is close to the threshold, the upper limit is in most cases 20 keV for the low mass ions and 200 keV for heavy ions.

ion	solid	$\lambda$	q	$\mu$	$E_{th}$	$\nu$	$\varepsilon_L$	$E_{sb}$
H	Li	6.136e+0	1.592e-3	2.361	5.407	1.117	1.85375e+2	1.67
D	Li	9.800e+0	2.510e-3	2.338	4.005	1.071	2.08692e+2	1.67
T	Li	1.916e+1	2.333e-3	2.659	3.455	1.002	2.32243e+2	1.67
<sup>4</sup> He	Li	9.362e+0	4.170e-3	2.055	5.866	1.066	5.56715e+2	1.67
Li	Li	4.947e+1	2.765e-3	1.847	6.803	1.355	1.12841e+3	1.67
H	Be	3.832e+0	1.165e-3	2.437	13.830	1.099	2.56510e+2	3.38
D	Be	7.991e+0	2.204e-3	2.946	9.090	1.072	2.82110e+2	3.38
T	Be	7.701e+0	2.512e-3	2.446	8.781	1.043	3.07966e+2	3.38
<sup>3</sup> He	Be	6.259e+0	4.154e-3	2.738	11.033	1.130	6.65344e+2	3.38
<sup>4</sup> He	Be	6.649e+0	4.206e-3	3.134	10.587	1.044	7.19545e+2	3.38
Be	Be	5.918e+1	3.100e-3	2.294	13.866	1.424	2.20796e+3	3.38
N	Be	8.341e+1	3.500e-3	2.665	17.642	1.362	5.46566e+3	3.38
O	Be	5.586e+1	3.800e-3	2.330	20.675	1.404	6.97104e+3	3.38
Ne	Be	1.824e+2	3.600e-3	3.172	17.726	1.302	1.06588e+4	3.38
Ar	Be	9.046e+1	3.400e-3	2.651	27.824	1.157	2.68450e+4	3.38
Kr	Be	2.797e+1	2.100e-3	2.070	62.004	1.488	1.67028e+5	3.38
Xe	Be	6.581e+1	1.500e-3	2.644	74.503	1.493	4.23834e+5	3.38
H	B	3.220e+0	6.000e-4	2.342	27.495	1.090	3.32864e+2	5.73
D	B	4.635e+0	1.500e-3	2.361	18.764	1.083	3.61025e+2	5.73
T	B	6.789e+0	1.800e-3	2.533	15.878	1.039	3.89468e+2	5.73
<sup>3</sup> He	B	1.118e+1	3.200e-3	2.843	17.366	1.111	8.35205e+2	5.73
<sup>4</sup> He	B	1.411e+1	3.300e-3	2.820	16.683	1.082	8.94388e+2	5.73
B	B	3.685e+1	3.000e-3	1.920	25.979	1.407	3.71634e+3	5.73
O	B	8.972e+1	6.800e-3	2.817	29.621	0.9664	8.02325e+3	5.73
Ne	B	6.744e+1	3.600e-3	2.480	34.389	1.362	1.21179e+4	5.73
H	C	4.809e+0	5.000e-4	2.056	38.296	1.111	4.14659e+2	7.41
D	C	7.327e+0	1.200e-3	2.299	24.545	1.079	4.46507e+2	7.41
T	C	8.409e+0	1.500e-3	2.257	21.003	1.061	4.78673e+2	7.41
<sup>3</sup> He	C	5.228e+0	2.600e-3	2.349	24.704	1.127	1.02061e+3	7.41
<sup>4</sup> He	C	3.640e+1	2.600e-3	3.359	16.709	1.046	1.08716e+3	7.41
C	C	3.509e+2	5.800e-3	2.517	20.726	1.013	5.68684e+3	7.41
N	C	5.291e+1	2.800e-3	2.219	38.405	1.367	7.37899e+3	7.41
O	C	3.836e+2	2.800e-3	3.133	29.512	1.317	9.29758e+3	7.41
Ne	C	1.107e+2	6.000e-3	2.648	38.414	0.8901	1.39308e+4	7.41
Ar	C	5.913e+1	3.300e-3	2.487	55.004	1.299	4.57989e+4	7.41
Kr	C	1.094e+2	2.200e-3	2.837	80.929	1.404	1.99609e+5	7.41
Xe	C	4.437e+1	1.700e-3	2.231	135.377	1.460	4.98349e+5	7.41
Mg	Mg	1.574e+1	3.900e-3	1.903	9.027	1.666	2.86599e+4	1.54
Ar	Mg	3.611e+1	3.100e-3	2.261	10.280	1.694	6.10685e+4	1.54
Kr	Mg	5.602e+1	1.800e-3	2.426	12.902	1.810	2.37254e+5	1.54

Table 2: Fitting parameters  $\lambda, q, \mu, E_{th}, \nu$ , for the energy dependence of the sputtered energy coefficient,  $Y_E$ , at normal incidence for different ions and targets. The lower limit is close to the threshold, the upper limit is in most cases 20 keV for the low mass ions and 200 keV for heavy ions.

ion	solid	$\lambda$	q	$\mu$	$E_{th}$	$\nu$	$\varepsilon_L$	$E_{sb}$
H	Al	6.154e+0	3.000e-4	2.520	29.061	1.236	1.05916e+3	3.36
D	Al	4.136e+0	1.100e-3	2.084	18.086	1.236	1.09700e+3	3.36
T	Al	4.981e+0	1.700e-3	2.170	13.614	1.247	1.13522e+3	3.36
<sup>3</sup> He	Al	5.472e+0	2.200e-3	2.758	14.185	1.280	1.37037e+3	3.36
<sup>4</sup> He	Al	4.085e+0	3.000e-3	2.384	12.875	1.260	2.44780e+3	3.36
N	Al	2.005e+1	3.600e-3	2.280	13.132	1.647	1.28804e+4	3.36
Ne	Al	2.525e+1	3.900e-3	2.403	16.144	1.601	2.22732e+4	3.36
Al	Al	4.345e+1	3.300e-3	2.142	16.009	1.658	3.45451e+4	3.36
Ar	Al	5.137e+1	3.900e-3	2.540	20.441	1.595	6.28194e+4	3.36
Kr	Al	4.492e+1	2.900e-3	2.489	26.580	1.622	2.39411e+5	3.36
Xe	Al	4.177e+1	2.400e-3	2.515	34.600	1.649	5.63459e+5	3.36
H	Si	5.208e+0	2.000e-4	2.104	45.013	1.222	1.16317e+3	4.70
D	Si	5.508e+0	7.000e-4	2.737	24.028	1.194	1.20314e+3	4.70
T	Si	5.110e+0	1.300e-3	2.122	19.859	1.226	1.24352e+3	4.70
<sup>3</sup> He	Si	5.497e+0	1.700e-3	2.431	20.654	1.261	2.59209e+3	4.70
<sup>4</sup> He	Si	4.363e+0	2.400e-3	2.459	17.853	1.223	2.67374e+3	4.70
N	Si	2.869e+1	3.200e-3	2.263	16.301	1.620	1.38909e+4	4.70
Ne	Si	2.357e+1	3.500e-3	2.017	21.902	1.591	2.39034e+4	4.70
Si	Si	5.598e+1	3.700e-3	2.247	18.844	1.568	4.10661e+4	4.70
Ar	Si	3.529e+1	3.600e-3	2.173	29.225	1.528	6.67979e+4	4.70
Kr	Si	3.892e+1	3.100e-3	2.261	37.005	1.577	2.52242e+5	4.70
Xe	Si	2.917e+2	2.500e-3	3.059	32.791	1.565	5.91044e+5	4.70
Ca	Ca	6.043e+1	2.000e-3	2.117	8.336	1.847	9.43891e+4	1.83
Sc	Sc	2.552e+1	2.700e-3	1.793	18.845	1.768	1.05770e+5	3.49
H	Ti	5.879e+0	1.000e-4	2.233	72.357	1.253	2.05415e+3	4.89
D	Ti	5.388e+0	4.000e-4	2.374	38.617	1.259	2.09615e+3	4.89
T	Ti	5.140e+0	8.000e-4	2.319	28.237	1.260	2.13856e+3	4.89
<sup>3</sup> He	Ti	5.147e+0	1.000e-3	2.279	30.416	1.324	4.41677e+3	4.89
<sup>4</sup> He	Ti	3.744e+0	1.400e-3	2.864	23.829	1.288	4.50177e+3	4.89
N	Ti	2.206e+1	3.100e-3	2.569	16.207	1.722	2.07557e+4	4.89
Ne	Ti	1.213e+1	3.400e-3	2.077	20.341	1.725	3.39688e+4	4.89
Ar	Ti	3.311e+1	3.200e-3	2.132	24.706	1.728	8.56428e+4	4.89
Ti	Ti	4.164e+1	3.200e-3	2.263	22.931	1.699	1.17898e+5	4.89
Kr	Ti	5.064e+1	2.900e-3	2.549	30.823	1.705	2.89844e+5	4.89
Xe	Ti	4.377e+1	2.700e-3	2.441	36.808	1.710	6.42730e+5	4.89
H	V	5.878e+0	1.000e-4	2.421	81.477	1.248	2.17329e+3	5.33
D	V	4.912e+0	4.000e-4	2.141	45.858	1.265	2.21513e+3	5.33
T	V	4.851e+0	8.000e-4	2.192	32.871	1.264	2.25738e+3	5.33
<sup>3</sup> He	V	5.466e+0	1.000e-3	2.629	33.594	1.320	4.65839e+3	5.33
<sup>4</sup> He	V	4.945e+0	1.500e-3	2.367	28.355	1.328	4.74299e+3	5.33
N	V	2.645e+1	3.200e-3	2.775	17.998	1.734	2.16246e+4	5.33
Ne	V	1.629e+1	3.500e-3	2.383	22.051	1.754	3.52128e+4	5.33
Ar	V	6.467e+1	3.600e-3	3.165	23.515	1.672	8.78018e+4	5.33
V	V	3.895e+1	1.470e-2	2.048	25.385	1.254	1.30783e+5	5.33
Kr	V	5.888e+1	3.100e-3	2.753	32.409	1.705	2.93342e+5	5.33
Xe	V	4.948e+1	2.400e-3	2.470	39.457	1.770	6.45981e+5	5.33

Table 3: Fitting parameters  $\lambda, q, \mu, E_{th}, \nu$ , for the energy dependence of the sputtered energy coefficient,  $Y_E$ , at normal incidence for different ions and targets. The lower limit is close to the threshold, the upper limit is in most cases 20 keV for the low mass ions and 200 keV for heavy ions.

ion	solid	$\lambda$	q	$\mu$	$E_{th}$	$\nu$	$\varepsilon_L$	$E_{sb}$
H	Cr	5.421e+0	2.000e-4	2.546	63.391	1.267	2.29573e+3	4.12
D	Cr	5.698e+0	5.000e-4	2.331	35.097	1.305	2.33904e+3	4.12
T	Cr	4.986e+0	1.000e-3	2.299	25.391	1.300	2.38278e+3	4.12
$^3\text{He}$	Cr	5.129e+0	1.200e-3	2.244	27.907	1.369	4.91344e+3	4.12
$^4\text{He}$	Cr	5.707e+0	1.600e-3	3.022	21.211	1.339	5.00096e+3	4.12
Ne	Cr	2.123e+1	4.000e-3	2.626	18.289	1.785	3.68638e+4	4.12
Ar	Cr	3.598e+1	3.700e-3	2.712	22.031	1.779	9.15022e+4	4.12
Cr	Cr	5.111e+1	3.500e-3	2.581	20.537	1.769	1.44437e+5	4.12
Kr	Cr	6.369e+1	2.900e-3	2.766	25.541	1.788	3.04062e+5	4.12
Xe	Cr	6.705e+1	2.500e-3	2.800	28.827	1.809	6.67613e+5	4.12
H	Mn	5.462e+0	2.000e-4	2.387	48.096	1.311	2.41819e+3	2.92
D	Mn	5.231e+0	6.000e-4	2.401	25.653	1.317	2.46141e+3	2.92
T	Mn	5.756e+0	1.100e-3	2.303	18.537	1.338	2.50506e+3	2.92
$^3\text{He}$	Mn	5.763e+0	1.200e-3	2.870	19.439	1.377	5.16191e+3	2.92
$^4\text{He}$	Mn	6.242e+0	1.700e-3	2.668	16.252	1.396	5.24919e+3	2.92
Ar	Mn	3.638e+1	4.000e-3	2.792	15.915	1.802	9.37995e+4	2.92
Kr	Mn	6.898e+1	3.000e-3	2.719	17.618	1.834	3.08095e+5	2.92
Xe	Mn	6.766e+1	2.100e-3	2.660	19.981	1.894	6.72160e+5	2.92
H	Fe	5.164e+0	1.000e-4	2.554	71.462	1.264	2.54382e+3	4.34
D	Fe	5.136e+0	5.000e-4	2.294	39.610	1.304	2.58856e+3	4.34
T	Fe	5.075e+0	9.000e-4	2.347	28.132	1.302	2.67374e+3	4.34
$^3\text{He}$	Fe	4.712e+0	1.100e-3	2.853	29.039	1.334	5.42342e+3	4.34
$^4\text{He}$	Fe	4.642e+0	1.500e-3	2.893	23.698	1.341	5.51371e+3	4.34
N	Fe	2.768e+1	3.300e-3	2.880	16.338	1.796	2.46747e+4	4.34
Ne	Fe	2.581e+1	3.700e-3	2.878	18.482	1.802	3.98491e+4	4.34
Ar	Fe	3.875e+1	3.700e-3	2.828	22.089	1.775	9.75914e+4	4.34
Fe	Fe	6.215e+1	3.400e-3	2.671	20.968	1.783	1.74096e+5	4.34
Kr	Fe	6.023e+1	3.100e-3	2.740	26.523	1.778	3.19107e+5	4.34
Xe	Fe	5.757e+1	2.300e-3	2.622	30.542	1.838	6.94435e+5	4.34
H	Co	5.105e+0	1.000e-4	2.583	76.460	1.258	2.66922e+3	4.43
D	Co	5.599e+0	5.000e-4	2.351	42.016	1.315	2.71375e+3	4.43
T	Co	5.441e+0	8.000e-4	2.340	29.926	1.312	2.75873e+3	4.43
$^3\text{He}$	Co	5.380e+0	1.000e-3	2.358	32.433	1.373	5.67719e+3	4.43
$^4\text{He}$	Co	5.480e+0	1.500e-3	2.613	25.665	1.362	5.76700e+3	4.43
Ne	Co	2.001e+1	3.900e-3	2.643	19.868	1.808	4.11463e+4	4.43
Ar	Co	3.105e+1	3.800e-3	2.673	23.445	1.802	9.98420e+4	4.43
Co	Co	6.266e+1	3.200e-3	2.670	21.955	1.923	1.90123e+5	4.43
Kr	Co	5.747e+1	3.100e-3	2.696	27.169	1.798	3.22806e+5	4.43
Xe	Co	5.800e+1	2.400e-3	2.606	30.448	1.838	6.98061e+5	4.43

Table 4: Fitting parameters  $\lambda, q, \mu, E_{th}, \nu$ , for the energy dependence of the sputtered energy coefficient,  $Y_E$ , at normal incidence for different ions and targets. The lower limit is close to the threshold, the upper limit is in most cases 20 keV for the low mass ions and 200 keV for heavy ions.

ion	solid	$\lambda$	q	$\mu$	$E_{th}$	$\nu$	$\varepsilon_L$	$E_{sb}$
H	Ni	6.007e+0	1.000e-4	2.388	78.040	1.286	2.79866e+3	4.46
D	Ni	5.240e+0	5.000e-4	2.366	42.151	1.314	2.84552e+3	4.46
T	Ni	5.503e+0	9.000e-4	2.337	30.038	1.315	2.89285e+3	4.46
<sup>3</sup> He	Ni	2.548e+0	2.000e-3	1.658	34.509	1.324	5.94964e+3	4.46
<sup>4</sup> He	Ni	5.885e+0	1.600e-3	2.737	24.885	1.349	6.04409e+3	4.46
N	Ni	2.306e+1	3.200e-3	2.538	18.182	1.836	2.67793e+4	4.46
O	Ni	2.304e+1	3.500e-3	2.752	18.122	1.813	3.18555e+4	4.46
Ne	Ni	1.070e+2	3.700e-3	3.526	14.896	1.789	4.30554e+4	4.46
Ar	Ni	3.289e+1	3.900e-3	2.647	23.075	1.794	1.04416e+5	4.46
Ni	Ni	6.410e+1	3.700e-3	2.719	21.190	1.770	2.06960e+5	4.46
Kr	Ni	7.971e+1	3.200e-3	2.949	24.873	1.761	3.37355e+5	4.46
Xe	Ni	2.113e+2	2.700e-3	3.296	24.930	1.789	7.29221e+5	4.46
H	Cu	5.207e+0	1.000e-4	1.970	70.973	1.352	2.92563e+3	3.52
D	Cu	4.506e+0	4.000e-4	2.203	37.024	1.332	2.97095e+3	3.52
T	Cu	5.517e+0	8.000e-4	2.585	24.308	1.321	3.01673e+3	3.52
<sup>3</sup> He	Cu	5.266e+0	1.000e-3	2.225	27.787	1.405	6.20088e+3	3.52
<sup>4</sup> He	Cu	5.263e+0	1.500e-3	2.944	21.017	1.355	6.29218e+3	3.52
N	Cu	3.415e+1	3.100e-3	3.352	14.034	1.807	2.75601e+4	3.52
Ne	Cu	2.656e+1	3.600e-3	2.852	15.451	1.853	4.40689e+4	3.52
Ar	Cu	2.133e+2	4.400e-3	4.240	13.968	1.759	1.05525e+5	3.52
Cu	Cu	9.833e+1	3.000e-3	2.851	15.819	1.848	2.24619e+5	3.52
Kr	Cu	7.062e+1	3.300e-3	2.839	20.256	1.806	3.35590e+5	3.52
Xe	Cu	6.280e+1	3.200e-3	2.714	22.503	1.790	7.18907e+5	3.52
Ar	Zn	5.637e+1	3.700e-3	3.227	6.993	1.897	1.08696e+5	1.35
Zn	Zn	1.356e+2	2.600e-3	2.756	5.993	1.968	2.43109e+5	1.35
Kr	Zn	7.339e+2	2.900e-3	3.643	5.318	1.888	3.43442e+5	1.35
D	Ga	5.379e+0	4.000e-4	2.493	29.574	1.317	3.23166e+3	2.82
T	Ga	7.273e+0	7.000e-4	2.235	21.110	1.333	3.27716e+3	2.82
Ga	Ga	2.148e+1	3.180e-2	2.003	15.410	0.903	2.62439e+5	2.82
H	Ge	5.548e+0	1.000e-4	2.087	85.473	1.290	3.31932e+3	3.88
D	Ge	5.184e+0	3.000e-4	2.228	43.890	1.295	3.36441e+3	3.88
T	Ge	5.285e+0	6.000e-4	2.288	30.468	1.293	3.40997e+3	3.88
<sup>3</sup> He	Ge	5.349e+0	6.000e-4	2.447	31.897	1.378	6.99838e+3	3.88
<sup>4</sup> He	Ge	5.240e+0	1.000e-3	2.345	25.864	1.366	7.08909e+3	3.88
Ne	Ge	2.081e+1	1.540e-2	2.602	13.795	1.278	4.82268e+4	3.88
Ar	Ge	3.103e+1	3.600e-3	2.883	15.212	1.745	1.12992e+5	3.88
Ge	Ge	5.796e+1	3.400e-3	2.504	17.156	1.758	2.82619e+5	3.88
Kr	Ge	3.305e+1	3.100e-3	2.373	23.248	1.772	3.49421e+5	3.88
Xe	Ge	5.927e+1	2.500e-3	2.615	23.960	1.806	7.36368e+5	3.88
Ar	Se	2.670e+1	3.800e-3	2.715	8.791	1.815	1.18037e+5	2.14

Table 5: Fitting parameters  $\lambda, q, \mu, E_{th}, \nu$ , for the energy dependence of the sputtered energy coefficient,  $Y_E$ , at normal incidence for different ions and targets. The lower limit is close to the threshold, the upper limit is in most cases 20 keV for the low mass ions and 200 keV for heavy ions.

ion	solid	$\lambda$	q	$\mu$	$E_{th}$	$\nu$	$\varepsilon_L$	$E_{sb}$
H	Zr	5.599e+0	4.000e-5	2.099	173.501	1.254	4.42211e+3	6.33
D	Zr	4.981e+0	2.000e-4	2.239	88.265	1.256	4.47714e+3	6.33
T	Zr	5.505e+0	3.000e-4	2.131	61.932	1.282	4.52564e+3	6.33
<sup>3</sup> He	Zr	5.900e+0	4.000e-4	2.220	63.577	1.339	9.25829e+3	6.33
<sup>4</sup> He	Zr	6.150e+0	6.000e-4	2.068	51.257	1.356	9.35457e+3	6.33
Ne	Zr	1.671e+1	2.900e-3	2.317	22.828	1.755	6.06862e+4	6.33
Ar	Zr	4.190e+1	3.300e-3	2.674	21.848	1.777	1.37106e+5	6.33
Kr	Zr	3.820e+1	2.500e-3	2.248	33.940	1.819	4.03685e+5	6.33
Zr	Zr	5.480e+1	3.500e-3	2.358	28.056	1.726	4.75691e+5	6.33
Xe	Zr	6.277e+1	3.300e-3	2.635	36.086	1.705	8.25496e+5	6.33
H	Nb	5.667e+0	3.417e-5	2.329	204.032	1.245	4.57351e+3	7.59
D	Nb	6.547e+0	1.000e-4	2.347	105.520	1.284	4.62220e+3	7.59
T	Nb	4.992e+0	3.000e-4	2.556	74.841	1.260	4.67139e+3	7.59
<sup>3</sup> He	Nb	5.486e+0	4.000e-4	2.105	78.922	1.336	9.55327e+3	7.59
<sup>4</sup> He	Nb	4.927e+0	6.000e-4	2.153	62.186	1.326	9.65087e+3	7.59
Ne	Nb	1.765e+1	3.000e-3	2.464	27.506	1.751	6.23657e+4	7.59
Ar	Nb	2.321e+1	3.800e-3	2.596	28.470	1.744	1.40484e+5	7.59
Kr	Nb	2.880e+1	2.900e-3	2.250	41.833	1.792	4.11932e+5	7.59
Nb	Nb	4.866e+1	3.200e-3	2.357	35.038	1.766	5.03904e+5	7.59
Xe	Nb	4.081e+1	2.500e-3	2.330	47.697	1.807	8.40173e+5	7.59
H	Mo	5.758e+0	4.102e-5	2.229	192.824	1.261	4.71832e+3	6.83
D	Mo	4.662e+0	2.000e-4	2.518	96.518	1.253	4.76698e+3	6.83
T	Mo	4.478e+0	3.000e-4	2.444	67.535	1.250	4.81614e+3	6.83
<sup>3</sup> He	Mo	5.196e+0	4.000e-4	2.171	72.550	1.342	9.84614e+3	6.83
<sup>4</sup> He	Mo	5.127e+0	6.000e-4	2.238	56.793	1.353	9.94365e+3	6.83
N	Mo	1.586e+1	2.200e-3	2.434	27.840	1.785	4.10879e+4	6.83
O	Mo	2.915e+1	2.400e-3	3.099	23.703	1.780	4.83320e+4	6.83
Ne	Mo	3.520e+1	2.800e-3	3.218	23.350	1.790	6.38956e+4	6.83
Ar	Mo	2.691e+1	3.500e-3	2.676	26.403	1.809	1.43274e+5	6.83
Kr	Mo	2.247e+1	3.000e-3	1.976	38.198	1.826	4.17411e+5	6.83
Mo	Mo	1.893e+2	4.500e-3	3.293	24.890	1.649	5.33049e+5	6.83
Xe	Mo	4.489e+1	2.800e-3	2.551	41.382	1.798	8.47848e+5	6.83
H	Ru	5.119e+0	4.199e-5	2.411	192.548	1.217	5.01173e+3	6.69
D	Ru	4.994e+0	2.000e-4	2.719	97.283	1.261	5.06083e+3	6.69
T	Ru	4.564e+0	3.000e-4	2.685	68.148	1.279	5.11042e+3	6.69
<sup>3</sup> He	Ru	5.676e+0	4.000e-4	2.213	73.544	1.368	1.04414e+4	6.69
<sup>4</sup> He	Ru	5.240e+0	6.000e-4	2.378	57.307	1.364	1.05397e+4	6.69
Ne	Ru	1.968e+1	2.900e-3	2.712	25.648	1.795	6.70985e+4	6.69
Ar	Ru	2.416e+1	3.800e-3	2.742	26.770	1.797	1.49334e+5	6.69
Kr	Ru	3.583e+1	3.400e-3	2.743	34.984	1.803	4.30460e+5	6.69
Xe	Ru	3.893e+1	3.400e-3	2.491	41.742	1.780	6.68372e+5	6.69

Table 6: Fitting parameters  $\lambda, q, \mu, E_{th}, \nu$ , for the energy dependence of the sputtered energy coefficient,  $Y_E$ , at normal incidence for different ions and targets. The lower limit is close to the threshold, the upper limit is in most cases 20 keV for the low mass ions and 200 keV for heavy ions.

ion	solid	$\lambda$	q	$\mu$	$E_{th}$	$\nu$	$\varepsilon_L$	$E_{sb}$	
H	Rh	5.541e+0	4.547e-5	2.453	168.212	1.253	5.16041e+3	5.78	
	D	5.046e+0	2.000e-4	2.367	88.652	1.295	5.21007e+3	5.78	
	T	5.143e+0	4.000e-4	2.326	61.466	1.312	5.26022e+3	5.78	
	<sup>3</sup> He	5.337e+0	4.000e-4	2.347	63.865	1.374	1.07444e+4	5.78	
	<sup>4</sup> He	5.113e+0	7.000e-4	2.668	49.073	1.357	1.08438e+4	5.78	
	Ne	2.029e+1	2.900e-3	2.676	22.804	1.823	6.87945e+4	5.78	
	Ar	2.087e+1	3.700e-3	2.698	24.272	1.824	1.52692e+5	5.78	
	Kr	2.545e+1	2.900e-3	2.447	32.956	1.877	4.38429e+5	5.78	
	Xe	5.547e+1	2.600e-3	2.715	33.869	1.866	8.82222e+5	5.78	
D	Pd	5.385e+0	1.000e-4	2.313	119.227	1.283	5.30935e+3	3.91	
	D	5.289e+0	2.000e-4	2.371	61.408	1.356	5.35878e+3	3.91	
	T	5.577e+0	4.000e-4	2.255	42.629	1.349	5.40870e+3	3.91	
	<sup>3</sup> He	5.865e+0	4.000e-4	2.574	43.684	1.403	1.10446e+4	3.91	
	<sup>4</sup> He	5.186e+0	7.000e-4	2.666	34.201	1.404	1.11435e+4	3.91	
	Ne	2.665e+1	2.900e-3	2.926	15.692	1.861	7.03218e+4	3.91	
	Ar	1.818e+1	3.390e-2	2.614	17.750	1.154	1.55391e+5	3.91	
	Kr	3.496e+1	2.700e-3	2.687	21.481	1.930	4.43321e+5	3.91	
	Pd	6.520e+1	2.300e-3	2.672	18.897	1.955	6.59103e+5	3.91	
	Xe	8.834e+1	2.300e-3	2.989	21.414	1.928	8.88306e+5	3.91	
T	H	Ag	5.488e+0	1.000e-4	2.280	92.472	1.319	5.46029e+3	2.97
	D	Ag	5.564e+0	2.000e-4	2.370	47.714	1.352	5.51044e+3	2.97
	T	Ag	5.039e+0	4.000e-4	2.259	33.421	1.360	5.56109e+3	2.97
	<sup>3</sup> He	Ag	5.621e+0	4.000e-4	2.402	33.938	1.428	1.13527e+4	2.97
	<sup>4</sup> He	Ag	3.465e+0	7.000e-4	2.771	26.286	1.382	1.14531e+4	2.97
	N	Ag	2.079e+1	2.000e-3	2.874	12.923	1.867	4.66664e+4	2.97
	O	Ag	1.952e+1	2.400e-3	2.750	12.794	1.863	5.47544e+4	2.97
	Ne	Ag	2.680e+1	2.800e-3	3.083	11.871	1.871	7.20736e+4	2.97
	Ar	Ag	2.218e+1	3.400e-3	2.660	13.287	1.917	1.58921e+5	2.97
	Ar(Mol)	Ag	5.122e+1	3.300e-3	2.860	13.484	2.005	1.58921e+5	2.97
	Ar(Mola)	Ag	3.583e+1	3.700e-3	2.893	11.764	1.891	1.58921e+5	2.97
	Ar(ZBL)	Ag	3.581e+1	3.500e-3	3.033	13.790	1.911	1.58921e+5	2.97
	Kr	Ag	4.488e+1	2.600e-3	2.874	15.582	1.955	4.51993e+5	2.97
	Ag	Ag	7.741e+1	6.000e-4	3.460	11.650	1.838	6.93021e+5	2.97
	Xe	Ag	6.920e+1	1.900e-3	2.767	16.908	1.989	9.03858e+5	2.97
Ar	Cd	3.366e+1	3.000e-3	2.742	5.323	2.015	1.61276e+5	1.16	
	Kr	Cd	6.279e+1	2.000e-3	3.047	6.034	2.078	4.55218e+5	1.16
	Cd	8.911e+1	1.800e-3	2.782	5.387	2.083	7.27916e+5	1.16	
In	H	In	5.489e+0	1.000e-4	2.136	82.640	1.330	5.76339e+3	2.49
	D	In	6.136e+0	2.000e-4	2.185	41.894	1.374	5.81315e+3	2.49
	T	In	5.421e+0	4.000e-4	2.071	28.799	1.357	5.86340e+3	2.49
	Ne	In	2.531e+1	2.500e-3	2.967	9.334	1.869	7.51927e+4	2.49
	Kr	In	2.683e+1	2.200e-3	2.357	13.168	1.981	4.62260e+5	2.49
	In	In	3.942e+1	1.800e-3	2.240	12.693	1.997	7.63793e+5	2.49

Table 7: Fitting parameters  $\lambda, q, \mu, E_{th}, \nu$ , for the energy dependence of the sputtered energy coefficient,  $Y_E$ , at normal incidence for different ions and targets. The lower limit is close to the threshold, the upper limit is in most cases 20 keV for the low mass ions and 200 keV for heavy ions.

ion	solid	$\lambda$	q	$\mu$	$E_{th}$	$\nu$	$\varepsilon_L$	$E_{sb}$
H	Sn	5.833e+0	4.310e-5	2.038	108.676	1.315	5.91631e+3	3.12
D	Sn	5.932e+0	2.000e-4	2.180	54.431	1.339	5.96574e+3	3.12
T	Sn	5.520e+0	3.000e-4	2.184	37.301	1.340	6.01566e+3	3.12
<sup>3</sup> He	Sn	6.021e+0	4.000e-4	2.272	38.542	1.405	1.22714e+4	3.12
<sup>4</sup> He	Sn	4.835e+0	5.000e-4	2.575	29.586	1.400	1.23702e+4	3.12
Ne	Sn	3.164e+1	2.400e-3	2.926	11.399	1.857	7.67367e+4	3.12
Ar	Sn	2.400e+1	3.000e-3	2.546	11.764	1.902	1.67157e+5	3.12
Kr	Sn	6.068e+1	2.500e-3	3.057	13.564	1.906	4.66941e+5	3.12
Sn	Sn	4.243e+1	2.400e-3	2.301	15.297	1.924	8.00660e+5	3.12
Xe	Sn	6.348e+1	1.700e-3	2.595	17.407	1.986	9.22556e+5	3.12
Kr	Sb	2.636e+1	3.200e-3	2.481	13.156	1.872	4.73059e+5	2.72
Ar	Te	2.519e+1	3.600e-3	2.881	7.262	1.871	1.72282e+5	2.02
Cs	Cs	6.170e+1	1.900e-3	2.229	4.276	2.010	1.00007e+6	0.82
Kr	Sm	3.739e+1	2.700e-3	2.857	9.104	1.953	5.50683e+5	2.16
H	Tb	6.656e+0	2.409e-5	1.967	181.849	1.322	8.32995e+3	3.89
D	Tb	6.391e+0	1.000e-4	1.883	92.781	1.349	8.38203e+3	3.89
T	Tb	6.345e+0	2.000e-4	2.415	58.866	1.325	8.43464e+3	3.89
<sup>3</sup> He	Tb	6.207e+0	2.000e-4	2.284	61.826	1.394	1.71555e+4	3.89
<sup>4</sup> He	Tb	5.456e+0	3.000e-4	2.299	47.928	1.390	1.72593e+4	3.89
Ar	Tb	2.363e+1	2.700e-3	2.585	13.797	1.894	2.15976e+5	3.89
H	Tm	6.422e+0	2.943e-5	2.137	120.687	1.340	9.00672e+3	2.52
D	Tm	6.102e+0	1.000e-4	2.159	60.859	1.366	9.05971e+3	2.52
T	Tm	5.921e+0	2.000e-4	2.511	39.465	1.366	9.11324e+3	2.52
<sup>3</sup> He	Tm	5.882e+0	2.000e-4	2.254	42.529	1.446	1.85244e+4	2.52
<sup>4</sup> He	Tm	5.599e+0	3.000e-4	2.149	33.313	1.463	1.86300e+4	2.52
Ar	Tm	2.276e+1	3.200e-3	2.816	9.234	1.899	2.29744e+5	2.52
H	Hf	5.089e+0	1.641e-5	2.281	316.511	1.222	9.52208e+3	6.31
D	Hf	5.555e+0	1.000e-4	2.038	166.154	1.301	9.57512e+3	6.31
T	Hf	5.746e+0	1.000e-4	2.060	111.740	1.319	9.62870e+3	6.31
<sup>3</sup> He	Hf	5.827e+0	1.683e-4	2.179	112.983	1.367	1.95639e+4	6.31
<sup>4</sup> He	Hf	6.015e+0	2.678e-4	2.300	86.190	1.377	1.96695e+4	6.31
Ne	Hf	1.482e+1	1.900e-3	2.318	28.468	1.832	1.15397e+5	6.31
Ar	Hf	1.912e+1	3.100e-3	2.544	23.165	1.848	2.39690e+5	6.31
Kr	Hf	2.063e+1	3.500e-3	2.415	26.235	1.865	6.21788e+5	6.31
Xe	Hf	2.991e+1	2.900e-3	2.438	31.643	1.891	1.16579e+6	6.31
H	Ta	6.971e+0	1.432e-5	1.917	441.289	1.324	9.69565e+3	8.10
D	Ta	6.933e+0	1.000e-4	2.115	213.454	1.304	9.74893e+3	8.10
T	Ta	5.521e+0	1.000e-4	2.300	141.668	1.292	9.80275e+3	8.10
<sup>3</sup> He	Ta	5.412e+0	2.000e-4	2.387	143.841	1.334	1.99149e+4	8.10
<sup>4</sup> He	Ta	5.499e+0	3.000e-4	2.151	113.986	1.362	2.00210e+4	8.10
Ne	Ta	1.423e+1	1.900e-3	2.633	35.975	1.797	1.17263e+5	8.10
Ar	Ta	2.286e+1	3.500e-3	3.302	27.761	1.768	2.43215e+5	8.10
Kr	Ta	2.263e+1	3.600e-3	2.613	33.078	1.858	6.29462e+5	8.10
Xe	Ta	2.676e+1	2.800e-3	2.414	41.065	1.893	1.17814e+6	8.10
Ta	Ta	4.506e+1	2.200e-3	2.312	39.858	1.932	1.93615e+6	8.10

Table 8: Fitting parameters  $\lambda, q, \mu, E_{th}, \nu$ , for the energy dependence of the sputtered energy coefficient,  $Y_E$ , at normal incidence for different ions and targets. The lower limit is close to the threshold, the upper limit is in most cases 20 keV for the low mass ions and 200 keV for heavy ions.

ion	solid	$\lambda$	q	$\mu$	$E_{th}$	$\nu$	$\varepsilon_L$	$E_{sb}$
H	W	6.453e+0	1.202e-5	3.302	392.000	1.141	9.86986e+3	8.68
D	W	3.665e+0	1.000e-4	2.279	229.743	1.210	9.92326e+3	8.68
T	W	4.524e+0	1.000e-4	2.436	152.506	1.250	9.97718e+3	8.68
<sup>3</sup> He	W	5.673e+0	1.606e-4	2.200	160.294	1.351	2.02666e+4	8.68
<sup>4</sup> He	W	5.211e+0	3.000e-4	2.331	121.307	1.342	2.03728e+4	8.68
N	W	1.398e+1	1.200e-3	2.812	44.876	1.764	7.90505e+4	8.68
O	W	1.308e+1	1.400e-3	2.370	44.105	1.820	9.19794e+4	8.68
Ne	W	1.527e+1	1.900e-3	2.649	38.147	1.792	1.19107e+5	8.68
Ar	W	4.869e+1	3.400e-3	3.105	26.501	1.803	2.46646e+5	8.68
Kr	W	2.845e+1	3.300e-3	2.875	34.518	1.878	6.36677e+5	8.68
Xe	W	2.909e+1	2.900e-3	2.597	43.078	1.890	1.18932e+6	8.68
W	W	2.983e+3	3.000e-3	3.363	18.144	1.839	1.99860e+6	8.68
H	Re	6.046e+0	5.189e-5	1.966	453.552	0.8489	1.00450e+4	8.09
D	Re	4.664e+0	2.000e-4	2.320	215.636	0.8173	1.00987e+4	8.09
T	Re	4.309e+0	4.000e-4	2.298	147.557	0.8440	1.01529e+4	8.09
<sup>3</sup> He	Re	6.008e+0	2.000e-4	2.326	149.646	1.373	2.06207e+4	8.09
<sup>4</sup> He	Re	5.765e+0	2.598e-4	2.279	115.262	1.379	2.07275e+4	8.09
Ne	Re	1.660e+1	1.900e-3	2.577	37.393	1.834	1.20995e+5	8.09
Ar	Re	1.902e+1	3.100e-3	2.553	31.766	1.864	2.50221e+5	8.09
Kr	Re	2.261e+1	3.400e-3	2.625	34.576	1.890	6.44513e+5	8.09
Xe	Re	2.638e+1	2.700e-3	2.510	41.972	1.933	1.20203e+6	8.09
H	Os	5.461e+0	1.500e-5	2.103	450.118	1.262	1.02204e+4	8.13
D	Os	5.282e+0	1.000e-4	2.068	229.171	1.302	1.02739e+4	8.13
T	Os	5.605e+0	1.000e-4	2.460	147.056	1.294	1.03279e+4	8.13
<sup>3</sup> He	Os	4.871e+0	1.714e-4	2.435	151.704	1.333	2.09735e+4	8.13
<sup>4</sup> He	Os	5.734e+0	2.606e-4	2.475	116.308	1.372	2.10799e+4	8.13
Ne	Os	1.586e+1	1.900e-3	2.859	37.415	1.835	1.22785e+5	8.13
Ar	Os	1.938e+1	3.100e-3	2.808	31.624	1.867	2.53422e+5	8.13
Kr	Os	2.093e+1	3.500e-3	2.698	34.946	1.885	6.50625e+5	8.13
Xe	Os	3.493e+1	2.900e-3	2.855	39.566	1.914	1.21043e+6	8.13
H	Ir	4.918e+0	1.703e-5	1.996	396.621	1.280	1.03972e+4	6.90
D	Ir	4.960e+0	1.000e-4	2.394	188.073	1.287	1.04510e+4	6.90
T	Ir	5.155e+0	1.000e-4	2.469	126.540	1.300	1.05053e+4	6.90
<sup>3</sup> He	Ir	5.759e+0	1.687e-4	2.182	132.546	1.384	2.13313e+4	6.90
<sup>4</sup> He	Ir	5.927e+0	3.000e-4	2.166	102.962	1.402	2.14384e+4	6.90
Ne	Ir	1.847e+1	1.800e-3	2.723	32.504	1.874	1.24708e+5	6.90
Ar	Ir	2.334e+1	3.100e-3	2.771	27.287	1.893	2.57103e+5	6.90
Kr	Ir	2.279e+1	3.100e-3	2.704	30.494	1.942	6.58875e+5	6.90
Xe	Ir	4.987e+1	2.700e-3	3.046	32.907	1.942	1.22412e+6	6.90

Table 9: Fitting parameters  $\lambda, q, \mu, E_{th}, \nu$ , for the energy dependence of the sputtered energy coefficient,  $Y_E$ , at normal incidence for different ions and targets. The lower limit is close to the threshold, the upper limit is in most cases 20 keV for the low mass ions and 200 keV for heavy ions.

ion	solid	$\lambda$	q	$\mu$	$E_{th}$	$\nu$	$\varepsilon_L$	$E_{sb}$
H	Pt	5.832e+0	1.769e-5	2.237	325.862	1.293	1.05744e+4	5.86
D	Pt	4.822e+0	1.000e-4	2.204	166.278	1.310	1.06283e+4	5.86
T	Pt	5.265e+0	1.000e-4	2.199	112.336	1.344	1.06828e+4	5.86
<sup>3</sup> He	Pt	5.305e+0	1.757e-4	2.320	113.322	1.386	2.16890e+4	5.86
<sup>4</sup> He	Pt	5.744e+0	2.676e-4	2.341	86.682	1.408	2.17963e+4	5.86
O	Pt	1.577e+1	1.400e-3	2.553	31.782	1.882	9.78987e+4	5.86
Ne	Pt	2.262e+1	1.800e-3	2.580	28.158	1.914	1.26583e+5	5.86
Ar	Pt	2.641e+1	3.100e-3	2.767	23.074	1.901	2.60590e+5	5.86
Kr	Pt	2.139e+1	3.100e-3	2.656	26.234	1.954	6.66218e+5	5.86
Xe	Pt	2.579e+1	2.400e-3	2.508	30.931	2.001	1.23553e+6	5.86
Pt	Pt	7.003e+1	1.700e-3	2.742	27.584	2.036	2.25981e+6	5.86
H	Au	5.354e+0	2.132e-5	2.562	204.563	1.311	1.07527e+4	3.80
D	Au	4.738e+0	1.000e-4	2.004	110.464	1.351	1.08070e+4	3.80
T	Au	5.337e+0	2.000e-4	2.179	73.546	1.382	1.08618e+4	3.80
<sup>3</sup> He	Au	5.140e+0	1.828e-4	2.217	75.044	1.437	2.20499e+4	3.80
<sup>4</sup> He	Au	4.982e+0	3.000e-4	2.295	57.083	1.433	2.21579e+4	3.80
N	Au	1.977e+1	1.200e-3	2.719	21.972	1.895	8.55290e+4	3.80
O	Au	2.187e+1	1.400e-3	3.163	19.433	1.859	9.94281e+4	3.80
Ne	Au	2.219e+1	1.700e-3	2.437	18.952	1.951	2.18526e+5	3.80
Ar	Au	2.621e+1	3.000e-3	2.846	15.554	1.935	2.64318e+5	3.80
Kr	Au	2.290e+1	2.500e-3	2.549	17.813	2.032	6.74618e+5	3.80
Xe	Au	4.778e+1	1.800e-3	2.749	19.454	2.098	1.24955e+6	3.80
Au	Au	6.954e+1	2.900e-3	2.773	17.621	1.941	2.32799e+6	3.80
Kr	Hg	2.546e+1	3.100e-3	2.703	24.009	1.883	6.81273e+5	6.36
Kr	Tl	5.582e+1	2.300e-3	3.393	7.228	2.058	6.87823e+5	1.88
He	Pb	4.165e+0	3.000e-4	2.333	31.654	1.447	2.32414e+4	2.03
Ne	Pb	2.009e+1	1.500e-3	2.853	9.642	1.928	1.34122e+5	2.03
Ar	Pb	1.750e+1	2.200e-3	2.545	8.269	2.004	2.74555e+5	2.03
Kr	Pb	2.004e+1	2.100e-3	2.483	8.903	2.068	6.95357e+5	2.03
Xe	Pb	2.561e+1	1.500e-3	2.416	10.602	2.136	1.28038e+6	2.03
Pb	Pb	6.874e+1	1.300e-3	2.566	9.845	2.121	2.53951e+6	2.03
Ar	Bi	1.961e+1	2.200e-3	2.700	8.373	1.978	2.78342e+5	2.17
Kr	Bi	2.368e+1	2.000e-3	2.479	9.019	2.068	7.03904e+5	2.17
<sup>4</sup> He	Th	6.615e+0	2.000e-4	2.201	103.060	1.381	2.61980e+4	5.93
Ne	Th	1.692e+1	1.500e-3	2.675	29.194	1.817	1.49508e+5	5.93
Ar	Th	1.502e+1	2.800e-3	2.252	23.280	1.855	3.02995e+5	5.93
Kr	Th	2.223e+1	3.400e-3	3.444	22.198	1.885	7.54519e+5	5.93
Xe	Th	3.329e+1	2.900e-3	2.464	25.470	1.919	1.37124e+6	5.93
H	U	3.816e+0	1.326e-5	2.146	367.066	1.206	1.31300e+4	5.42
D	U	5.365e+0	1.000e-4	2.170	184.355	1.315	1.31849e+4	5.42
<sup>4</sup> He	U	5.220e+0	2.000e-4	2.322	95.736	1.402	2.69513e+4	5.42
Ne	U	1.418e+1	1.500e-3	2.332	28.734	1.873	1.53434e+5	5.42
Ar	U	1.872e+1	2.800e-3	2.748	21.333	1.878	3.10275e+5	5.42
Kr	U	1.860e+1	2.900e-3	2.524	22.120	1.960	7.69792e+5	5.42
Xe	U	2.229e+1	2.400e-3	2.454	25.780	2.009	1.39494e+6	5.42
Rn	U	3.942e+1	1.700e-3	2.613	30.993	2.044	2.96732e+6	5.42
U	U	8.512e+1	1.700e-3	2.854	24.144	2.021	3.32167e+6	5.42

Table 10: Fitting values  $f, b, c$  for the angular dependence of the sputtered energy coefficient for several ion-target combinations and incident ion energies,  $E_0$ . Furthermore, the values for the sputtered energy coefficient at normal incidence,  $Y_E(E_0, 0)$ , the binding energy,  $E_{sp}$ (eV), for the projectiles, the value  $\theta_0^*$  (deg.), (6), and the angular position,  $\theta_{0m}$  (deg.), of the maximum sputtered energy coefficient, (7), are given.

ion	target	$E_0$ (eV)	f	b	c	$Y(E_0, 0)$	$E_{sp}$	$\theta_0^*$	$\theta_{0m}$
T	Li	100	10.2362	3.9529	0.7761	1.57e-3	1.00	95.71	74.95
T	Li	300	8.0979	2.6148	0.7435	9.69e-4	1.00	93.30	79.50
Li	Li	100	16.2355	7.5529	0.6936	2.72e-3	1.67	97.36	69.90
Li	Li	200	12.0024	4.9215	0.7101	3.17e-3	1.67	95.22	73.65
Li	Li	1000	8.6850	2.8498	0.6935	2.08e-3	1.67	92.34	79.84
H	Be	17	15.0192	12.2994	0.6534	5.30e-6	1.00	103.63	31.06
H	Be	20	13.1894	10.4764	0.5934	3.14e-5	1.00	102.60	31.85
H	Be	22	11.3554	8.7815	0.6254	6.21e-5	1.00	102.04	35.62
H	Be	25	9.8625	7.1791	0.6663	1.22e-4	1.00	101.31	42.34
H	Be	30	7.5942	4.9722	0.7687	2.42e-4	1.00	100.35	52.26
H	Be	40	6.5908	3.5658	0.9001	4.61e-4	1.00	98.98	62.96
H	Be	50	6.2148	2.9708	0.9559	6.19e-4	1.00	98.05	67.16
H	Be	70	5.9604	2.4433	1.0058	7.72e-4	1.00	96.82	70.73
H	Be	100	5.4833	1.9514	1.0351	8.25e-4	1.00	95.71	73.07
H	Be	140	5.2556	1.6886	1.0386	7.78e-4	1.00	94.83	74.48
H	Be	200	5.1949	1.5446	1.0241	6.59e-4	1.00	94.04	75.55
H	Be	300	5.1756	1.4477	0.9921	5.02e-4	1.00	93.30	76.62
H	Be	500	5.1718	1.3557	0.9362	3.13e-4	1.00	92.56	78.34
H	Be	1000	5.2614	1.2434	0.8281	1.39e-4	1.00	91.81	82.64
D	Be	11	13.5302	10.2782	0.7530	1.21e-6	1.00	106.78	42.98
D	Be	12	13.1593	9.6932	0.4965	4.88e-6	1.00	106.10	37.11
D	Be	13	13.3940	9.5880	0.5074	1.30e-5	1.00	105.50	40.43
D	Be	14	12.5003	8.7410	0.5374	2.79e-5	1.00	104.96	43.75
D	Be	15	11.7442	7.9688	0.5699	5.04e-5	1.00	104.48	47.46
D	Be	17	11.2812	7.2662	0.6167	1.13e-4	1.00	103.63	52.73
D	Be	20	10.6565	6.4178	0.6964	2.51e-4	1.00	102.60	58.36
D	Be	25	10.1966	5.7049	0.7740	5.28e-4	1.00	101.31	62.59
D	Be	30	10.0263	5.3137	0.8192	7.87e-4	1.00	100.35	64.84
D	Be	40	9.3179	4.5386	0.8830	1.20e-3	1.00	98.98	67.46
D	Be	50	9.1102	4.2137	0.9064	1.43e-3	1.00	98.05	68.64
D	Be	70	8.4246	3.5596	0.9434	1.60e-3	1.00	96.82	70.46
D	Be	100	7.6933	2.9730	0.9653	1.63e-3	1.00	95.71	71.95
D	Be	140	7.3337	2.6468	0.9660	1.48e-3	1.00	94.83	73.01
D	Be	200	6.6082	2.1695	0.9733	1.30e-3	1.00	94.04	74.45
D	Be	300	6.3383	1.9598	0.9468	1.01e-3	1.00	93.30	75.60
D	Be	500	6.1678	1.7951	0.8947	6.64e-4	1.00	92.56	77.34
D	Be	1000	5.8465	1.5024	0.8107	3.22e-4	1.00	91.81	81.62
D	Be	3000	5.8554	1.2982	0.7851	7.49e-5	1.00	91.05	84.73
T	Be	10	14.4920	8.5512	0.5089	1.09e-6	1.00	107.55	60.59
T	Be	11	13.9500	8.2032	0.5366	4.65e-6	1.00	106.78	60.83
T	Be	12	14.2935	8.3295	0.5698	1.22e-5	1.00	106.10	61.58
T	Be	13	14.2308	8.1893	0.5914	2.51e-5	1.00	105.50	62.42
T	Be	15	14.7444	8.3054	0.6323	6.76e-5	1.00	104.48	63.64
T	Be	17	14.7802	8.1839	0.6634	1.33e-4	1.00	103.63	64.39
T	Be	20	15.0025	8.1597	0.7015	2.64e-4	1.00	102.60	64.92
T	Be	25	14.5955	7.6980	0.7447	5.19e-4	1.00	101.31	65.82

Table 11: Fitting values  $f, b, c$  for the angular dependence of the sputtered energy coefficient for several ion-target combinations and incident ion energies,  $E_0$ . Furthermore, the values for the sputtered energy coefficient at normal incidence,  $Y_E(E_0, 0)$ , the binding energy,  $E_{\text{sp}}$ (eV), for the projectiles, the value  $\theta_0^*$  (deg.), and the angular position,  $\theta_{0m}$  (deg.), of the maximum sputtered energy coefficient, are given.

ion	target	$E_0$ (eV)	f	b	c	$Y(E_0, 0)$	$E_{\text{sp}}$	$\theta_0^*$	$\theta_{0m}$
T	Be	30	13.8986	7.1225	0.7739	7.78e-4	1.00	100.35	66.60
T	Be	50	12.1179	5.6621	0.8511	1.42e-3	1.00	98.05	68.67
T	Be	100	9.9135	4.0246	0.9120	1.69e-3	1.00	95.71	71.28
T	Be	200	8.3666	2.9625	0.9226	1.42e-3	1.00	94.04	73.54
T	Be	300	7.6936	2.5468	0.9049	1.16e-3	1.00	93.30	74.90
T	Be	500	7.2432	2.2535	0.8576	8.22e-4	1.00	92.56	76.75
T	Be	1000	7.7269	1.8637	0.7788	4.28e-4	1.00	91.81	81.06
${}^4\text{He}$	Be	10	11.7360	5.5326	0.7401	1.61e-7	0.00	90.00	63.57
${}^4\text{He}$	Be	11	16.8676	9.0611	0.6483	8.90e-7	0.00	90.00	57.64
${}^4\text{He}$	Be	12	14.9305	7.5641	0.6967	2.60e-6	0.00	90.00	60.57
${}^4\text{He}$	Be	13	13.8713	6.6181	0.7855	5.89e-6	0.00	90.00	62.69
${}^4\text{He}$	Be	15	15.2507	7.6048	0.7387	2.21e-5	0.00	90.00	61.13
${}^4\text{He}$	Be	17	13.8177	6.6277	0.8086	6.21e-5	0.00	90.00	62.33
${}^4\text{He}$	Be	20	14.0793	6.8823	0.8001	1.75e-4	0.00	90.00	61.63
${}^4\text{He}$	Be	25	13.7252	6.6588	0.8297	4.72e-4	0.00	90.00	61.84
${}^4\text{He}$	Be	30	14.5509	7.3087	0.7616	8.45e-4	0.00	90.00	60.67
${}^4\text{He}$	Be	40	12.3386	5.7482	0.8415	1.60e-3	0.00	90.00	63.21
${}^4\text{He}$	Be	50	11.5880	5.2287	0.8587	2.17e-3	0.00	90.00	64.20
${}^4\text{He}$	Be	70	10.5461	4.4969	0.8820	2.82e-3	0.00	90.00	65.83
${}^4\text{He}$	Be	100	9.5087	3.7939	0.9042	3.22e-3	0.00	90.00	67.54
${}^4\text{He}$	Be	140	8.4665	3.1385	0.9246	3.39e-3	0.00	90.00	69.22
${}^4\text{He}$	Be	200	7.8958	2.7481	0.9312	3.19e-3	0.00	90.00	70.64
${}^4\text{He}$	Be	300	7.3588	2.4033	0.9304	2.83e-3	0.00	90.00	72.08
${}^4\text{He}$	Be	400	7.2910	2.3336	0.9180	2.46e-3	0.00	90.00	72.74
${}^4\text{He}$	Be	500	7.0485	2.1981	0.9094	2.27e-3	0.00	90.00	73.47
${}^4\text{He}$	Be	700	7.1312	2.2116	0.8757	1.80e-3	0.00	90.00	74.29
${}^4\text{He}$	Be	1000	7.2610	2.2521	0.8258	1.39e-3	0.00	90.00	75.47
${}^4\text{He}$	Be	2000	6.9172	1.9656	0.7569	7.58e-4	0.00	90.00	79.61
${}^4\text{He}$	Be	5000	6.2585	1.4569	0.7205	2.80e-4	0.00	90.00	85.64
${}^4\text{He}$	Be	10000	5.8372	1.1935	0.7357	1.18e-4	0.00	90.00	87.45
Be	Be	11	42.1620	21.4302	0.4771	3.57e-7	3.38	119.00	81.85
Be	Be	12	42.7381	21.9715	0.5047	6.92e-7	3.38	117.96	79.75
Be	Be	13	43.3572	22.5293	0.5170	1.18e-6	3.38	117.02	78.05
Be	Be	15	43.5882	22.9716	0.5302	2.97e-6	3.38	115.39	75.65
Be	Be	17	42.3287	22.4482	0.5318	6.75e-6	3.38	114.03	74.21
Be	Be	20	40.1586	21.4314	0.5262	1.84e-5	3.38	112.35	72.60
Be	Be	25	36.3672	19.5125	0.5282	6.59e-5	3.38	110.19	70.74
Be	Be	30	33.6694	18.1104	0.5328	1.53e-4	3.38	108.55	69.48
Be	Be	40	30.1803	16.2633	0.5459	4.26e-4	3.38	106.21	67.83
Be	Be	50	27.9672	15.0459	0.5613	7.62e-4	3.38	104.57	66.90
Be	Be	70	24.9109	13.2867	0.5919	1.47e-3	3.38	102.39	66.09
Be	Be	100	21.8061	11.3811	0.6348	2.37e-3	3.38	100.42	66.13
Be	Be	200	16.7135	8.0539	0.7303	3.69e-3	3.38	97.41	67.86
Be	Be	300	14.1990	6.3993	0.7792	4.03e-3	3.38	96.06	69.37
Be	Be	500	11.9262	4.9331	0.8130	3.96e-3	3.38	94.70	71.16
Be	Be	700	10.9538	4.3181	0.8125	3.68e-3	3.38	93.97	72.24
Be	Be	1000	10.0619	3.7686	0.8030	3.19e-3	3.38	93.33	73.55
Be	Be	3000	8.0780	2.5319	0.7678	1.87e-3	3.38	91.92	78.42
Be	Be	5000	8.1179	2.4454	0.7093	1.22e-3	3.38	91.49	81.11

Table 12: Fitting values  $f, b, c$  for the angular dependence of the sputtered energy coefficient for several ion-target combinations and incident ion energies,  $E_0$ . Furthermore, the values for the sputtered energy coefficient at normal incidence,  $Y_E(E_0, 0)$ , the binding energy,  $E_{\text{sp}}$ (eV), for the projectiles, the value  $\theta_0^*$  (deg.), and the angular position,  $\theta_{0m}$  (deg.), of the maximum sputtered energy coefficient, are given.

ion	target	$E_0$ (eV)	f	b	c	$Y(E_0, 0)$	$E_{\text{sp}}$	$\theta_0^*$	$\theta_{0m}$
N	Be	15	56.6431	28.9991	0.5349	4.08e-8	1.00	104.48	70.72
N	Be	20	55.5253	29.3086	0.5132	4.78e-7	1.00	102.60	67.21
N	Be	25	46.9703	25.0400	0.5453	5.53e-6	1.00	101.31	65.51
N	Be	27	39.8702	22.1580	0.5309	2.23e-4	1.00	100.89	62.01
N	Be	30	37.4299	20.9914	0.5363	4.97e-4	1.00	100.35	60.99
N	Be	40	32.2237	18.4203	0.5534	2.72e-3	1.00	98.98	58.78
N	Be	50	27.1013	15.5100	0.5983	7.94e-3	1.00	98.05	58.46
N	Be	70	23.2661	13.3500	0.6312	2.53e-2	1.00	96.82	56.99
N	Be	100	18.5794	10.4007	0.6958	6.02e-2	1.00	95.71	58.90
N	Be	140	14.9483	8.0322	0.7602	1.08e-1	1.00	94.83	60.25
N	Be	200	11.8204	5.9812	0.8224	1.72e-1	1.00	94.04	62.81
N	Be	500	7.1837	2.9571	0.9262	3.38e-1	1.00	92.56	68.30
N	Be	1000	5.3902	1.8661	0.9559	4.48e-1	1.00	91.81	71.80
Ne	Be	13	68.9814	35.1891	0.5128	1.40e-10	0.00	90.00	61.33
Ne	Be	14	57.2937	28.0867	0.5380	9.30e-10	0.00	90.00	63.68
Ne	Be	15	56.4498	27.8171	0.5466	2.47e-9	0.00	90.00	63.25
Ne	Be	17	48.5543	23.5463	0.5840	2.32e-8	0.00	90.00	63.77
Ne	Be	20	45.0078	21.9259	0.6003	1.78e-7	0.00	90.00	63.33
Ne	Be	22	42.0286	20.3619	0.6159	4.86e-7	0.00	90.00	63.47
Ne	Be	25	41.2355	20.2883	0.6090	1.54e-6	0.00	90.00	62.70
Ne	Be	30	37.3313	18.3767	0.6261	7.40e-6	0.00	90.00	62.52
Ne	Be	35	35.7019	17.8136	0.6269	2.01e-5	0.00	90.00	61.78
Ne	Be	40	33.3821	16.6783	0.6383	4.63e-5	0.00	90.00	61.63
Ne	Be	45	31.5807	15.7937	0.6476	8.74e-5	0.00	90.00	61.51
Ne	Be	50	30.0601	15.0243	0.6566	1.44e-4	0.00	90.00	61.48
Ne	Be	60	27.1695	13.4712	0.6778	3.10e-4	0.00	90.00	61.75
Ne	Be	70	24.9841	12.2665	0.6972	5.29e-4	0.00	90.00	62.09
Ne	Be	100	20.6541	9.8332	0.7402	1.32e-3	0.00	90.00	63.14
Ne	Be	150	16.6374	7.4867	0.7915	2.53e-3	0.00	90.00	64.93
Ne	Be	200	14.4401	6.2187	0.8223	3.47e-3	0.00	90.00	66.16
Ne	Be	300	12.0017	4.8124	0.8594	4.67e-3	0.00	90.00	67.97
Ne	Be	500	10.0255	3.7004	0.8862	5.69e-3	0.00	90.00	69.90
Ne	Be	700	9.1663	3.2222	0.8937	5.96e-3	0.00	90.00	71.02
Ne	Be	1000	8.6970	2.9677	0.8855	5.97e-3	0.00	90.00	71.89
Ar	Be	25	48.5911	23.2142	0.5856	9.80e-7	0.00	90.00	64.59
Ar	Be	30	40.2406	18.8679	0.6308	2.75e-7	0.00	90.00	64.99
Ar	Be	35	37.4509	17.6139	0.6419	1.23e-6	0.00	90.00	64.70
Ar	Be	40	35.8857	17.1765	0.6423	3.64e-6	0.00	90.00	63.82
Ar	Be	45	34.5918	16.7293	0.6436	8.67e-6	0.00	90.00	63.28
Ar	Be	50	32.2093	15.3993	0.6588	1.78e-5	0.00	90.00	63.70
Ar	Be	60	29.9442	14.4066	0.6671	5.17e-5	0.00	90.00	63.31
Ar	Be	70	27.4376	13.0662	0.6852	1.11e-4	0.00	90.00	63.63
Ar	Be	100	22.4140	10.3549	0.7295	4.26e-4	0.00	90.00	64.53
Ar	Be	150	18.1024	8.0272	0.7749	1.19e-3	0.00	90.00	65.66
Ar	Be	200	15.5926	6.6292	0.8078	1.92e-3	0.00	90.00	66.78
Ar	Be	300	12.8666	5.1316	0.8471	3.09e-3	0.00	90.00	68.31
Ar	Be	500	10.4208	3.8104	0.8832	4.48e-3	0.00	90.00	70.20
Ar	Be	700	9.2687	3.1987	0.8997	5.21e-3	0.00	90.00	71.37
Ar	Be	1000	8.6051	2.8505	0.9014	5.58e-3	0.00	90.00	72.29

Table 13: Fitting values  $f, b, c$  for the angular dependence of the sputtered energy coefficient for several ion-target combinations and incident ion energies,  $E_0$ . Furthermore, the values for the sputtered energy coefficient at normal incidence,  $Y_E(E_0, 0)$ , the binding energy,  $E_{sp}$ (eV), for the projectiles, the value  $\theta_0^*$  (deg.), and the angular position,  $\theta_{0m}$  (deg.), of the maximum sputtered energy coefficient, are given.

ion	target	$E_0$ (eV)	f	b	c	$Y(E_0, 0)$	$E_{sp}$	$\theta_0^*$	$\theta_{0m}$
D	B	30	11.6693	7.4278	0.7198	6.71e-5	1.00	100.35	53.56
	B	50	8.7790	4.4206	0.8912	4.48e-4	1.00	98.05	65.45
	B	100	6.8440	2.5986	1.0072	9.26e-4	1.00	95.71	71.89
	B	400	5.9861	1.7614	0.9519	6.45e-4	1.00	92.86	76.13
	B	500	6.3174	1.8409	0.9137	4.95e-4	1.00	92.56	76.88
	B	8000	5.5522	1.0900	0.7914	1.91e-5	1.00	90.64	86.15
B	B	1000	10.3371	3.9627	0.7589	3.51e-3	5.73	94.33	74.47
	B	2000	9.1373	3.2150	0.7516	2.82e-3	5.73	93.06	76.45
H	C	40	25.1377	16.8180	0.8164	1.26e-7	1.00	98.98	50.74
	C	50	11.3083	7.6579	0.7594	6.48e-6	1.00	98.05	48.60
	C	70	6.2750	3.4977	0.9006	5.02e-5	1.00	96.82	60.24
	C	100	4.4547	1.7320	1.0321	1.27e-4	1.00	95.71	71.03
	C	140	4.1224	1.2451	1.0706	1.94e-4	1.00	94.83	75.14
	C	200	4.0616	1.0525	1.0682	2.35e-4	1.00	94.04	77.02
	C	300	3.9732	0.9309	1.0465	2.55e-4	1.00	93.30	78.25
	C	500	4.5761	1.0786	0.9697	1.79e-4	1.00	92.56	79.25
	C	1000	4.9595	1.1242	0.8424	1.00e-4	1.00	91.81	82.89
	C	2000	5.2103	1.1392	0.8804	4.53e-5	1.00	91.28	81.74
D	C	30	18.7020	12.7582	0.5994	3.32e-6	1.00	100.35	45.88
	C	40	13.9859	8.3859	0.7022	3.58e-5	1.00	98.98	56.64
	C	50	9.1046	4.7171	0.8423	1.18e-4	1.00	98.05	64.36
	C	70	6.8357	2.9145	0.9611	3.26e-4	1.00	96.82	70.01
	C	100	6.1142	2.1925	1.0137	5.27e-4	1.00	95.71	73.18
	C	140	5.5800	1.7856	1.0228	6.77e-4	1.00	94.83	74.80
	C	200	5.4183	1.6184	1.0124	7.12e-4	1.00	94.04	75.66
	C	300	5.4718	1.5643	0.9764	6.56e-4	1.00	93.30	76.54
	C	350	5.3398	1.4866	0.9908	6.57e-4	1.00	93.06	76.53
	C	500	5.5508	1.5347	0.9123	5.02e-4	1.00	92.56	77.94
D	C	1000	5.2293	1.2861	0.8339	2.94e-4	1.00	91.81	81.71
	C	2000	5.1506	1.1281	0.8779	1.39e-4	1.00	91.28	81.79
T	C	25	22.0075	14.0078	0.5594	2.26e-6	1.00	101.31	51.41
	C	30	16.7368	9.7905	0.6356	1.41e-5	1.00	100.35	58.54
	C	40	12.8519	6.5908	0.7794	8.27e-5	1.00	98.98	65.54
	C	50	11.1855	5.2720	0.8488	1.96e-4	1.00	98.05	68.34
	C	70	8.9010	3.6518	0.9388	4.54e-4	1.00	96.82	71.40
	C	100	8.2697	3.1125	0.9528	6.68e-4	1.00	95.71	72.81
	C	140	7.2448	2.4653	0.9755	8.37e-4	1.00	94.83	74.24
	C	200	7.2269	2.3719	0.9540	8.51e-4	1.00	94.04	74.79
	C	300	6.7254	2.0851	0.9294	8.36e-4	1.00	93.30	75.88
	C	500	6.1973	1.7780	0.8939	6.78e-4	1.00	92.56	77.65
T	C	1000	6.3026	1.7218	0.7847	3.92e-4	1.00	91.81	81.18

Table 14: Fitting values  $f, b, c$  for the angular dependence of the sputtered energy coefficient for several ion-target combinations and incident ion energies,  $E_0$ . Furthermore, the values for the sputtered energy coefficient at normal incidence,  $Y_E(E_0, 0)$ , the binding energy,  $E_{sp}$ (eV), for the projectiles, the value  $\theta_0^*$  (deg.), and the angular position,  $\theta_{0m}$  (deg.), of the maximum sputtered energy coefficient, are given.

ion	target	$E_0$ (eV)	$f$	$b$	$c$	$Y(E_0, 0)$	$E_{sp}$	$\theta_0^*$	$\theta_{0m}$
${}^4\text{He}$	C	20	28.4708	18.0764	0.4335	1.01e-7	0.00	90.00	43.36
${}^4\text{He}$	C	25	17.6336	10.1800	0.6108	2.34e-6	0.00	90.00	53.17
${}^4\text{He}$	C	27	9.6634	5.0493	0.8006	1.00e-5	0.00	90.00	58.80
${}^4\text{He}$	C	30	11.8456	6.0631	0.7740	2.00e-5	0.00	90.00	59.79
${}^4\text{He}$	C	35	13.2392	6.6339	0.7592	5.00e-5	0.00	90.00	60.79
${}^4\text{He}$	C	40	11.5719	5.3259	0.8543	1.10e-4	0.00	90.00	63.55
${}^4\text{He}$	C	50	10.9140	4.7947	0.8726	2.80e-4	0.00	90.00	64.75
${}^4\text{He}$	C	60	10.1895	4.3257	0.8877	5.00e-4	0.00	90.00	65.91
${}^4\text{He}$	C	70	9.3806	3.8211	0.9059	7.40e-4	0.00	90.00	66.93
${}^4\text{He}$	C	100	8.3345	3.1351	0.9289	1.29e-3	0.00	90.00	68.79
${}^4\text{He}$	C	140	7.7229	2.7292	0.9397	1.68e-3	0.00	90.00	70.16
${}^4\text{He}$	C	200	7.0738	2.3334	0.9477	1.95e-3	0.00	90.00	71.57
${}^4\text{He}$	C	300	6.7220	2.1202	0.9394	2.01e-3	0.00	90.00	72.82
${}^4\text{He}$	C	400	6.5491	2.0103	0.9288	1.93e-3	0.00	90.00	73.41
${}^4\text{He}$	C	500	6.3449	1.9008	0.9205	1.85e-3	0.00	90.00	74.06
${}^4\text{He}$	C	700	6.5586	1.9844	0.8077	1.55e-3	0.00	90.00	74.72
${}^4\text{He}$	C	1000	6.7335	2.0552	0.8317	1.26e-3	0.00	90.00	75.69
${}^4\text{He}$	C	2000	6.3927	1.7781	0.7622	7.40e-4	0.00	90.00	79.94
${}^4\text{He}$	C	3000	6.0934	1.5671	0.7528	5.30e-4	0.00	90.00	82.07
${}^4\text{He}$	C	5000	6.2421	1.5564	0.8125	2.94e-4	0.00	90.00	80.54
${}^4\text{He}$	C	10000	6.1393	1.3482	0.7271	1.24e-4	0.00	90.00	86.52
${}^4\text{He}$	C	20000	4.7871	0.3771	0.6108	5.20e-5	0.00	90.00	90.00
C	C	25	50.5913	26.2291	0.4926	2.49e-7	7.41	118.57	79.48
C	C	30	48.6907	25.5043	0.5177	1.09e-6	7.41	116.44	76.95
C	C	40	42.9993	22.5078	0.5206	8.28e-6	7.41	113.29	74.90
C	C	50	38.3944	19.9900	0.5194	2.98e-5	7.41	111.06	73.89
C	C	70	32.5113	16.7415	0.5356	1.32e-4	7.41	108.02	72.65
C	C	100	27.6668	14.0728	0.5588	4.06e-4	7.41	105.23	71.51
C	C	140	23.6811	11.8531	0.5893	8.92e-4	7.41	102.96	70.81
C	C	200	20.2369	9.8676	0.6211	1.57e-3	7.41	100.90	70.71
C	C	300	17.3540	8.1805	0.6569	2.35e-3	7.41	98.93	70.83
C	C	500	14.4607	6.4252	0.7055	3.12e-3	7.41	96.94	71592
C	C	1000	11.7081	4.7573	0.7358	3.48e-3	7.40	94.92	73.27
C	C	3000	7.4737	2.4240	0.8103	2.80e-3	7.40	92.85	77.12
N	C	30	56.7514	29.3830	0.4995	4.60e-8	1.00	100.35	67.33
N	C	40	52.4678	27.6459	0.5241	7.69e-7	1.00	98.98	64.93
N	C	50	46.9726	24.9876	0.5453	5.63e-6	1.00	98.05	63.56
N	C	70	39.4092	20.9578	0.5840	5.03e-5	1.00	96.82	62.70
N	C	100	30.8064	15.9042	0.6481	2.35e-4	1.00	95.71	63.61
N	C	140	25.9364	13.0187	0.7027	6.37e-4	1.00	94.83	64.27
N	C	200	20.5931	9.7878	0.7635	1.31e-3	1.00	94.04	65.86
N	C	300	16.2957	7.2354	0.8127	2.20e-3	1.00	93.30	67.59
N	C	500	12.9519	5.2966	0.8454	3.13e-3	1.00	92.56	69.48
N	C	1000	10.6909	4.0567	0.8328	3.74e-3	1.00	91.81	71.42
N	C	15000	7.3988	2.0549	0.7707	1.21e-3	1.00	90.47	80.09
N	C	30000	6.6358	1.5883	0.7081	6.40e-4	1.00	90.33	85.94

Table 15: Fitting values  $f, b, c$  for the angular dependence of the sputtered energy coefficient for several ion-target combinations and incident ion energies,  $E_0$ . Furthermore, the values for the sputtered energy coefficient at normal incidence,  $Y_E(E_0, 0)$ , the binding energy,  $E_{sp}$ (eV), for the projectiles, the value  $\theta_0^*$  (deg.), and the angular position,  $\theta_{0m}$  (deg.), of the maximum sputtered energy coefficient, are given.

ion	target	$E_0$ (eV)	$f$	$b$	$c$	$Y(E_0, 0)$	$E_{sp}$	$\theta_0^*$	$\theta_{0m}$
Ne	C	35	54.7818	26.5272	0.5841	1.87e-8	0.00	90.00	63.85
Ne	C	40	50.4972	24.7654	0.5904	1.31e-7	0.00	90.00	63.06
Ne	C	45	47.7550	23.3495	0.6069	4.11e-7	0.00	90.00	63.06
Ne	C	50	45.5534	22.6656	0.6019	1.29e-6	0.00	90.00	62.13
Ne	C	60	40.5180	19.9867	0.6275	6.14e-6	0.00	90.00	62.39
Ne	C	70	35.9979	17.6089	0.6497	1.90e-5	0.00	90.00	62.64
Ne	C	100	28.7287	13.7417	0.6952	1.27e-4	0.00	90.00	63.33
Ne	C	140	22.8934	10.5205	0.7432	4.34e-4	0.00	90.00	64.60
Ne	C	200	18.4156	8.0568	0.7857	1.02e-3	0.00	90.00	66.03
Ne	C	300	14.6882	6.0268	0.8268	1.95e-3	0.00	90.00	67.70
Ne	C	500	11.9158	4.5590	0.8534	3.12e-3	0.00	90.00	69.43
Ne	C	1000	9.9254	3.5596	0.8495	4.24e-3	0.00	90.00	71.29
Ne	C	2000	8.9429	3.0841	0.8089	4.41e-3	0.00	90.00	73.17
Ne	C	5000	8.2880	2.6952	0.7299	3.53e-3	0.00	90.00	76.90
Ne	C	10000	7.7430	2.3088	0.7059	2.53e-3	0.00	90.00	80.21
Ne	C	20000	7.0896	1.8716	0.7048	1.56e-3	0.00	90.00	83.47
Ar	C	40	53.8120	25.5764	0.5836	3.51e-9	0.00	90.00	64.91
Ar	C	50	47.2296	22.2438	0.6164	6.13e-8	0.00	90.00	64.95
Ar	C	70	39.2650	18.5960	0.6429	1.97e-6	0.00	90.00	64.34
Ar	C	100	31.3496	14.6218	0.6842	2.58e-5	0.00	90.00	64.60
Ar	C	140	25.2253	11.4111	0.7284	1.37e-4	0.00	90.00	65.42
Ar	C	200	20.1819	8.7482	0.7717	4.66e-4	0.00	90.00	66.55
Ar	C	300	16.1136	6.6068	0.8127	1.15e-3	0.00	90.00	67.93
Ar	C	500	12.6380	4.8076	0.8496	2.32e-3	0.00	90.00	69.66
Ar	C	1000	9.9118	3.4546	0.8683	3.91e-3	0.00	90.00	71.69
Ar	C	30000	7.0849	1.8749	0.8506	2.62e-3	0.00	90.00	78.21
Xe	C	120	31.9066	13.2717	0.6516	2.12e-7	0.00	90.00	70.23
Xe	C	150	29.0901	12.0036	0.6798	1.27e-6	0.00	90.00	69.96
Xe	C	170	30.5088	12.9240	0.6428	1.72e-6	0.00	90.00	69.62
Xe	C	200	29.5114	12.7084	0.6117	5.65e-6	0.00	90.00	69.52
Xe	C	250	26.8356	11.4893	0.6481	2.28e-5	0.00	90.00	69.03
Xe	C	300	24.0982	10.1112	0.6739	5.51e-5	0.00	90.00	69.39
Xe	C	500	17.1118	6.8047	0.6677	3.36e-4	0.00	90.00	71.73
Xe	C	1000	12.0951	4.3406	0.6714	1.20e-3	0.00	90.00	75.52
Xe	C	3000	7.7765	2.1766	0.6714	2.91e-3	0.00	90.00	83.44
Xe	C	10000	7.9932	2.4154	0.7415	3.43e-3	0.00	90.00	78.57
Xe	C	30000	8.4171	2.5635	0.7402	3.05e-3	0.00	90.00	78.40
Xe	C	100000	7.4986	2.0008	0.7538	2.19e-3	0.00	90.00	81.21
Ar	Al	100	15.4861	7.2384	0.7823	3.67e-3	0.00	90.00	63.55
Ar	Al	500	8.1319	3.0446	0.9028	1.33e-2	0.00	90.00	69.28
Ar	Al	1000	7.1393	2.4672	0.9111	1.38e-2	0.00	90.00	71.14
Ar	Al	1050	7.7844	2.8077	0.8600	1.19e-2	0.00	90.00	70.95
Ar	Al	10000	6.7766	2.1285	0.7615	7.29e-3	0.00	90.00	76.91
${}^4\text{He}$	Si	200	3.6245	1.0495	0.9943	3.40e-3	0.00	90.00	73.27
${}^4\text{He}$	Si	2000	3.3519	0.6560	0.9469	1.19e-3	0.00	90.00	80.13
${}^4\text{He}$	Si	3000	3.5064	0.6972	0.9086	8.57e-4	0.00	90.00	81.06
Ar	Si	4500	6.4334	1.9135	0.8696	8.30e-3	0.00	90.00	75.34

Table 16: Fitting values  $f, b, c$  for the angular dependence of the sputtered energy coefficient for several ion-target combinations and incident ion energies,  $E_0$ . Furthermore, the values for the sputtered energy coefficient at normal incidence,  $Y_E(E_0, 0)$ , the binding energy,  $E_{\text{sp}}$ (eV), for the projectiles, the value  $\theta_0^*$  (deg.), and the angular position,  $\theta_{0m}$  (deg.), of the maximum sputtered energy coefficient, are given.

ion	target	$E_0$ (eV)	$f$	$b$	$c$	$Y(E_0, 0)$	$E_{\text{sp}}$	$\theta_0^*$	$\theta_{0m}$
Si	Si(KrC)	200	15.7808	7.9103	0.6307	6.40e-3	4.70	98.72	67.46
	Si(Mol)	200	15.4820	8.0233	0.6312	8.63e-3	4.70	98.72	65.45
	Si(ZBL)	200	15.5639	7.5687	0.6357	5.30e-3	4.70	98.72	69.18
	Si(SiSi)	200	11.6349	5.0235	0.6077	5.39e-3	4.70	98.72	76.21
	Si	500	11.1924	4.9698	0.7029	9.04e-3	4.70	95.54	70.62
	Si	2000	8.2975	3.1245	0.7702	9.22e-3	4.70	92.78	73.60
He	Ti	100000	3.7323	0.4330	0.8357	7.57e-6	0.00	90.00	89.71
Ne	Ti	38	11.0490	5.5016	0.8092	8.60e-4	0.00	90.00	60.83
	Ti	380	6.1891	2.4364	0.9095	1.57e-2	0.00	90.00	67.85
	Ti	3800	5.4236	1.7711	0.8012	8.92e-3	0.00	90.00	74.80
Ar	Ti	1050	6.8672	2.5265	0.8686	1.57e-2	0.00	90.00	70.27
	Ti	150000	4.7928	0.9731	0.8107	1.24e-3	0.00	90.00	84.20
	Ti	900000	4.9290	0.8382	0.7637	1.80e-4	0.00	90.00	89.01
H	V	100	5.0277	3.6559	0.8791	7.11e-7	1.00	95.71	44.37
	V	120	3.8885	2.6073	0.9520	4.50e-6	1.00	95.22	50.21
	V	140	3.2942	2.0953	0.9769	1.22e-5	1.00	94.83	53.05
	V	200	2.5482	1.2451	1.0109	4.29e-5	1.00	94.04	63.44
	V	400	2.0197	0.4542	1.0764	1.05e-4	1.00	92.86	77.80
	V	1000	2.3039	0.3558	1.0563	9.32e-5	1.00	91.81	81.71
	V	3000	2.5607	0.2834	1.0233	3.59e-5	1.00	91.05	83.89
	V	10000	3.8538	0.5612	0.7785	7.23e-6	1.00	90.57	90.85
D	V	55	6.6566	5.2254	0.8363	3.37e-6	1.00	97.68	38.39
	V	60	5.8706	4.5525	0.8601	9.10e-6	1.00	97.36	39.81
	V	70	4.7156	3.5188	0.9095	3.06e-5	1.00	96.82	43.50
	V	100	3.3371	2.0957	0.9670	1.44e-4	1.00	95.71	54.13
	V	200	2.0014	0.5997	1.1103	4.43e-4	1.00	94.04	74.07
	V	500	2.4001	0.5014	1.0632	4.96e-4	1.00	92.56	78.71
	V	1000	2.3533	0.3817	1.0483	3.60e-4	1.00	91.81	81.00
	V	3000	2.7207	0.4118	0.9669	1.37e-4	1.00	91.05	83.23
T	V	10000	3.5648	0.5515	0.8333	2.58e-5	1.00	90.57	87.49
	V	40	8.1413	6.5657	0.8046	6.63e-6	1.00	98.98	35.67
	V	50	5.7712	4.5030	0.8757	5.20e-5	1.00	98.05	39.90
	V	70	4.2463	2.8658	0.9166	2.41e-4	1.00	96.82	50.30
	V	100	2.7393	1.3505	1.0385	5.50e-4	1.00	95.71	64.17
	V	300	2.7455	0.7452	1.0561	1.08e-3	1.00	93.30	75.92
	V	1000	2.5013	0.4347	1.0403	6.59e-4	1.00	91.81	80.55
	V	3000	2.7076	0.4224	0.9657	2.57e-4	1.00	91.05	82.98
${}^4\text{He}$	V	10000	3.2739	0.4819	0.8799	5.18e-5	1.00	90.57	86.10
	V	35	2.8053	3.3535	0.9154	1.18e-5	0.00	90.00	0.00
	V	40	3.2722	3.3277	0.9028	5.07e-5	0.00	90.00	0.00
	V	50	3.3637	2.9172	0.8821	2.26e-4	0.00	90.00	27.37
	V	70	2.5622	1.7173	0.9467	7.71e-4	0.00	90.00	47.43
	V	100	2.4528	1.1898	1.0046	1.54e-3	0.00	90.00	60.96
	V	300	2.7208	0.8019	1.0221	2.86e-3	0.00	90.00	72.48
	V	1000	2.4294	0.4784	1.0209	2.01e-3	0.00	90.00	78.13
${}^4\text{He}$	V	3000	2.5290	0.4066	0.9931	9.08e-4	0.00	90.00	80.94
	V	10000	2.7076	0.3499	0.9717	2.41e-4	0.00	90.00	83.46

Table 17: Fitting values  $f, b, c$  for the angular dependence of the sputtered energy coefficient for several ion-target combinations and incident ion energies,  $E_0$ . Furthermore, the values for the sputtered energy coefficient at normal incidence,  $Y_E(E_0, 0)$ , the binding energy,  $E_{sp}$ (eV), for the projectiles, the value  $\theta_0^*$  (deg.), and the angular position,  $\theta_{0m}$  (deg.), of the maximum sputtered energy coefficient, are given.

ion	target	$E_0$ (eV)	$f$	$b$	$c$	$Y(E_0, 0)$	$E_{sp}$	$\theta_0^*$	$\theta_{0m}$
H	Fe	4000	2.5041	0.2715	1.0224	3.50e-5	1.00	90.91	83.92
	Fe	8000	3.0021	0.3747	0.9597	1.41e-5	1.00	90.64	84.72
H	Ni	200	1.9070	1.0298	0.9915	6.94e-5	1.00	94.04	59.89
	Ni	450	1.8639	0.4115	1.1068	1.52e-4	1.00	92.70	77.30
	Ni	1000	2.2729	0.3926	1.0546	1.30e-4	1.00	91.81	80.26
	Ni	4000	2.8450	0.4218	0.9645	3.87e-5	1.00	90.91	83.37
	Ni	8000	2.8233	0.3245	0.9808	1.53e-5	1.00	90.64	84.61
D	Ni	1000	2.2869	0.4115	1.0572	4.68e-4	1.00	91.81	79.80
	Ni	4000	2.2225	0.2382	1.0304	1.29e-4	1.00	90.91	83.75
	Ni	8000	2.5159	0.2718	0.9941	5.23e-5	1.00	90.64	84.59
${}^4\text{He}$	Ni	100	2.2293	1.3338	0.9941	2.21e-3	0.00	90.00	53.23
${}^4\text{He}$	Ni	500	2.6193	0.7645	1.0198	3.42e-3	0.00	90.00	72.69
${}^4\text{He}$	Ni	1000	2.7140	0.6842	0.9982	2.51e-3	0.00	90.00	75.44
${}^4\text{He}$	Ni	4000	2.3470	0.3576	1.0033	8.75e-4	0.00	90.00	81.14
${}^4\text{He}$	Ni	8000	2.7309	0.4336	0.9496	4.09e-4	0.00	90.00	82.36
Ne	Ni	1000	4.3283	1.5651	0.9595	2.27e-2	0.00	90.00	69.34
Ar	Ni	40	22.4349	11.8142	0.6384	2.21e-4	0.00	90.00	58.76
	Ni	50	17.8626	9.2923	0.7155	8.68e-4	0.00	90.00	59.20
	Ni	70	14.6729	7.6957	0.7426	3.29e-3	0.00	90.00	58.74
	Ni	100	12.0784	6.3193	0.7733	8.04e-3	0.00	90.00	58.80
	Ni	290	9.1839	4.6777	0.7755	2.33e-2	0.00	90.00	60.00
	Ni(ZBL)	290	8.6332	4.4235	0.7871	2.57e-2	0.00	90.00	59.70
	Ni	300	8.0355	3.8274	0.8542	2.37e-2	0.00	90.00	62.31
	Ni	1000	6.4513	2.6293	0.8945	2.54e-2	0.00	90.00	67.05
	Ni	3000	5.2675	1.7573	0.9129	1.99e-2	0.00	90.00	71.92
	Ni	30000	5.7290	1.6679	0.8266	6.16e-3	0.00	90.00	76.90
Ni	Ni	100	20.0427	11.5441	0.5787	5.01e-3	4.46	101.92	60.14
	Ni	500	11.2194	5.7958	0.7868	2.38e-2	4.46	95.40	62.89
	Ni	1000	9.1490	4.2319	0.8484	2.42e-2	4.46	93.82	66.11
	Ni	2500	7.7451	3.2410	0.8536	2.14e-2	4.46	92.42	68.53
	Ni	5000	6.8163	2.5285	0.8608	1.81e-2	4.46	91.71	71.51
	Ni	10000	5.3814	1.5904	0.9351	1.41e-2	4.46	91.21	75.03
Kr	Ni	45000	6.3511	1.9125	0.8001	7.97e-3	0.00	90.00	76.86

Table 18: Fitting values  $f, b, c$  for the angular dependence of the sputtered energy coefficient for several ion-target combinations and incident ion energies,  $E_0$ . Furthermore, the values for the sputtered energy coefficient at normal incidence,  $Y_E(E_0, 0)$ , the binding energy,  $E_{\text{sp}}$ (eV), for the projectiles, the value  $\theta_0^*$  (deg.), and the angular position,  $\theta_{0m}$  (deg.), of the maximum sputtered energy coefficient, are given.

ion	target	$E_0$ (eV)	f	b	c	$Y(E_0, 0)$	$E_{\text{sp}}$	$\theta_0^*$	$\theta_{0m}$
H	Cu	100	1.9357	1.6131	0.9636	8.46e-6	1.00	95.71	34.97
	Cu	1000	2.1449	0.3519	1.0178	1.40e-4	1.00	91.81	81.69
D	Cu	50	4.7874	3.8414	0.7252	1.67e-5	1.00	98.05	33.70
	Cu	100	2.4362	1.5123	0.9385	3.40e-4	1.00	95.71	54.53
D	Cu	300	1.8961	0.4634	0.9663	7.60e-4	1.00	93.30	79.41
	Cu	1000	2.2203	0.3926	0.9570	4.75e-4	1.00	91.81	82.64
${}^4\text{He}$	Cu	3000	2.7615	0.4505	0.8231	1.69e-4	1.00	91.05	87.76
	Cu	1000	2.5612	0.6312	0.9998	2.59e-3	0.00	90.00	75.74
Ne	Cu	1000	3.9584	1.4320	0.9634	2.58e-2	0.00	90.00	69.27
	Cu	45000	4.9079	1.2599	0.7871	2.05e-3	0.00	90.00	80.84
Ar	Cu	14	13.7310	5.7877	0.8333	1.89e-6	0.00	90.00	66.75
	Cu	16	18.7112	8.5696	0.7458	3.65e-6	0.00	90.00	64.71
Ar	Cu	18	24.7634	12.3464	0.7428	6.24e-6	0.00	90.00	61.09
	Cu	20	24.6295	12.3216	0.6482	1.21e-5	0.00	90.00	61.49
Ar	Cu	25	23.3516	11.9356	0.6401	5.57e-5	0.00	90.00	60.40
	Cu	30	20.8176	10.9010	0.6536	2.16e-4	0.00	90.00	59.03
Ar	Cu	40	17.3105	9.3354	0.6690	1.10e-3	0.00	90.00	57.40
	Cu	50	14.9756	8.1564	0.6894	2.72e-3	0.00	90.00	56.87
Ar	Cu	100	9.8335	5.1621	0.7996	1.35e-2	0.00	90.00	58.60
	Cu	300	7.1143	3.3917	0.8648	2.87e-2	0.00	90.00	62.22
Ar	Cu	1050	5.3984	2.0893	0.9212	2.97e-2	0.00	90.00	68.16
	Cu	20000	5.8574	1.8610	0.7437	8.12e-3	0.00	90.00	77.13
Ar	Cu	27000	5.5357	1.6507	0.7489	6.97e-3	0.00	90.00	78.67
	Cu	30000	5.4438	1.5641	0.8263	6.32e-3	0.00	90.00	77.20
Ar	Cu	37000	5.7062	1.6555	0.7997	5.48e-3	0.00	90.00	77.75
	Cu	100000	6.2447	1.7499	0.7226	2.42e-3	0.00	90.00	81.22
Ar	Cu	300000	6.1299	1.5126	0.7428	8.75e-4	0.00	90.00	83.39
	Cu	1000000	5.9758	1.2645	0.7952	2.24e-4	0.00	90.00	84.16
Cu	Cu	12	27.7552	14.5099	0.9554	4.09e-6	3.52	118.44	77.03
	Cu	20	38.3428	20.3793	0.5498	9.71e-6	3.52	112.76	73.15
Cu	Cu	50	24.3745	13.7797	0.5491	1.30e-3	3.52	104.86	63.15
	Cu	100	18.1600	10.5588	0.5972	8.00e-3	3.52	100.63	58.82
Cu	Cu	300	12.3753	6.7171	0.7439	2.27e-2	3.52	96.18	60.99
	Cu	1000	8.0849	3.6489	0.8654	2.78e-2	3.52	93.40	66.56
Cu	Cu	3000	6.7296	2.5810	0.8793	2.17e-2	3.52	91.96	70.48
	Cu	10000	6.6936	2.4081	0.7855	1.46e-2	3.52	91.07	73.34
Cu	Cu	100000	6.9856	2.0525	0.6500	3.32e-3	3.52	90.34	83.33
	Cu	1050	7.3296	3.0297	0.8541	2.59e-2	0.00	90.00	67.12
Kr	Cu	45000	6.2228	1.8712	0.7977	8.33e-3	0.00	90.00	76.96
	Cu	550	9.4977	4.3466	0.7681	1.99e-2	0.00	90.00	64.52
Xe	Cu	1050	8.1860	3.5048	0.7833	2.27e-2	0.00	90.00	66.85
	Cu	2050	7.1193	2.8012	0.7967	2.30e-2	0.00	90.00	69.51
Xe	Cu	5000	6.2234	2.1229	0.8652	1.98e-2	0.00	90.00	72.28
	Cu	9500	6.1966	2.0514	0.8330	1.69e-2	0.00	90.00	73.70
Xe	Cu	10000	6.1730	2.0302	0.8319	1.66e-2	0.00	90.00	73.89
	Cu	30000	6.1932	1.9197	0.7634	1.16e-2	0.00	90.00	77.20
Xe	Cu	50000	6.0859	1.7877	0.8112	9.76e-3	0.00	90.00	77.13

Table 19: Fitting values  $f, b, c$  for the angular dependence of the sputtered energy coefficient for several ion-target combinations and incident ion energies,  $E_0$ . Furthermore, the values for the sputtered energy coefficient at normal incidence,  $Y_E(E_0, 0)$ , the binding energy,  $E_{sp}$ (eV), for the projectiles, the value  $\theta_0^*$  (deg.), and the angular position,  $\theta_{0m}$  (deg.), of the maximum sputtered energy coefficient, are given.

ion	target	$E_0$ (eV)	$f$	$b$	$c$	$Y(E_0, 0)$	$E_{sp}$	$\theta_0^*$	$\theta_{0m}$
Ga	Ga	100	16.7743	9.1242	0.5864	8.31e-3	2.97	99.78	62.98
	Ga	150	14.5728	7.7966	0.6435	1.30e-2	2.97	98.01	63.00
	Ga	200	13.1886	6.9186	0.6731	1.59e-2	2.97	96.95	63.43
	Ga	300	11.0053	5.4774	0.6833	1.94e-2	2.97	95.68	65.41
	Ga	900	7.9624	3.4643	0.6967	2.33e-2	2.97	93.29	69.94
	Ga	1000	7.9552	3.4752	0.7365	2.36e-2	2.97	93.12	69.03
Ar	Zr	1050	5.3413	2.0603	0.7646	2.11e-2	0.00	90.00	70.73
Ar	Zr	150000	4.7423	1.0523	0.7811	1.44e-3	0.00	90.00	83.90
Ar	Zr	900000	4.4915	0.7419	0.7528	1.97e-4	0.00	90.00	90.00
D	Nb	12200	2.8181	0.3387	0.8739	2.11e-5	1.00	90.52	88.18
He	Nb	36500	3.1127	0.3956	0.8138	4.33e-5	0.00	90.00	89.94
Nb	Nb	60000	6.4767	2.0352	0.7366	8.06e-3	7.59	90.64	78.22
H	Mo	210	4.6644	2.9517	0.8643	4.65e-8	1.00	93.95	51.97
H	Mo	220	3.6330	2.2019	0.9352	1.21e-7	1.00	93.86	54.63
H	Mo	230	3.1907	1.9175	0.9526	2.45e-7	1.00	93.77	55.07
H	Mo	250	2.7190	1.5689	0.9722	6.55e-7	1.00	93.62	56.89
H	Mo	300	2.2515	1.1942	1.0034	2.79e-6	1.00	93.30	60.09
H	Mo	400	1.9520	0.8627	1.0206	9.84e-6	1.00	92.86	65.66
H	Mo	700	1.4779	0.2899	1.0688	2.91e-5	1.00	92.16	78.95
H	Mo	1400	1.8636	0.2342	1.0501	3.72e-5	1.00	91.53	82.72
H	Mo	2000	1.9287	0.2042	1.0456	3.25e-5	1.00	91.28	83.71
H	Mo	3000	2.1113	0.2134	1.0306	2.63e-5	1.00	91.05	84.21
H	Mo	4000	2.3192	0.2394	1.0158	1.98e-5	1.00	90.91	84.42
H	Mo	7000	2.6671	0.3054	0.9701	1.17e-5	1.00	90.68	85.04
H	Mo	8000	2.7199	0.3128	0.9599	1.02e-5	1.00	90.64	85.32

Table 20: Fitting values  $f, b, c$  for the angular dependence of the sputtered energy coefficient for several ion-target combinations and incident ion energies,  $E_0$ . Furthermore, the values for the sputtered energy coefficient at normal incidence,  $Y_E(E_0, 0)$ , the binding energy,  $E_{\text{sp}}$ (eV), for the projectiles, the value  $\theta_0^*$  (deg.), and the angular position,  $\theta_{0m}$  (deg.), of the maximum sputtered energy coefficient, are given.

ion	target	$E_0$ (eV)	$f$	$b$	$c$	$Y(E_0, 0)$	$E_{\text{sp}}$	$\theta_0^*$	$\theta_{0m}$
D	Mo	100	9.2449	6.3222	0.7675	9.47e-9	1.00	95.71	46.88
	Mo	110	4.5633	3.1434	0.9213	2.53e-7	1.00	95.45	47.70
	Mo	120	3.8837	2.6794	0.9308	1.17e-6	1.00	95.22	47.70
	Mo	200	2.2299	1.2745	1.0126	4.27e-5	1.00	94.04	57.65
	Mo	300	1.6086	0.6050	1.0563	1.12e-4	1.00	93.30	69.77
	Mo	450	1.4770	0.3135	1.0959	1.73e-4	1.00	92.70	77.97
	Mo	2000	2.0847	0.2813	1.0241	1.41e-4	1.00	91.28	82.71
	Mo	8000	2.3447	0.2517	0.9775	4.03e-5	1.00	90.64	85.18
T	Mo	75	7.4824	5.3754	0.8200	3.25e-7	1.00	96.59	44.16
	Mo	80	5.6512	4.1123	0.8648	1.29e-6	1.00	96.38	44.39
	Mo	90	4.4689	3.2241	0.8973	6.22e-6	1.00	96.02	45.34
	Mo	100	3.6744	2.6229	0.9321	1.63e-5	1.00	95.71	46.41
	Mo	170	2.2730	1.2376	1.0060	1.59e-4	1.00	94.39	59.79
	Mo	300	1.5604	0.4187	1.1002	3.74e-4	1.00	93.30	75.35
	Mo	1000	1.9048	0.3003	1.0546	4.34e-4	1.00	91.81	81.09
	Mo	3000	2.1799	0.3009	0.9934	2.20e-4	1.00	91.05	83.22
${}^3\text{He}$	Mo	10000	2.4168	0.2769	0.9544	6.11e-5	1.00	90.57	85.47
	Mo	90	3.0383	2.5660	0.9041	5.70e-6	0.00	90.00	30.84
	Mo	100	2.9563	2.3990	0.8977	1.66e-5	0.00	90.00	33.89
	Mo	140	1.9207	1.3512	0.9838	1.15e-4	0.00	90.00	45.12
	Mo	300	1.5030	0.4882	1.0442	5.75e-4	0.00	90.00	70.40
	Mo	1000	1.9136	0.3602	1.0272	8.04e-4	0.00	90.00	78.48
	Mo	3000	2.0905	0.3084	1.0032	4.72e-4	0.00	90.00	81.42
	Mo	10000	2.5428	0.3733	0.9149	1.63e-4	0.00	90.00	84.28
${}^4\text{He}$	Mo	70	3.1096	2.7963	0.8979	7.04e-6	0.00	90.00	23.71
	Mo	80	3.0181	2.5721	0.8945	2.83e-5	0.00	90.00	29.40
	Mo	100	2.1032	1.6710	0.9695	1.15e-4	0.00	90.00	36.89
	Mo	140	1.6576	1.0307	1.0014	3.75e-4	0.00	90.00	51.56
	Mo	1500	1.9766	0.3334	1.0214	1.09e-3	0.00	90.00	79.72
	Mo	4000	2.0874	0.3033	0.9926	6.11e-4	0.00	90.00	81.86
	Mo	8000	2.4273	0.3663	0.9363	3.19e-4	0.00	90.00	83.28
Ar	Mo	160	7.0007	3.2720	0.8926	1.28e-2	0.00	90.00	62.74
	Mo	1601	5.4856	2.1707	0.7863	2.16e-2	0.00	90.00	69.50
	Mo	16010	4.8797	1.5105	0.7697	9.79e-3	0.00	90.00	77.05
	Mo	27500	4.5978	1.2991	0.8287	8.13e-3	0.00	90.00	77.49
Mo	Mo	300	15.3790	8.0915	0.6545	9.82e-3	6.83	98.58	64.37
	Mo	350	14.7949	7.7319	0.6522	1.10e-2	6.83	97.95	64.37
	Mo	1000	10.0595	4.7559	0.7080	1.89e-2	6.83	94.72	67.08
	Mo	2000	8.3594	3.6172	0.7205	1.99e-2	6.83	93.34	69.83
Xe	Mo	9500	6.3001	2.1680	0.7909	1.75e-2	0.00	90.00	73.64
	Mo	30000	6.2240	2.0219	0.7289	1.28e-2	0.00	90.00	76.96

Table 21: Fitting values  $f, b, c$  for the angular dependence of the sputtered energy coefficient for several ion-target combinations and incident ion energies,  $E_0$ . Furthermore, the values for the sputtered energy coefficient at normal incidence,  $Y_E(E_0, 0)$ , the binding energy,  $E_{\text{sp}}$ (eV), for the projectiles, the value  $\theta_0^*$  (deg.), and the angular position,  $\theta_{0m}$  (deg.), of the maximum sputtered energy coefficient, are given.

ion	target	$E_0$ (eV)	$f$	$b$	$c$	$Y(E_0, 0)$	$E_{\text{sp}}$	$\theta_0^*$	$\theta_{0m}$
Ar	Pd	1050	4.7874	2.0382	0.8265	3.46e-2	0.00	90.00	66.50
D	Ag	100	2.0113	1.3599	0.9395	8.55e-5	0.00	90.00	46.89
Ne	Ag	45000	3.5361	0.8029	0.8260	2.63e-3	0.00	90.00	81.79
Na	Ag	30000	4.0818	1.1588	0.8259	4.15e-3	0.00	90.00	77.47
Ar	Ag	1050	4.3998	1.8099	0.8285	3.61e-2	0.00	90.00	67.60
Ar	Ag	150000	4.9279	1.2176	0.7883	2.19e-3	0.00	90.00	81.57
Ar	Ag	900000	4.4318	0.6692	0.6653	2.63e-4	0.00	90.00	90.00
K	Ag	30000	4.4784	1.2806	0.7592	8.42e-3	0.00	90.00	79.38
Kr	Ag	45000	5.5426	1.6991	0.7254	1.07e-2	0.00	90.00	78.73
H	In	2000	2.0993	0.2668	0.9898	5.16e-5	1.00	91.28	84.19
In	In	100	15.0918	7.9243	0.6185	9.76e-3	2.52	99.02	64.88
In	In	200	11.4998	5.7702	0.6699	1.79e-2	2.52	96.40	65.56
In	In	1000	7.3248	3.1485	0.7132	2.76e-2	2.52	92.87	69.87
${}^4\text{He}$	Ta	150000	2.7842	0.2865	0.9195	1.07e-5	0.00	90.00	86.97
Ne	Ta	45000	2.7053	0.5405	0.8807	2.59e-3	0.00	90.00	81.89
Ar	Ta	1050	3.7749	1.5167	0.8503	2.55e-2	0.00	90.00	68.04
Kr	Ta	45000	4.4589	1.3533	0.7498	1.42e-2	0.00	90.00	78.18
H	W	500	2.9896	1.5460	0.9382	1.85e-8	1.00	92.56	60.64
H	W	550	2.9665	1.5154	0.9223	8.45e-8	1.00	92.44	61.06
H	W	600	2.1320	1.0397	0.9630	2.37e-7	1.00	92.34	62.54
H	W	700	1.8691	0.8504	0.9839	7.82e-7	1.00	92.16	64.55
H	W	800	2.2265	0.9849	0.9428	1.53e-6	1.00	92.02	65.60
H	W	900	1.6453	0.6802	0.9714	2.66e-6	1.00	91.91	67.24
H	W	1000	1.4684	0.5018	1.0082	3.55e-6	1.00	91.81	71.31
H	W	2000	1.2970	0.1244	1.0630	1.01e-5	1.00	91.28	83.75
H	W	4000	1.7925	0.1535	1.0319	1.08e-5	1.00	90.91	84.90
D	W	250	3.9269	2.5577	0.8242	6.43e-8	1.00	93.62	49.74
D	W	270	3.3257	1.9540	0.9277	2.80e-7	1.00	93.48	55.85
D	W	300	2.4382	1.4079	0.9691	1.04e-6	1.00	93.30	56.66
D	W	350	2.2277	1.2410	0.9674	3.89e-6	1.00	93.06	58.02
D	W	400	1.9710	1.0176	0.9898	8.04e-6	1.00	92.86	60.81
D	W	500	1.5306	0.6843	1.0177	1.87e-5	1.00	92.56	65.13
D	W	600	1.0222	0.3585	1.0601	3.03e-5	1.00	92.34	70.50
D	W	700	1.2293	0.3613	1.0416	3.77e-5	1.00	92.16	73.95
D	W	1000	1.2531	0.2141	1.0543	5.60e-3	1.00	91.81	80.37
T	W	170	4.9883	3.2765	0.8428	1.47e-7	1.00	94.39	49.84
T	W	180	2.7166	1.7643	0.9784	4.98e-7	1.00	94.26	51.68
T	W	200	2.7572	1.7937	0.9434	2.18e-6	1.00	94.04	51.18
T	W	250	2.0253	1.2204	0.9902	1.26e-5	1.00	93.62	55.03
T	W	300	1.7568	0.9622	1.0136	2.90e-5	1.00	93.30	58.88
T	W	400	1.4228	0.6303	1.0284	6.61e-5	1.00	92.86	65.54
T	W	500	1.3307	0.4476	1.0410	9.71e-5	1.00	92.56	71.76
T	W	700	1.0453	0.1849	1.0952	1.47e-4	1.00	92.16	79.41
T	W	1000	1.1420	0.1278	1.1154	1.72e-4	1.00	91.81	81.99

Table 22: Fitting values  $f, b, c$  for the angular dependence of the sputtered energy coefficient for several ion-target combinations and incident ion energies,  $E_0$ . Furthermore, the values for the sputtered energy coefficient at normal incidence,  $Y_E(E_0, 0)$ , the binding energy,  $E_{\text{sp}}$ (eV), for the projectiles, the value  $\theta_0^*$  (deg.), and the angular position,  $\theta_{0m}$  (deg.), of the maximum sputtered energy coefficient, are given.

ion	target	$E_0$ (eV)	$f$	$b$	$c$	$Y(E_0, 0)$	$E_{\text{sp}}$	$\theta_0^*$	$\theta_{0m}$
${}^4\text{He}$	W	130	5.1575	3.8507	0.8157	1.27e-7	0.00	90.00	38.81
${}^4\text{He}$	W	140	3.5583	2.7388	0.8582	8.49e-7	0.00	90.00	37.34
${}^4\text{He}$	W	150	2.6570	2.0178	0.9114	2.53e-6	0.00	90.00	39.25
${}^4\text{He}$	W	170	2.4647	1.8831	0.8837	1.03e-5	0.00	90.00	38.35
${}^4\text{He}$	W	200	1.4856	1.0769	0.9891	3.17e-5	0.00	90.00	43.41
${}^4\text{He}$	W	250	1.4122	0.9127	0.9964	8.64e-5	0.00	90.00	49.71
${}^4\text{He}$	W	300	1.4279	0.7910	0.9984	1.46e-4	0.00	90.00	56.36
${}^4\text{He}$	W	350	1.1183	0.5393	1.0225	2.10e-4	0.00	90.00	61.08
${}^4\text{He}$	W	400	1.3948	0.5660	1.0149	2.53e-4	0.00	90.00	65.92
${}^4\text{He}$	W	500	1.1808	0.3512	1.0428	3.46e-4	0.00	90.00	71.99
${}^4\text{He}$	W	600	1.2887	0.3085	1.0471	3.96e-4	0.00	90.00	75.18
${}^4\text{He}$	W	700	1.2115	0.2418	1.0579	4.56e-4	0.00	90.00	77.15
${}^4\text{He}$	W	1000	1.3706	0.2331	1.0510	5.38e-4	0.00	90.00	78.91
${}^4\text{He}$	W	1400	1.5298	0.2485	1.0347	5.63e-4	0.00	90.00	79.73
${}^4\text{He}$	W	2000	1.6609	0.2619	1.0147	5.35e-4	0.00	90.00	80.52
${}^4\text{He}$	W	5000	1.9571	0.2970	0.9444	3.57e-4	0.00	90.00	82.96
${}^4\text{He}$	W	10000	2.1752	0.3004	0.8837	2.09e-4	0.00	90.00	86.03
${}^4\text{He}$	W	20000	2.4066	0.3207	0.8765	1.04e-4	0.00	90.00	86.66
${}^4\text{He}$	W	50000	2.6944	0.3119	0.8399	3.38e-5	0.00	90.00	89.53
N	W	48	9.7828	11.4444	1.2564	2.19e-7	1.00	98.21	0.00
N	W	50	0.8114	2.8579	1.1923	8.42e-7	1.00	98.05	0.00
N	W	52	0.03809	2.6284	0.9957	2.44e-6	1.00	97.90	0.00
N	W	55	5.2029	6.4120	0.8114	7.80e-6	1.00	97.68	0.00
N	W	60	2.1282	3.7146	0.9422	2.61e-5	1.00	97.36	0.00
N	W	70	4.7589	5.1059	0.8143	1.16e-4	1.00	96.82	0.00
N	W	80	4.1131	4.3528	0.8253	2.85e-4	1.00	96.38	0.00
N	W	90	3.1672	3.3717	0.8778	5.22e-4	1.00	96.02	0.00
N	W	100	2.4983	2.6452	0.9128	7.88e-4	1.00	95.71	0.00
N	W	120	1.8889	1.7769	0.9901	1.35e-3	1.00	95.22	20.76
N	W	140	2.1218	1.6462	1.0064	1.92e-3	1.00	94.83	41.32
N	W	200	2.1655	1.2550	1.0442	3.56e-3	1.00	94.04	57.15
N	W	300	2.3710	1.1075	1.0461	5.49e-3	1.00	93.30	64.20
N	W	500	2.5141	0.9912	1.0372	7.36e-3	1.00	92.56	68.30
N	W	1000	2.5727	0.8754	1.0109	8.26e-3	1.00	91.81	71.36
Ne	W	45	5.4930	6.6565	0.7267	4.44e-6	0.00	90.00	0.00
Ne	W	50	1.6099	3.2847	0.8404	2.59e-5	0.00	90.00	0.00
Ne	W	60	0.1495	1.6421	0.9372	1.63e-4	0.00	90.00	0.00
Ne	W	70	1.4400	2.1022	0.8779	4.42e-4	0.00	90.00	0.00
Ne	W	80	1.1669	1.6922	0.8964	8.87e-4	0.00	90.00	0.00
Ne	W	100	0.8879	1.0161	1.0011	1.91e-3	0.00	90.00	0.00
Ne	W	140	1.6541	1.0860	0.9993	4.12e-3	0.00	90.00	48.96
Ne	W	200	2.2658	1.1498	0.9936	6.81e-3	0.00	90.00	59.52
Ne	W	300	2.4474	1.0814	0.9929	9.82e-3	0.00	90.00	63.83
Ne	W	400	2.5851	1.0684	0.9879	1.15e-2	0.00	90.00	65.70
Ne	W	500	2.6379	1.0350	0.9872	1.26e-2	0.00	90.00	67.03
Ne	W	700	2.5324	0.9299	0.9861	1.38e-2	0.00	90.00	68.63
Ne	W	1000	2.5126	0.8610	0.9836	1.42e-2	0.00	90.00	70.19

Table 23: Fitting values  $f, b, c$  for the angular dependence of the sputtered energy coefficient for several ion-target combinations and incident ion energies,  $E_0$ . Furthermore, the values for the sputtered energy coefficient at normal incidence,  $Y_E(E_0, 0)$ , the binding energy,  $E_{sp}$ (eV), for the projectiles, the value  $\theta_0^*$  (deg.), and the angular position,  $\theta_{0m}$  (deg.), of the maximum sputtered energy coefficient, are given.

ion	target	$E_0$ (eV)	f	b	c	$Y(E_0, 0)$	$E_{sp}$	$\theta_0^*$	$\theta_{0m}$
Ar	W	30	20.4440	14.9485	0.5109	4.34e-7	0.00	90.00	32.69
Ar	W	35	8.8750	7.1742	0.5088	5.98e-6	0.00	90.00	23.07
Ar	W	40	0.002166	0.6590	1.0153	2.65e-5	0.00	90.00	0.00
Ar	W	45	0.000351	0.4903	1.0779	7.98e-5	0.00	90.00	0.00
Ar	W	50	0.5698	0.7801	1.0144	1.94e-4	0.00	90.00	0.00
Ar	W	55	0.6882	0.6881	1.0715	3.72e-4	0.00	90.00	1.28
Ar	W	60	1.4902	1.0925	0.9989	6.12e-4	0.00	90.00	42.84
Ar	W	70	2.1776	1.4073	0.9687	1.33e-3	0.00	90.00	49.51
Ar	W	80	2.4754	1.4780	0.9736	2.27e-3	0.00	90.00	53.24
Ar	W	100	2.8236	1.5583	0.9659	4.45e-3	0.00	90.00	56.48
Ar	W	140	3.3495	1.6875	0.9577	8.70e-3	0.00	90.00	59.86
Ar	W	200	3.6552	1.7211	0.9533	1.35e-2	0.00	90.00	62.14
Ar	W	300	3.5837	1.5800	0.9568	1.88e-2	0.00	90.00	64.15
Ar	W	500	3.4196	1.4194	0.9548	2.40e-2	0.00	90.00	65.89
Ar	W	700	3.5047	1.4030	0.9476	2.55e-2	0.00	90.00	66.95
Ar	W	1000	3.3911	1.2869	0.9478	2.64e-2	0.00	90.00	68.32
Ar	W	1005	3.3469	1.2588	0.9514	2.60e-2	0.00	90.00	68.50
Ar	W	1050	3.3949	1.2820	0.9453	2.59e-2	0.00	90.00	68.48
Ar	W	30000	3.2210	0.8253	0.8795	9.52e-3	0.00	90.00	78.00
Xe	W	9500	5.2942	1.8868	0.8020	2.58e-2	0.00	90.00	72.40
Xe	W	30000	5.2338	1.7352	0.7524	1.89e-2	0.00	90.00	75.69
W	W	35	38.9214	19.3927	0.4803	1.06e-6	8.68	116.47	81.98
W	W	40	38.7481	19.6182	0.5111	2.79e-6	8.68	114.98	79.02
W	W	50	36.5132	18.4183	0.5099	9.81e-6	8.68	112.62	77.73
W	W	60	34.9177	18.0217	0.5214	3.15e-5	8.68	110.82	74.46
W	W	70	31.7802	16.4397	0.5209	8.20e-5	8.68	109.40	73.32
W	W	80	29.3956	15.2327	0.5224	1.70e-4	8.68	108.23	72.38
W	W	100	25.6694	13.3290	0.5375	4.90e-4	8.68	106.42	70.91
W	W	120	23.3024	12.1541	0.5347	1.00e-3	8.68	105.05	69.67
W	W	140	21.4480	11.2129	0.5469	1.67e-3	8.68	103.98	68.72
W	W	200	18.3650	9.6309	0.5779	3.88e-3	8.68	101.77	66.91
W	W	300	15.5941	8.1239	0.6203	8.09e-3	8.68	99.65	65.79
W	W	350	14.6047	7.5244	0.6377	9.48e-3	8.68	98.95	65.94
W	W	400	14.0761	7.2438	0.6391	1.10e-2	8.68	98.38	65.62
W	W	500	12.7467	6.4829	0.6683	1.37e-2	8.68	97.51	65.57
W	W	800	10.8164	5.2902	0.7212	1.88e-2	8.68	95.95	66.20
W	W	1000	9.8530	4.6927	0.7465	2.10e-2	8.68	95.32	66.81
W	W	2000	7.9586	3.5143	0.6958	2.47e-2	8.68	93.77	69.66
W	W	2500	7.7404	3.3309	0.7891	2.52e-2	8.68	93.37	69.08
W	W	5000	6.9226	2.7745	0.7989	2.56e-2	8.68	92.39	70.70

Table 24: Fitting values  $f, b, c$  for the angular dependence of the sputtered energy coefficient for several ion-target combinations and incident ion energies,  $E_0$ . Furthermore, the values for the sputtered energy coefficient at normal incidence,  $Y_E(E_0, 0)$ , the binding energy,  $E_{sp}$ (eV), for the projectiles, the value  $\theta_0^*$  (deg.), and the angular position,  $\theta_{0m}$  (deg.), of the maximum sputtered energy coefficient, are given.

ion	target	$E_0$ (eV)	f	b	c	$Y(E_0, 0)$	$E_{sp}$	$\theta_0^*$	$\theta_{0m}$
H	Au	1000	1.1296	0.1502	1.0382	2.89e-5	0.00	90.00	81.27
H	Au	4000	1.7580	0.1565	1.0106	2.27e-5	0.00	90.00	84.54
D	Au	130	2.6208	1.8618	0.8021	9.75e-7	0.00	90.00	42.08
D	Au	140	2.1189	1.4799	0.8627	2.39e-6	0.00	90.00	44.08
D	Au	150	2.3862	1.6368	0.8266	4.32e-6	0.00	90.00	44.73
D	Au	160	2.0048	1.3376	0.8743	6.81e-6	0.00	90.00	46.96
D	Au	200	1.7763	1.1120	0.8909	2.27e-5	0.00	90.00	50.55
D	Au	250	1.7577	0.9500	0.9203	4.54e-5	0.00	90.00	57.28
D	Au	300	1.3509	0.5861	0.9533	6.60e-5	0.00	90.00	64.65
D	Au	500	0.9831	0.1896	1.0331	1.28e-4	0.00	90.00	78.08
D	Au	1000	1.2250	0.1462	1.0429	1.64e-4	0.00	90.00	81.88
D	Au	3000	1.6463	0.1815	1.0034	1.09e-4	0.00	90.00	83.56
Na	Au	30000	3.0835	0.7467	0.7976	4.12e-3	0.00	90.00	81.63
Ne	Au	6000	2.4325	0.6801	0.9071	1.09e-2	0.00	90.00	75.70
Ne	Au	14000	2.5594	0.6470	0.8641	6.78e-3	0.00	90.00	78.68
Ar	Au	1050	2.8462	1.0853	0.9517	3.61e-2	0.00	90.00	68.15
Ar	Au	3000	2.7213	0.8977	0.9330	2.98e-2	0.00	90.00	71.82
Ar	Au	6000	2.9131	0.9221	0.8911	2.35e-2	0.00	90.00	73.52
Ar	Au	10000	2.9991	0.9154	0.8602	1.91e-2	0.00	90.00	75.00
Ar	Au	30000	3.2141	0.8796	0.8070	1.05e-2	0.00	90.00	78.82
K	Au	30000	3.1960	0.8585	0.8180	1.03e-2	1.00	90.33	78.88
Xe	Au	10000	4.7282	1.6621	0.8059	3.11e-2	0.00	90.00	72.70
Kr	Hg	762	4.8632	1.9141	0.8621	2.87e-2	0.00	90.00	68.49
H	U	2000	1.2630	0.1048	1.0576	1.29e-5	1.00	91.28	84.60
Kr	U	17900	3.7641	1.1963	0.7999	2.25e-2	0.00	90.00	75.53

Table 25: Fitting values  $f, b, c$  for the angular dependence of the sputtering yield (examples not covered in [1]) for several ion-target combinations and incident ion energies,  $E_0$ . Furthermore, the values for the sputtered energy coefficient at normal incidence,  $Y_E(E_0, 0)$ , the binding energy,  $E_{sp}$ (eV), for the projectiles, the value  $\theta_0^*$  (deg.), and the angular position,  $\theta_{0m}$  (deg.), of the maximum sputtered energy coefficient, are given.

ion	target	$E_0$ (eV)	$f$	$b$	$c$	$Y(E_0, 0)$	$E_{sp}$	$\theta_0^*$	$\theta_{0m}$
Be	Be	11	35.2434	18.1188	0.4655	6.78e-6	3.38	119.00	80.86
N	Be	15	50.6281	26.5932	0.5153	1.13e-6	1.00	104.48	68.83
Ne	Be	13	50.9814	24.8654	0.6084	7.45e-9	0.00	90.00	63.18
Ne	Be	14	53.4544	27.2431	0.5297	3.91e-8	0.00	90.00	61.25
Ne	Be	15	47.3351	23.4632	0.5710	1.20e-7	0.00	90.00	62.63
Ne	Be	17	43.0239	21.5378	0.5586	8.18e-7	0.00	90.00	62.15
Ne	Be	20	39.8480	19.9341	0.5988	5.80e-6	0.00	90.00	61.85
${}^4\text{He}$	C	20	27.5649	18.3805	0.4229	2.42e-6	0.00	90.00	38.03
C	C	25	44.0500	23.3049	0.5027	5.00e-6	7.41	118.57	77.50
C	C	3000	5.1035	1.6174	0.8516	2.49e-1	7.41	92.85	76.70
N	C	30	51.6695	27.5605	0.4891	1.12e-6	1.00	100.35	64.96
Ne	C	35	48.5603	24.0988	0.5889	6.40e-7	0.00	90.00	62.40
Ne	C	40	45.1001	22.7553	0.5898	3.74e-6	0.00	90.00	61.43
Ar	C	40	46.8448	22.6117	0.5960	1.80e-7	0.00	90.00	63.89
Ar	C	50	41.9448	20.3107	0.6165	2.46e-6	0.00	90.00	63.49
Xe	C	120	34.4756	15.3041	0.5892	5.62e-6	0.00	90.00	68.49
H	Cu	100	1.5911	1.4083	0.9787	1.01e-3	0.00	90.00	27.30
H	Cu	1000	2.2149	0.4473	1.0021	2.18e-2	0.00	90.00	78.30
Ar	Cu	14	30.0095	15.0053	0.5866	1.84e-6	0.00	90.00	61.98
H	Mo	210	4.4225	2.8066	0.8589	1.64e-5	1.00	93.95	51.76
H	Mo	220	2.9123	1.7804	0.9661	3.64e-5	1.00	93.86	54.38
D	Mo	100	13.1903	9.8965	0.8739	3.76e-6	1.00	95.71	41.99
H	Ta	25000	2.7064	0.0344	0.6684	1.95e-3	1.00	90.36	90.00